A Gestalt in Primary Visual Cortex?

Applying neurophysiological methods to capture a psychophysical phenomenon

Dissertation

zur Erlangung des Doktorgrades

der Naturwissenschaften

vorgelegt beim Fachbereich Psychologie und Sportwissenschaften

der Johann Wolfgang Goethe Universität, Frankfurt/Main

von

Anne Schmidt

aus Bernburg

Frankfurt/Main 2009
D30

vom Fachbereich Psychologie der Johann Wolfgang Goethe Universität Frankfurt/Main als Dissertation angenommen.

Dekan:
Prof. Dr. Helfried Moosbrugger

Gutachter:
Prof. Dr. Helfried Moosbrugger, J.-W. Goethe Universität Frankfurt/Main
Prof. Dr. Dieter Heyer, Martin-Luther Universität Halle/Saale

Datum der Disputation:

To

Ruxandra Sireteanu

(1945 – 2008)

Acknowledgments

First of all, I want to thank my supervisor at the Max Planck Institute for Brain Research, Kerstin E. Schmidt. I am very grateful for the opportunity she gave me to work in her research group, her patience teaching me about neuroscience, and the various chances I got to participate at conferences and course programs. I would also like to thank my close colleagues and office mates Thomas Wunderle and David Eriksson for their enduring support through my data analysis, helping me to overcome my non-existent programming skills and answering all my questions even if I asked the same one for the fifth time. Thank you also to Ana Luiza Turchetti Maia. Her visiting year in our research group was one of my best and I will always cherish her beautiful friendship. I would like to thank Sergio Neuenschwander for technical support in the lab. Thank you to all my colleagues in the department of Neurophysiology at the Max Planck Institute for Brain Research as well to the staff members in the administration, IT department, mechanical workshop, and animal house.

I thank my university advisors Helfried Moosbrugger and Dieter Heyer for their guidance through the process of writing my thesis in the department of psychology and providing me with the essential confidence to get it done.

My gratitude goes to my dear friends whom I met in Frankfurt during the last three years who gave me the strength to keep going: Sarah Weigelt, Christine Grützner, Jutta Mayer, Sandra Anti – our soul sushi let me keep my mind and smile; Valérie Wespatat, Ellen Städtler, Thomas Orban, Ines Streu – soccer, sauna, and ice cream are the best stress releasers; and all those that listened patiently and gave me good advice: Maria Olkkonen, Ovidiu Jurjut, Bruss Lima, Ulrike Radden, Petra Janson, Mirko Schmidt, Friederike Wiedemann, Ursula Werder, Birke Stubbendieck, Hermann Josef Abs, Lauri Stemmler, my friends from Fulbright Alumni, and many more.

All my love and gratefulness to my parents Jörg and Elke Schmidt and to my brother Konrad Schmidt who give me roots when I need to stay on the ground and offer me wings to fly through my life.

Abstract

‘The whole is more than the sum of its parts.’ This idea has been brought forward by psychologists such as Max Wertheimer who formulated Gestalt laws that describe our perception. One law is that of collinearity: elements that correspond in their local orientation to their global axis of alignment form a collinear line, compared to a non-collinear line where local and global orientations are orthogonal. Psychophysical studies revealed a perceptual advantage for collinear over non-collinear stimulus context. It was suggested that this behavioral finding could be related to underlying neuronal mechanisms already in the primary visual cortex (V1).

Studies have shown that neurons in V1 are linked according to a common fate: cells responding to collinearly aligned contours are predominantly interconnected by anisotropic long-range lateral connections. In the cat, the same holds true for visual interhemispheric connections. In the present study we aimed to test how the perceptual advantage of a collinear line is reflected in the anatomical properties within or between the two primary visual cortices. We applied two neurophysiological methods, electrode and optical recording, and reversibly deactivated the topographically corresponding contralateral region by cooling in eight anesthetized cats.

In electrophysiology experiments our results revealed that influences by stimulus context significantly depend on a unit’s orientation preference. Vertical preferring units had on average a higher spike rate for collinear over non-collinear context. Horizontal preferring units showed the opposite result. Optical imaging experiments confirmed these findings for cortical areas assigned to vertical orientation preference. Further, when deactivating the contralateral region the spike rate for horizontal preferring units in the intact hemisphere significantly decreased in response to a collinear stimulus context. Most of the optical imaging experiments revealed a decrease in cortical activity in response to either stimulus context crossing the vertical midline.

In conclusion, our results support the notion that modulating influences from stimulus context can be quite variable. We suggest that the kind of influence may depend on a cell’s orientation preference. The perceptual advantage of a collinear line as one of the Gestalt laws proposes is not uniformly represented in the activity of individual cells in V1. However, it is likely that the combined activity of many V1 neurons serves to activate neurons further up the processing stream which eventually leads to the perceptual phenomenon.

Table of contents

1 INTRODUCTION

> *What led me to my science and what fascinated me from a young age was the, by no means self-evident, fact that our laws of thought agree with the regularities found in the succession of impressions we receive from the external world, that it is thus possible for the human being to gain enlightenment regarding these regularities by means of pure thought.*
>
> *- Max Planck, Scientific Autobiography, 1948 -*

Consider an example to these words by Max Planck. Assume a ball that is thrown by hand into the air. One can 'by means of pure thought' calculate the exact position, time, speed, angle, etc. of that ball to fall back on earth and this is indeed what will happen with that ball.

Had Max Planck been a neuroscientist instead he would have known to use his words on the fascinating study of the brain as well. And yet by considering all the facts of what drives the brain he would have not been able to capture the whole with his thought. Brain mechanisms of course underlie natural laws in that for example sensory information entering the cortical system is processed and output is generated in form of behavior. The anatomy of the brain and underlying functional properties such as how one cell communicates with another can in most cases be reliably described. However, along the line of cortical processing there are entities that lie beyond the mere summation of all individual pieces of input information. For example in vision our sensation is not equivalent to our perception. Seeing is considered a mere physical process performed by the eyes and the nervous system. On the other hand, perceiving is what our mind does as it is related to individual experiences. While research in neurophysiology concentrates on the anatomical and functional properties of the brain to describe the process of sensation, perceptual phenomena are rather attended to in the field of psychology. It was the aim of this thesis to unite both fields of research and thus contribute to increase our understanding in how the brain works.

The following sections describe in more detail the theoretical and empirical background in psychology and neurophysiology vision research on a common topic: collinearity. Section 1.1 addresses collinearity as a law of perception formulated in Gestalt psychology, followed by section 1.2 that describes a selection of psycho-

physical studies which used collinear context in their visual stimulus setting. Section 1.3 gives an overview of the visual system. Following, section 1.4 describes in more detail the cat primary visual cortex (V1) as an experimental model which was used in our project. This includes a description of anatomical (1.4.1) and functional properties (1.4.2 - 1.4.4) of cat V1 which have been suggested by other researchers to stand in relation to collinearity as a perceptual phenomenon. The introduction chapter will conclude in section 1.5 with a summary of the proposed research hypotheses.

Chapter 2 describes the methodology including a description of the animals and surgery procedures (2.1), and the independent variables of the study (2.2). It was the main interest of this thesis work to provide a detailed explanation of both recording methods used in this project, optical imaging (2.3) and electrophysiology (2.4), as they are not common in the field of psychology research. The methods description will eventually lead to an understanding what dependent variables were derived from each. The chapter closes with a description of the experimental design of this study (2.5).

Chapter 3 presents the results of the experiments for both recording methods successively. Electrophysiology data (3.1) are addressed with an analysis of variance, optical imaging data (3.2) are described qualitatively.

Chapter 4 provides a discussion of this study's findings addressing the proposed research questions (4.1 and 4.2) and drawing inferences to known cortical functions (4.3). Further, methodological considerations (4.4), and implications for further studies (4.5) are presented before giving concluding remarks (4.6).

A detailed summary in German language will be provided in chapter 5.

1.1 Gestalt Psychology

The perceptual whole is more than the sum of its sensory parts. This concept was motivated by the Austrian Philosopher Christian Ehrenfels (1859 – 1932). His work 'Über Gestaltqualitäten' [On Gestalt qualities] (1980) laid the basis for the pioneers of Gestalt Psychology, including Kurt Koffka (1886 – 1941), Wolfgang Köhler (1887 – 1969), and Max Wertheimer (1880 – 1943). As members of the Frankfurt / Berlin Gestalt School in the 1920s they contributed much to the just upcoming research field in Germany, but they eventually had to flee Nazi Germany in the 1930s, all three emigrated to the USA. Based on their own experimental work they formulated the basic concepts of Gestalt theory, published for example in 'Principles of Gestalt Psychology' (Koffka, 1935), 'Gestalt Psychology' (Köhler, 1929), 'Studies in the Theories of Gestalt' (Wertheimer, 1923). Gestalt theory underlies the observation that our perceptual experience is beyond our mere sensations and that grouping is the main process in visual perception. According to the Gestaltists, our perception underlies certain organizing principles, so called Gestalt laws. As the German term Gestalt literally means 'form', 'figure' or 'shape', the most common rules according to which our perception groups incoming sensory information include: proximity, similarity, and closure (Wertheimer, 1923).

The law of proximity says that a temporal or spatial nearness of objects makes us perceive them as a collective entity (Figure 1.1 A). The law of similarity says that elements which are similar in size, color, or form are grouped together in perception to form a collective entity (Figure 1.1 B). The law of closure says that elements which are missing in an otherwise complete figure will be added in our perception (Figure 1.1 C).

All these laws underlie the idea of Prägnanz [conciseness], in that we perceive the simplest, most balanced, and regular organization possible under the given circumstances (Wertheimer, 1923). Despite numerous laudatory references, the Gestalt laws put together by Wertheimer and colleagues also received some critical remarks (Vicario, 1998 In G. Stemberger). For example, the Gestalt law of Prägnanz had been formulated by Wertheimer on the same hierarchical level as other Gestalt laws, although it rather serves as a superordinate term. Further, the two Gestalt laws of proximity and similarity refer to the perception of single elements while the Gestalt

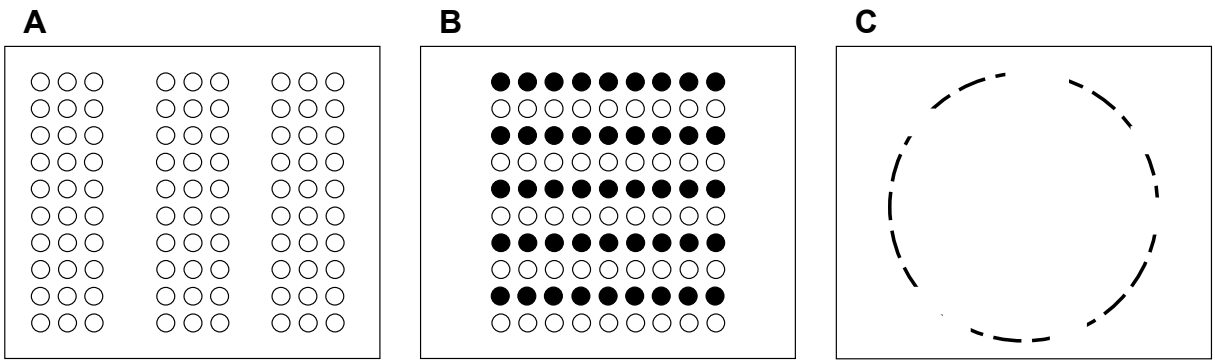

Figure 1.1 | Examples of Gestalt laws.
(A) Gestalt law of proximity - the circles spatially near each other are perceived as a collective entity, i.e. three columnar groups of circles, rather than six columns of circles. **(B)** Gestalt law of similarity - the circles that share a common characteristic are grouped together in perception, i.e. rows of full circles and rows of empty circles, rather than columns of alternating full and empty circles. **(C)** Gestalt law of closure - Physically the image shows a collection of line fragments which in their aligned composition create the percept of a circle. The gaps in their alignment are closed up in our perception.

law of closure refers to an already unified whole.

In the following example the complexity of the Gestalt law application grows even more acute: the law of collinearity (Figure 1.2): A set of oriented elements that correspond in their local orientation to their global axis of alignment is considered collinear (Figure 1.2 A). On the other hand, if their local orientation is orthogonal to their global axis of alignment the resulting collective entity is considered non-collinear (Figure 1.2 B). The law states that a collinear line is the 'better' Gestalt compared to the non-collinear line (Wertheimer, 1923).

Neglecting for a moment the Gestalt law of collinearity and applying other Gestalt laws on the object constructs shown in Figure 1.2 the following insights derive. In both instances (Figure 1.2 A + B), the set is composed of elements that are co-oriented, and according to the law of *similarity* either would be grouped together in a Gestalt percept by this characteristic. Further, both types of element alignments (Figure 1.2 A + B) can be perceived as lines, i.e. a thin horizontal line (Figure 1.2 A) and a thick vertical line (Figure 1.2 B) despite the gaps in their Gestalt, i.e. the Gestalt law of *closure*. Finally, the nearness of the elements is the same for both lines in terms of their inter-element distance, i.e. the Gestalt law of *proximity*. According to these three Gestalt law examples both constructs (Figure 1.2 A + B) go along with

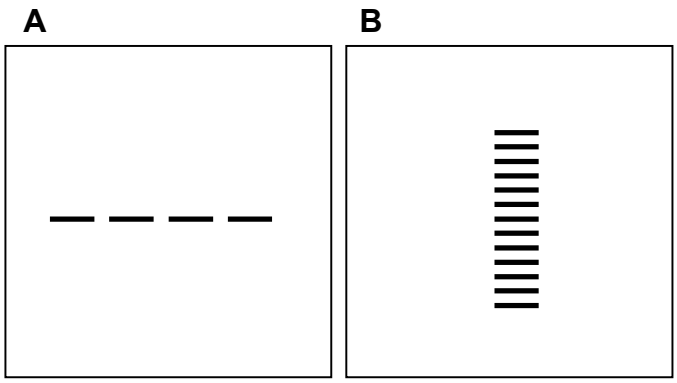

Figure 1.2 | Gestalt law of collinearity.
A set of oriented elements aligned end-to-end is considered collinear **(A)** and described as the 'better' Gestalt (Wertheimer, 1923), while a set of oriented elements aligned side-to-side is considered non-collinear **(B)**.

the rules. However, there are obvious differences between the two object constructs (Figure 1.2 A + B). First, only the elements of the collinear line are *also* co-aligned. Second, to complete the collinear line one depends on less line material compared to the amount for filling the gaps for the non-collinear line. Third, the collinear line (Figure 1.2 A) is only composed of four elements, while the non-collinear line (Figure 1.2 B) contains many more and would probably not be perceived as a line any longer if it also only had four elements.

These additional characteristics that the collinear line fulfills in comparison to a non-collinear line, i.e. co-alignment, total of perceptual filling in, and quantity of elements, could conceptually be considered as additional Gestalt laws. Without the aim to provide a complete listing, one should note that other researchers of Gestalt Psychology, for example, Metzger (1966) and Beck (1966) have specified more Gestalt laws beyond the seven originally defined by Wertheimer and his colleagues (1923). Eventually in this debate the term of 'Neo-Gestalt' theories had been introduced under the demand for a unification of the proposed Gestalt laws (Henle, 1990 In I. Rock). Apparently, under given circumstances different Gestalt laws have to be considered in combination to argue for their application in the perceptual phenomenon.

This comparison of a collinear and a non-collinear line reveals an interesting aspect in the light of Gestalt laws. Given two sets of elements like those presented in Figure 1.2 A and B both may follow certain laws of Gestalt and are thus each considered as a figure. However, when judging their relative goodness of a Gestalt figure, further criteria need to be considered.

1.2 Psychophysical Studies on Collinearity

Despite the complexity of the Gestalt law of collinearity the perceptual phenomenon of collinear facilitation has been extensively studied, i.e. that a collinear contour embedded in a field of randomly oriented elements is more easily detected than a contour of non-collinearly aligned elements (e.g., Field & Hess, 1993). Subsequent studies were designed to test the detection threshold of an oriented element of varying contrast surrounded by collinear or non-collinear elements. In particular, it was asked how much contrast of that target element being part of a line contour is needed to be detected by an observer. The minimal contrast required has been shown to vary with certain stimulus parameters, such as inter-element distance (e.g., Polat & Sagi 1993), relative element orientation (e.g., Polat & Sagi, 1994), attention to the elements (e.g., Freeman et al. 2001, 2005), and temporal relationship of elements (e.g., Cass & Alais, 2006; Polat & Sagi, 2006; Huang & Hess, 2008). One visualization for each experimental paradigm topic is presented in Figure 1.3 A - E.

Two major aspects argue for an attempt to briefly describe the aforementioned psychophysical studies. First, it is always impressive to learn about the elaborated experimental designs, each trying to tackle an otherwise hard to capture aspect of perception. Second, all authors at one point or another attempt to relate the behavioral outcomes of their studies to underlying neuronal mechanisms. These aspects will be presented in more detail after a descriptive overview of the listed experiments.

In the study by Field and Hess (1993), see Figure 1.3 A, both variations of line stimuli consist of a smooth path of spatially separate elements, embedded in a field of randomly oriented elements. The elements were sinusoidal gratings enveloped by a Gaussian window, so called Gabors (for a more detailed description see also Methods section chapter 2.2.1 of this thesis). In one of the settings, the oriented Gabor elements were collinearly aligned along the path of the contour, in the other condition the elements laid orthogonal to the path. The results of their study showed that the observers were significantly slower at detecting the line when the Gabor elements were placed side-to-side (non-collinear) as opposed to end-to-end (collinear).

Polat and Sagi (1993, 1994) asked their subjects to detect the presence of a Gabor under varying conditions. The experimenters compared the threshold of contrast needed for a single Gabor element with that when it was surrounded by flanking Gabors.

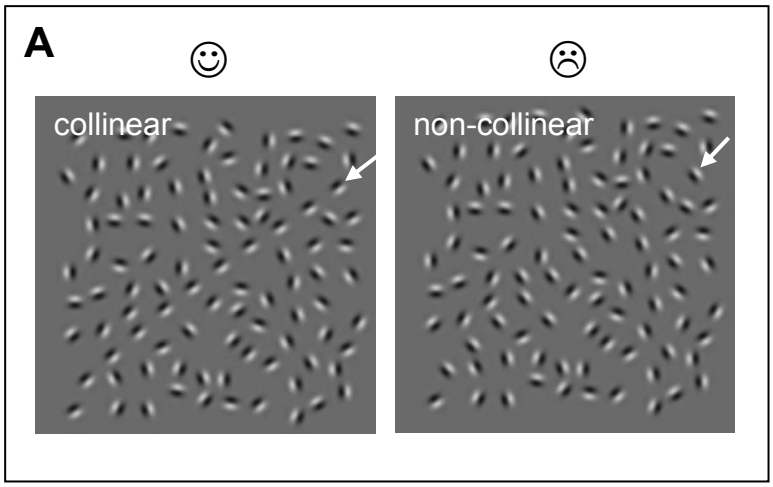
A
collinear
non-collinear

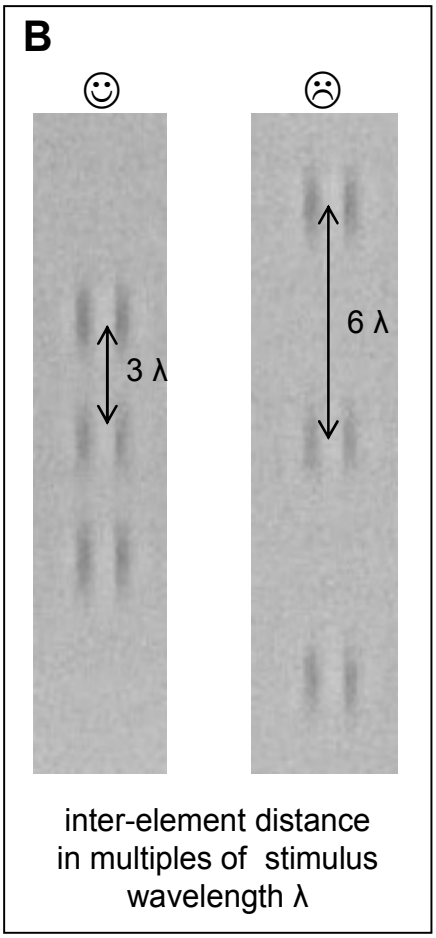
B
3 λ
6 λ
inter-element distance
in multiples of stimulus
wavelength λ

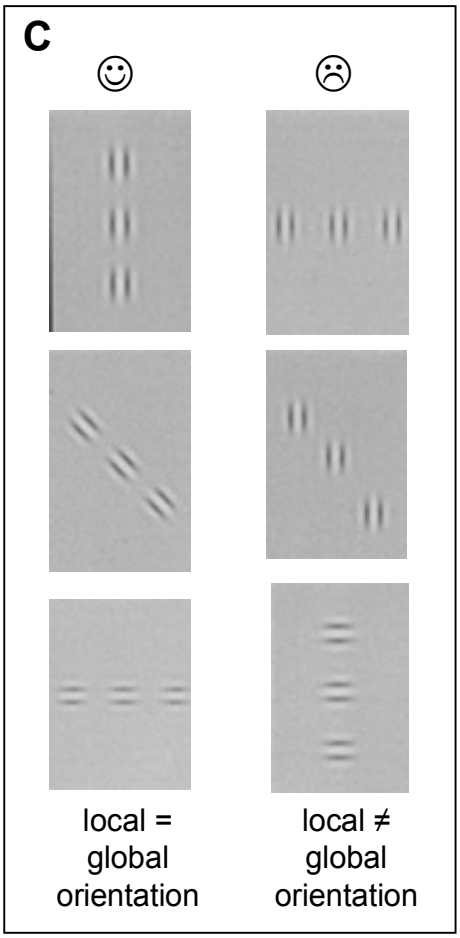
C
local =
global
orientation
local ≠
global
orientation

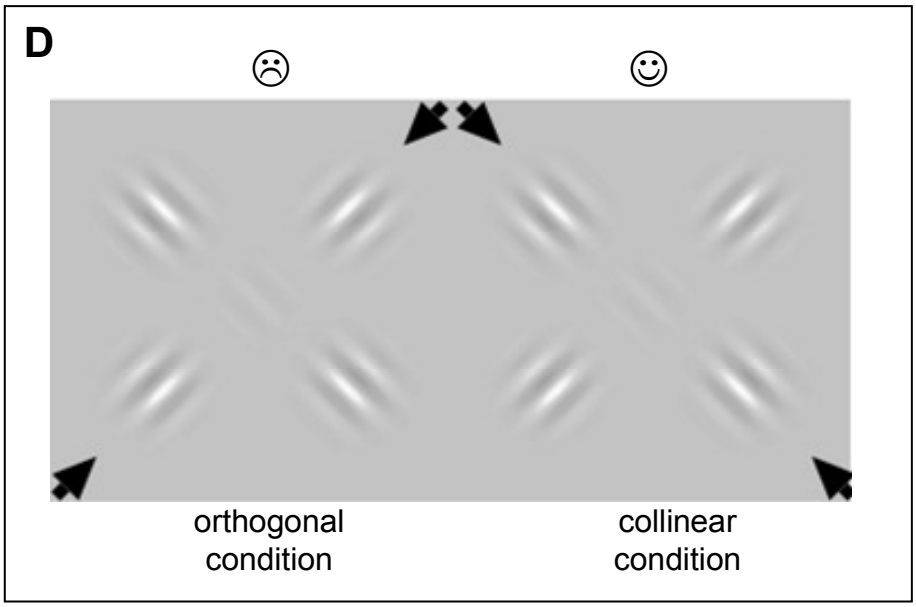

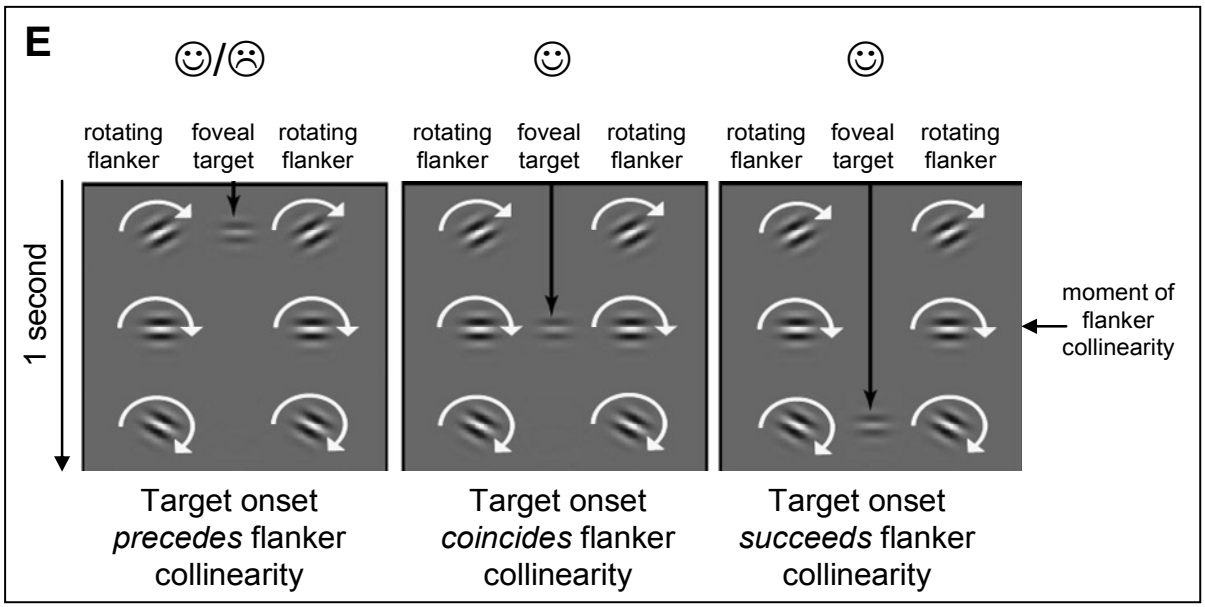

Figure 1.3 | Examples of psychophysical studies on collinearity.
A) Field & Hess (1993) asked their subjects to detect a line of oriented Gabors which were aligned either collinearly or non-collinearly.
B) Polat & Sagi (1993) tested their subjects on how much contrast of the center element was sufficient for its detection by varying the inter-stimulus distance of collinearly aligned Gabor elements or **(C)** combining different local orientations and global axes of Gabor alignment (Polat & Sagi, 1994).
D) Freeman et al. (2001) tested their subjects for the detection threshold of a center Gabor element in dependence of which axis they attended to, either with orthogonal flankers (left example) or with collinear flanker elements (right example). Black arrows indicate the axes that the subjects were drawn to attend to, respectively.
E) Caas & Alais (2006) varied the order of stimulus element onset with the target Gabor either preceding, coinciding or succeeding the onset of collinearly aligned Gabors. Smiley faces above the images indicate which respective stimulus configuration in each of the experiments led to a better detection or decision performance in the subjects. For a more detailed descriptions of the studies refer to section 1.2.

In their studies they varied the distance between the center Gabor and the flankers (Polat & Sagi, 1993) or the relative orientation of the individual elements (Polat & Sagi, 1994). The distance between Gabor elements was defined in multiples of the Gabor wavelength λ, i.e. a value derived from the spatial frequency of the Gabor. They found the contrast threshold for detecting the center Gabor lowest when the distance between the elements was 2 - 3 λ and the effect leveled off when the distance between the elements increased (Figure 1.3 B). Further, the target detectability was best at this optimal distance when the local orientation of the center and flanker Gabors agreed with their global axis of alignment, i.e. collinear (Figure 1.3 C). If the elements were misaligned by 15° or more a noticeable reduction in detection performance was observed.

Based on an ongoing debate whether attention can modulate our perception, Freemann and colleagues (2001) attempted to address this question in psychophysical studies on the effect of collinearity. In drawing their subjects' attention to one of two Gabor line constructs while ignoring the other one, they asked their subjects to detect a central element which was either collinearly or orthogonally aligned relative to the flankers. Both examples are presented in Figure 1.3 D, orthogonal condition (= non-collinear) on the left, and the collinear version on the right of the picture. In the experiment the relevant axis for a detection task was marked on an initial fixation display (not shown in the image, but indicated in Figure 1.3 D by arrows which were themselves not present in the experiment). They found that the detection thresholds were lower when subjects had to attend to the pair of collinear flankers than when attending to the orthogonal pair of flankers. In a later study Freemann & Driver (2005; not shown in Figure 1.3) found similar results when giving their subjects an additional task to perform to better control where they were attending to.

Several studies have reported facilitation effects even when the relative timing of target and flankers do not coincide. The experimental design from Caas & Alais (2006) for different timing situations is exemplarily presented in Figure 1.3 E. They varied the onset of the target Gabor presented in the point of focus for the subjects, in relation to that moment in time when the constantly rotating Gabor flankers were collinearly aligned. In their study they found a collinear facilitation effect in all three timings, when the target onset preceded flanker collinearity (by about 20 - 80ms), when the target onset was coincident with flanker collinearity, and also when the target onset succeeded flanker collinearity. In contrast, Polat & Sagi (2006; not shown

in Figure 1.3) found no collinearity effect for detecting a target that preceded the presence of flankers, and Huang & Hess (2008; not shown in Figure 1.3) disagree on the finding when the target presentation followed the flanker presentation. The studies differ in a variety of settings that one but not the others controlled for, or did not mention in the description of their research paper. For example, Caas & Alais (2006) used rotating flankers while the other two studies used static ones. Also, they tested only three subjects (themselves and one naïve subject) to draw their conclusion on the existence of all three collinearity timings (before, coincident, succeeding). The other two studies had three or eight subjects, respectively. These factors could be of relevance in explaining their different findings.

Results from all psychophysical studies presented here emphasize the relevance of Gestalt criteria for an optimal percept, here in particular that of collinearity. Despite their quite different approaches to narrow down optimal settings to show the advantage of collinearly aligned elements, all researchers share their quest for the underlying neuronal mechanisms of the behavioral outcomes. Especially the primary visual cortex has been a matter of debate in this context. Of particular interest for this thesis project is the discussion of intrinsic lateral connections between neurons of similar orientation preference. A detailed description of the anatomical and functional properties of the cat primary visual cortex will be given after a basic overview to the visual system in the following chapter. In brief, neurons in V1 are grouped together in a patchy manner according to their preference for a particular stimulus orientation. Patches of one particular orientation specificity are spaced about 900 – 1000 μm and neurons therein connect among each other via lateral connections. A center–to–center distance between Gabor elements of 2 - 3 times the elements' wavelength λ (Polat & Sagi, 1993) was described to be optimal for collinear facilitation. This suggests that the cortical spacing of orientation columns and the optimal distance of stimulus elements are related.

In conclusion, stimulus parameters such as inter-element distance and relative orientation appear to play a crucial role in planning visual stimuli for studying collinearity in V1. Anatomical structures in V1 such as lateral connections hold the potential to integrate information over visual space and it has been suggested that they serve as the underlying neuronal structure that the advantage of a collinear line in perception might rely on (e.g., Polat & Sagi, 1993, 1994; Chisum et al., 2003).

1.3 The Visual System – an Overview

The following overview of the visual system appears more compact on the example of the human brain. However, all descriptions in the order up to the primary visual cortex are anatomically similar to that of a cat or will be noted otherwise and can therefore be consigned in description. The subsequent chapter will then focus in more detail on the primary visual cortex of the cat.

The sensation of seeing begins when an object in sight reflects light into our eyes. Figure 1.4 visualizes the anatomical properties of the human eye in a schematic cross section. Information on the following overview of the visual system were extracted from lecture books on perception and neuroscience such as Goldstein (2001), Kandel, Schwartz, & Jessel (2000), and Palmer (1999).

The cornea and the lens of the eye transmit and focus the light entering through the pupil into the eye. The light further passes through the central chamber of the eye that is filled with a clear fluid, the vitreous humor, before reaching the light-sensitive receptors in the retina. The human retina comprises different types of neurons organized in layers. At point of focus, the light is bundled onto a particular spot on the retina, the fovea or 'yellow spot' (refer to Figure 2.11 in the 'Materials and Methods' chapter for more details), where the density of photo receptors is highest. The photo receptors are located at the innermost layer and they are the first to receive the electromagnetic energy of light photons and transforming it into electric activity by a photochemical transduction process. The neuronal activity is passed on through the different layers of neurons until it reaches the ganglion cells of the retina. The axons of the ganglion cells bundle into the optic nerve, which then projects to the thalamus. The location where the optic nerve leaves the back of the eye is called optic disc or 'blind spot' as here the retina does not contain any photo receptors.

Each ganglion cell in the retina receives information from a restricted area in the visual field, the receptive field (RF) (Kandel, Schwartz, & Jessel, 2000). These receptive fields are organized in a retinotopic way, i.e., adjacent cells in the retina have neighboring receptive fields. Thus, the visual field is coextensively mapped onto retinal space. Behind the eye the optic nerve fibers are led to the optic chiasm where the projections from the nasal side of each retina cross over to the opposite side of the brain, while fibers from the temporal side of each retina remain on their side. After the chiasm intersection a small portion of the fibers in either hemisphere

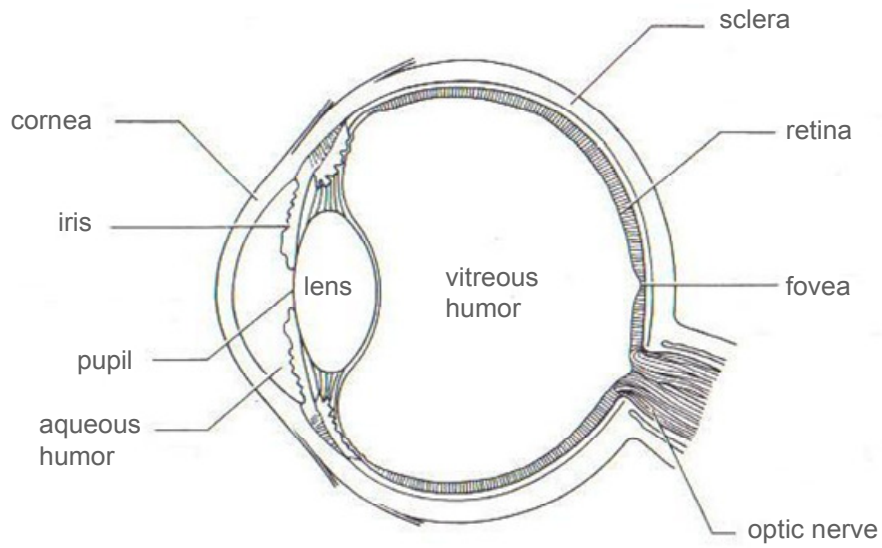

Figure 1.4 | A cross section of the human eye.
Anatomical properties include the cornea, the pupil, the lens the center chamber of the eye filled with vitreous humor, the retina, the fovea, the optic disc, and the optic nerve. Graphic modified after Goldstein 2001.

are led to the superior colliculus, a nucleus located in the midbrain. Within each hemisphere the remaining larger portion of the optic track fibers are led to the respective lateral geniculate nucleus (LGN) of the thalamus. Figure 1.5 visualizes the anatomical properties of the human visual system with its pathway from the eye to the visual cortex.

The axon projections from the retinal ganglion cells to the LGN via the optic nerve also carry along the receptive field information. Cells in the LGN are very similar in their receptive field properties, i.e. they are also retinotopically organized with neighboring positions in the visual field also being adjacent cells in the LGN. The LGN is divided into six laminar layers, three of them receive input from the left eye, the other three from the right eye. In primates, four of the LGN layers are referred to as magnocellular layers, because they contain large cell bodies with large RFs and are especially sensitive to contrast differences but not so to color. The remaining two of the LGN layers are referred to as parvocellular layers, because they contain small cell bodies with small RF and they are very selective to color but in turn not very sensitive to differences in contrast. Note that in the cat these systems are referred to as y-input (alias magnocellular) and x-input (alias parvocellular).

From the LGN, neurons project further on to the primary visual cortex. Here the cortical tissue is also divided into six laminar layers, where neurons in layer IV

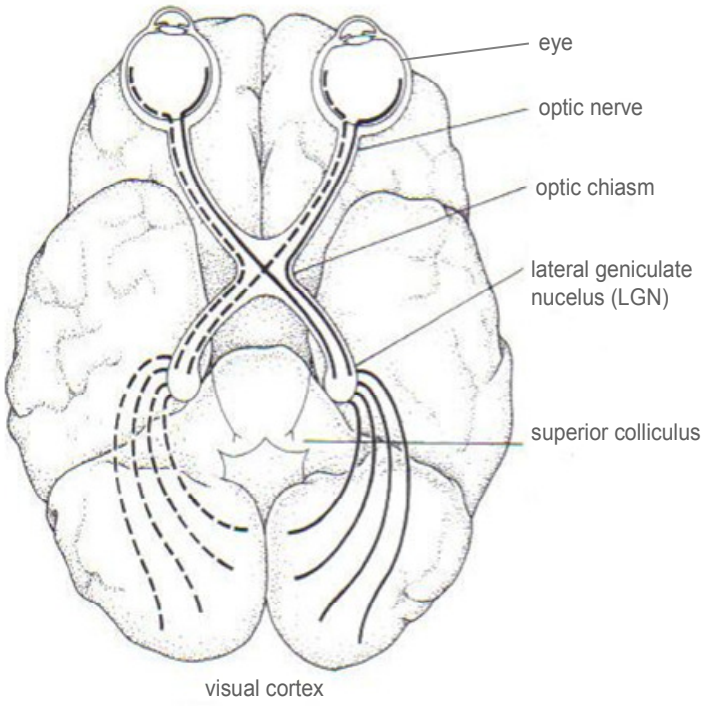

Figure 1.5 | Graphical outlay of the human visual system.
Anatomical properties include the eye, the optic nerve, the optic chiasm, the lateral geniculate nucleus (LGN), the superior colliculus, and the visual cortex. Graphic modified after Goldstein 2001.

receive the direct input coming from LGN cells and then project further on to other layers. Figure 1.6 visualizes the visual pathways in the human cortex. The primary visual cortex (V1) is considered the first stage of cortical processing of incoming visual information. From there two pathways linking higher visual areas can be distinguished. The ventral pathway comprises the cortical area V4 which is strongly modulated by attention (e.g., Reynolds & Desimone, 2003) and finally projects to the inferotemporal cortex including areas that are involved in face and object recognition. Thus, this pathway is also called the 'what' pathway. The dorsal pathway projects to the posterior parietal cortex and includes cortical area V3 and area V5 = MT which are both considered to be involved in the processing of visual motion (Braddick et al., 2001, Born & Bradley, 2005). This pathway is considered specialized for locating objects, thus is also called the 'where' pathway. Pioneer work on the existence and function of these two cortical visual systems came from lesion studies in the macaque monkey by Ungerleider & Mishkin (1982 In D. J. Ingle, M. A. Goodale, & R. J. W. Mansfield). They found monkeys to be impaired in either task, object identification or locating depending on which cortical areas were lesioned.

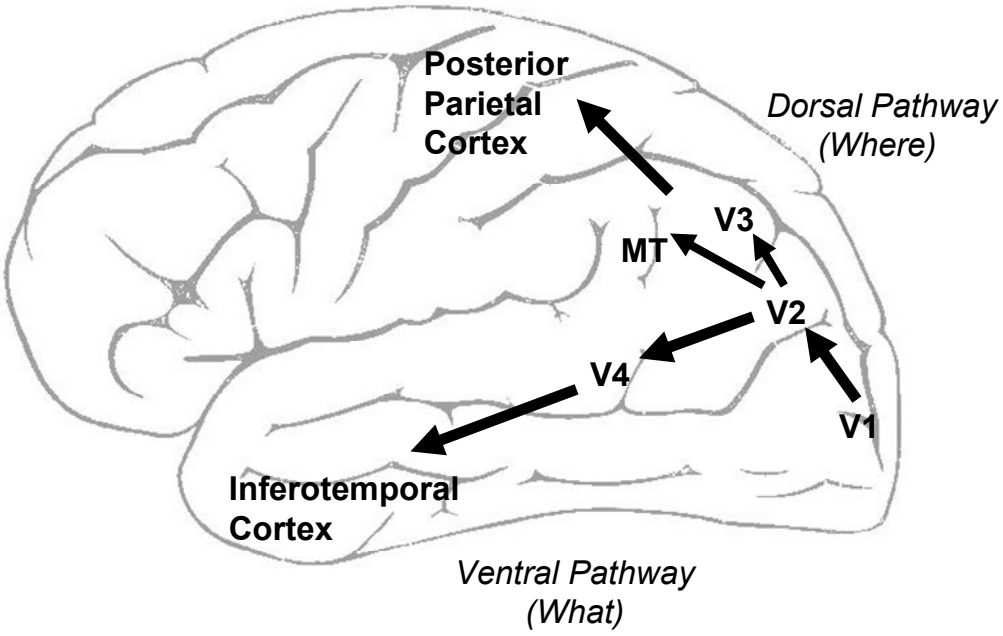

Figure 1.6 | The two visual pathways in human cortex.
The ventral ('what') pathway is specialized in object recognition and dorsal ('where') pathway specialized in object localization. Graphic modified after http://etc.usf.edu/clipart.

1.4 The Cat Primary Visual Cortex (V1)

1.4.1 Topographic Representation of the Visual Field

The cat primary visual cortex (V1) is represented on the first gyrus to either side of both hemispheres (Figure 1.7 A with V1 of the left hemisphere shaded in grey). A study by Tusa and colleagues (1978) has shown that there is a retinotopic representation of visual field longitudes and altitudes on the primary visual cortex. Locations adjacent in the visual outside world are also neighboring in V1 (Figure 1.7 B & C). The cat primary visual cortex includes both cortical area 17 (A17) and area 18 (A18), numbered after the cortical classification of Brodmann (1909). Both areas are considered primary as they both receive direct input from the thalamus, but they are also interconnected with each other and to subsequent areas of the visual system. The two visual areas 17 and 18 have an overlapping topographical representation of the visual field (Figure 1.7 C). In using micro-electrode recordings the visuotopic maps for both areas 17 and 18 were generated, mainly under the work of Hubel and Wiesel (e.g., 1962). In brief, this method allowed them to identify the position in the visual field to which a neuron that is recorded from responds best. After recording from many positions in V1 a retinotopic map could be generated.

Major landmarks in the retinotopic representation of the visual field within the primary visual cortex are the following (see Figure 1.7 B & C below for visualization): the horizontal midline (HM), the vertical midline (VM), and the adjacent spherical coordinates. The horizontal midline is represented at about 8mm posterior to the zero point of the anterior-posterior Horseley-Clarke coordinates (Tusa et al., 1978). In the back the cortex curves downwards. Experiments in the cat primary visual cortex are commonly performed on the caudal surface of the cerebrum, thus positioned in the cortical area anterior to the horizontal midline, i.e. representation of the lower half of the visual field. The vertical midline is represented on the primary visual cortex between area 17 and area 18, also referred to as the transition zone (TZ). Notably, each hemisphere has such a TZ, which implies a double representation of the vertical midline in the primary visual cortex.

Apparently, for the border between area 17 and area 18 there is no marking line visible on the cortical surface but there are several functional and organizational differences between the two areas that may help to distinguish one from another. These differences arise from the kind of input that either area receives from the retina

cells via the LGN inter-connection. While area 18 receives only input from retinal y-cells which hold large receptive field properties and preferably respond to stimuli of small spatial and high temporal frequency, neurons in area 17 receive y-input and also input from the x-cell type that has small receptive field properties and preferably respond to high spatial and small temporal frequency stimuli.

Consequently, neurons in area 18 have larger receptive fields, about 5°, than those in area 17 with about 2° in size. Accordingly, neurons in these two areas prefer different stimulus properties. Neurons in area 18 preferably respond to thick and fast moving bars crossing their RF, while neurons in area 17 display their optimal response to both thin and slow moving bars, but also respond to thick and fast moving bars. Therefore in studying V1 properties it is absolutely legitimate to use stimulus properties optimal for area 18 neurons as neurons in area 17 both are also respond to that. Neurons in area 17 and 18 also share other stimulus response properties such as their modular organization according to orientation preference and lateral connectivity. These properties will be addressed more closely in the next chapters. Orientation selectivity and specific lateral connectivity are common to both areas.

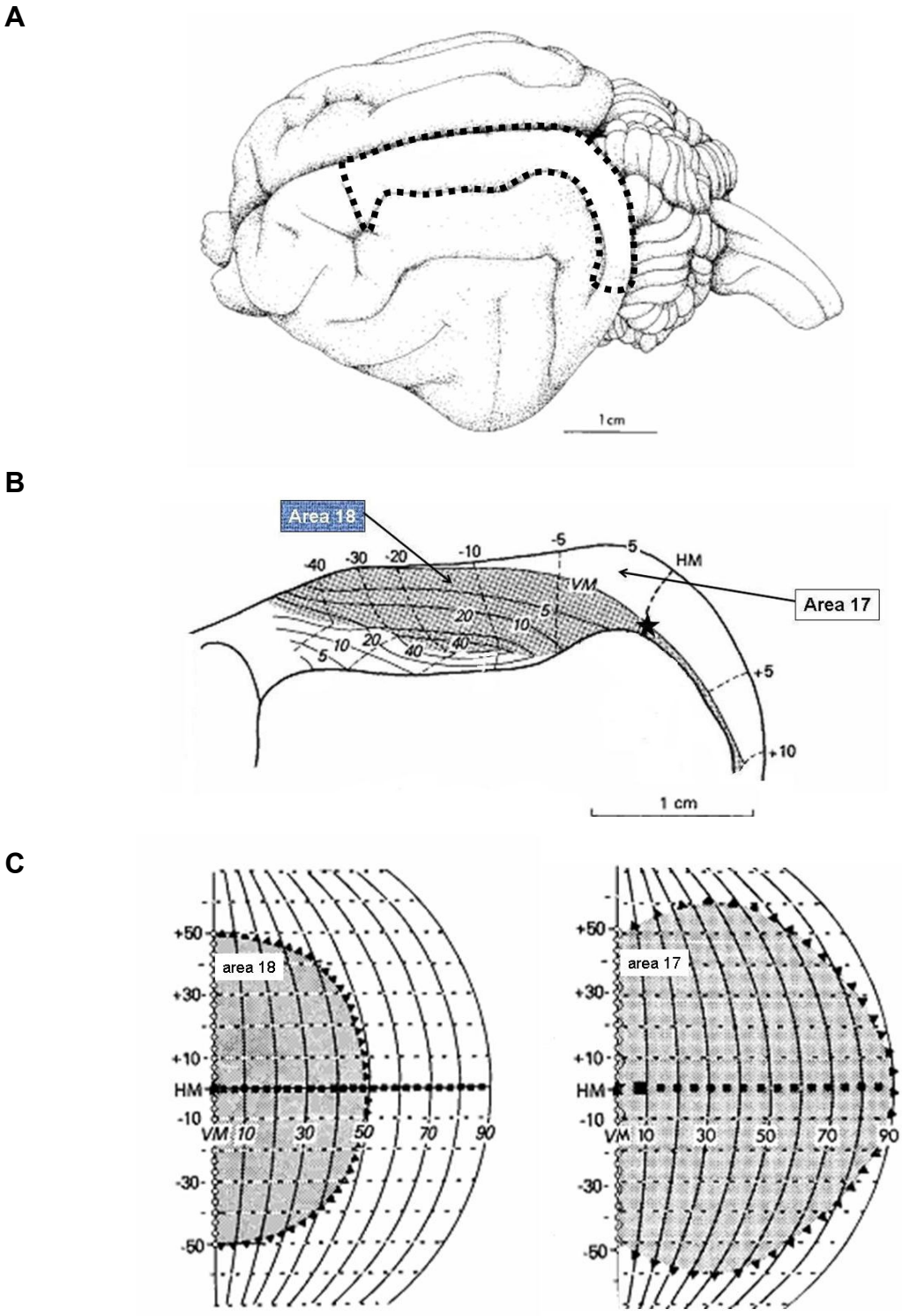

Figure 1.7 | Topographic representation of the visual field in the cat visual cortex.
A graphical display of the cat brain **(A)** with anterior to the left and posterior to the right. The outlined area in **(A)** is enlarged in **(B)** and overlaid with longitudinal and azimuth coordinates of the visual hemifield representation in **(C)** for both primary visual areas 17 and 18. The vertical midline (VM) is represented by the 17/18 border. The cortical area accessible during an experiment is always anterior to the horizontal midline (HM), i.e. representing the lower half of the contralateral visual hemifield. (Graphics modified after Tusa et al., 1978).

1.4.2 Orientation Selectivity of Neurons in V1

In V1, neurons that share receptive field properties such as input from the same eye (ocular dominance), or their preference for a particular stimulus orientation are organized in a columnar system (Hubel & Wiesel, 1962, 1967). As visualized in the model in Figure 1.8 A these columns are organized regularly across V1 in forming a so called hypercolumn, which includes a full set of all orientation and ocular dominance columns (Hubel & Wiesel, 1974). This concept of columnar organization in the cat primary visual cortex earned the researchers, David Hubel & Torsten Wiesel, the Nobel Price in 1981. In the following excerpt of David Hubel's Noble lecture that he gave at the ceremony one gets a good impression into the circumstances of their amazing discovery story:

'In the early spring of 1958 I drove over to Baltimore from Washington, D.C., and in a cafeteria at Johns Hopkins Hospital met Stephen Kuffler and Torsten Wiesel, for a discussion that was more momentous for Torsten's and my future than either of us could have possibly imagined. […]. Torsten and I didn't waste much time. Within a week of my coming to Hopkins (to a dark and dingy inner windowless room of the Wilmer Institute basement, deemed ideal for visual studies) we did our first experiment. […] A piece of apparatus resembling a small cyclotron held the anesthetized and paralyzed cat with its head facing almost directly upwards. A modified ophthalmoscope projected a background light and a spot stimulus onto the retina […]. After a month or so we decided to have the cat face a projection screen […].

Small spots of light were produced by sliding 2 cm x 5 cm metal rectangles containing various sizes of holes into a slot in the apparatus, just as one puts a slide into a slide projector. To obtain a black spot on a light background one used a piece of glass like a microscope slide, onto which a black dot had been glued. […] Our first real discovery came about as a surprise. We had been doing experiments for about a month […] and were not getting very far: the cells simply would not respond to our spots and annuli. One day we made an especially stable recording. […] The cell in question lasted 9 hours, and by the end we had a very different feeling about what the cortex might be doing. For 3 or 4 hours we got absolutely nowhere. Then gradually we began to elicit some vague and inconsistent responses by stimulating somewhere in the midperiphery of the retina. We were inserting the glass slide with its black spot into the slot of the ophthalmoscope when suddenly over the audiomonitor the cell went off like a machine gun. After some fussing and fiddling we found out what was happening. The response had nothing to do with the black dot. As the glass slide was inserted its edge was casting onto the retina a faint but sharp shadow, a straight dark line on a light background. That was what the cell wanted, and it wanted it, moreover, in just one narrow range of orientations. This was unheard of. It is hard, now, to think back and realize just how free we were from any idea of what cortical cells might be doing in an animal's daily life.'
(David Hubel (1981), Nobel lecture, Evolution of ideas on the primary visual cortex, 1955 – 1978: A biased historical account, retrieved June 25th from http://nobelprize.org/nobel_prizes/medicine/laureates/1981/hubel-lecture.pdf)

Mapping the cortical surface with electrode recordings, position by position, to allocate columns of neurons with particular orientation preference is quite an extensive work and very time consuming. In advancement of experimental methods, nowadays a special camera system (Optical Imaging) can quite uncomplicatedly take images of the cortical surface while simultaneously the animal is visually stimulated with oriented bars. Cortical areas can then be color-coded according to what stimulus orientation they were most responsive to (see Figure 1.8 B).

The cortex is divided into six laminar layers (Figure 2.9 A) and all neurons throughout the layers within an orientation column share the common orientation preference property and are densely interconnected with each other.

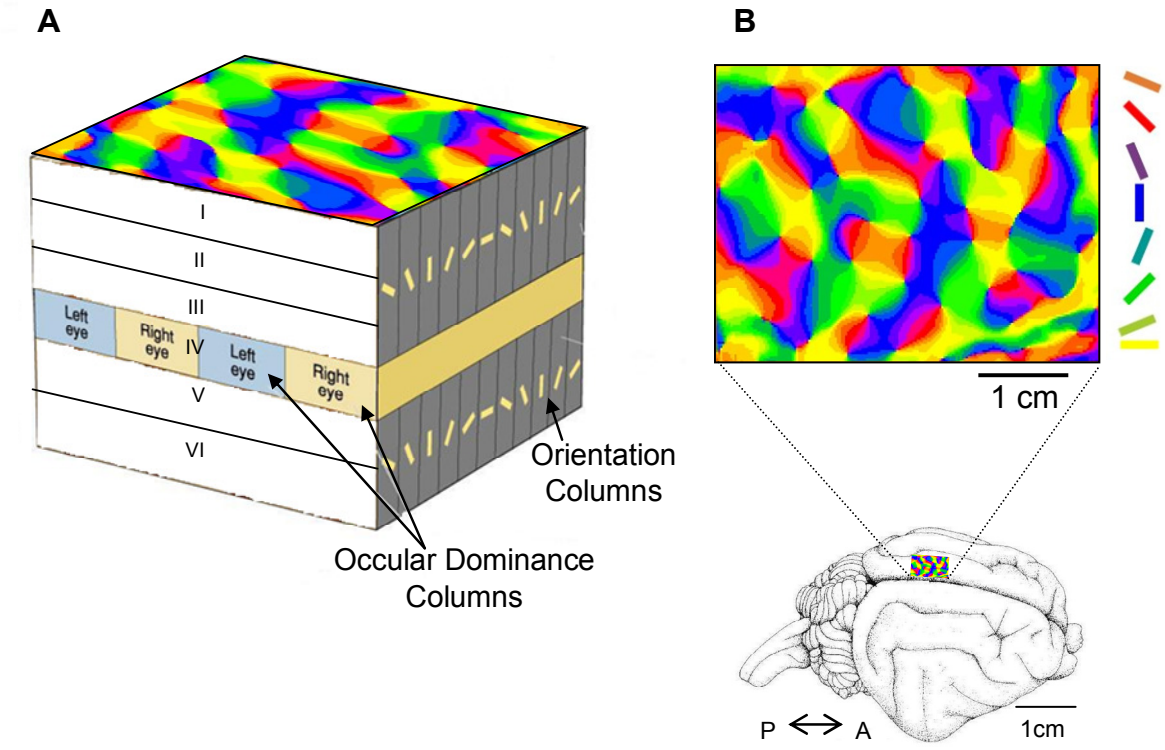

Figure 1.8 | Columnar system of the cat primary visual cortex.
(A) Hubel and Wiesel (1962, 1967) proposed that the visual system is organized according to properties such as cells' orientation preference in response to visual stimuli, and ocular dominance according to which eye is the source of input information. This pattern is regularly and persistent throughout the six cortical laminar layers, forming so called 'hypercolumns', i.e. a icecube like entity. Image modified after http://thebrain.mcgill.ca/
(B) As seen from the top of V1, cortical areas can be coded according to their most pronounced orientation preference in response to visual stimulation (upper panel). This so called angle map is an enlargement of the rectangular cortex region shown in the lower panel. Brain graphic modified after Tusa et al. (1978).

1.4.3 Lateral Interactions Between V1 Neurons

Neurons in V1 are not only interconnected over the different laminar layers, but they also are interconnected parallel to the cortical surface via lateral (horizontal) connections. Despite the more common use of the term 'horizontal connections' throughout the literature, its orientation idiom might be confusing later on when introducing orientation as an experimental variable of this study. Therefore only the term 'lateral connections' will be used throughout this thesis.

In anatomical studies in cats (e.g., Gilbert & Wiesel 1979, 1983) and tree shrews (Rockland & Lund, 1983) chemical tracers had been injected in the primary visual cortex. This labeled neuronal dendrites and axon collaterals which could then be reconstructed. Gilbert and Wiesel (1983) noted that the branching of axon collaterals was far reaching and the projection terminals showed a specific cluster-like distribution within the same cortical layer (see Figure 1.9). The authors suggested a possible relationship to the orientation column system. Subsequent studies could confirm that these lateral connections in V1 are primarily between neurons of similar orientation preference (e.g., Gilbert & Wiesel 1989) even over rather long distances, i.e. long-range connections. As can be seen in Figure 1.10 Gilbert and Wiesel (1989) had injected locally (filled circle) a retrograde tracer. This tracer was then transported back (i.e. retrograde) to those cells (small dots) which are projecting to the injection site. They then determined orientation domains (here columns of vertical orientation preference marked in dark grey) by injecting 2-deoxyglucose intravenously while simultaneously stimulating with vertical contours. Following, they compared the orientation specificity of the injection site with those of the labeled cells. The clusters of marked cells complied nicely with the orientation specificity of the columns that the injection had been placed in, namely preferring vertical orientation columns.

Lateral connections exist along all cortical axes. However, as could be shown in different animal species, connections are much further reaching among neurons if their cortical axis corresponds to that of the stimulus axis, i.e. the collinear axis (Schmidt et al., 1997a in the cat; Bosking et al., 1997 in the tree shrew; Sincich & Blasdel, 2001 in the monkey). In particular, Schmidt and colleagues determined by autoradiographic procedures a map of orientation preference, in Figure 1.11 exemplarily displaying vertical orientation columns. They had also injected a tracer into a column of neurons with vertical orientation preference which retrogradely labelled those cell bodies that projected to the injection side.

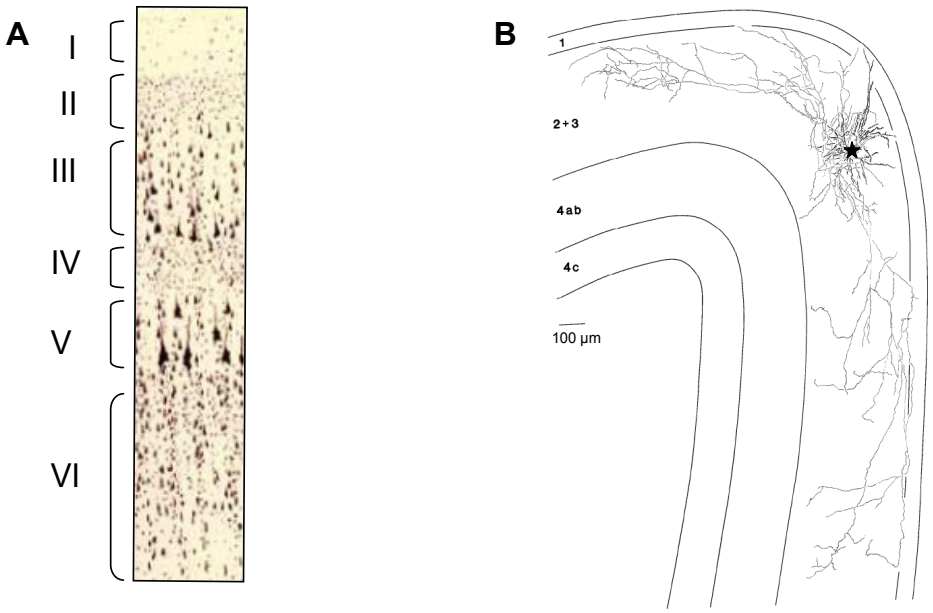

Figure 1.9 | Cells in visual system and their lateral extent.
(A) The coronal cut through the grey matter shows the cellular structure of the visual cortex including different layers I - VI with various types of neurons that are specialized in receiving and sending information. Above layer I lies the pia mater of the brain, and below layer VI joins the white matter consisting of myelinated axon fibers. Graphic modified after http://thebrain.mcgill.ca/
(B) A coronal cut through the first lateral gyrus, here displaying only layer I – IV shows the axon collaterals of a layer II pyramidal cell in cat V1 extending laterally within that same layer. The cell body had been injected (star) with an anterograde tracer that labels the axonal and dendrite branching of the cell to their end projections. (Adapted from Gilbert & Wiesel, 1983)

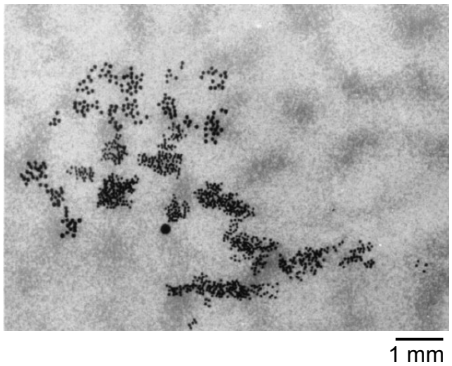

Figure 1.10 | Relationship between clustered distribution of lateral connections and cortical orientation columns in cat V1.
Top view on an approximately 8 x 6 mm region of V1 cortex surface. Dark grey regions scattered over the entire picture indicate vertical orientation columns. A retrograde tracer was injected locally in one of the vertical orientation columns (solid circle). This tracer was then transported back (i.e. retrograde) to those cells (small black dots) that project themselves to the injection site. One can see that these clusters of cells are located on other domains of vertical orientation preference. Adopted from Gilbert & Wiesel (1989, 1990).

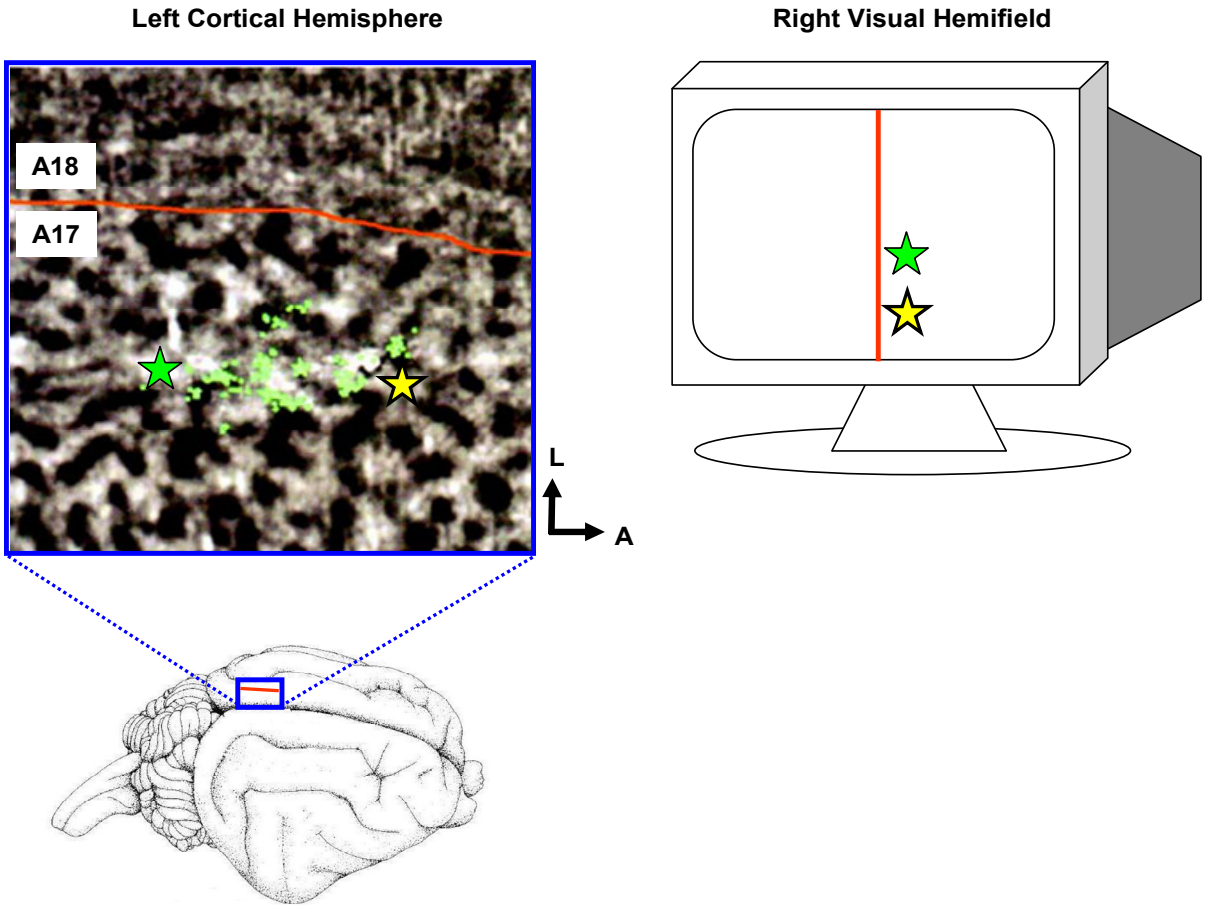

Figure 1.11 | Lateral connections in V1 between neurons of similar orientation preference are elongated along one cortical axis.
Orientation columns in area 17 of cat V1 were 2-deoxyglucose-labeled according to their response to vertical stimulation (dark patches on the cortical image to the left). A tracer was injected into a vertical orientation column that retrogradely labeled cells (small neon-green dots) overlaid with the map of orientation columns. Red line on cortical hemisphere and on stimulation PC graphic indicate the vertical midline. Green and yellow stars are placed in both images to clarify the analogy of labeled cells located in vertical orientation domains which are distributed along a line parallel to the vertical midline representation. The RF of those cells are located in the contralateral visual hemifield.
Graphic modified after Schmidt et al., 1997a.

Then both maps of information were superimposed for conformance. Results revealed a clustering of the labelled neurons (small neon-green dots) precisely in those orientation columns that were of similar orientation preference to the injection site. Furthermore, the distribution of labelling was farther reaching among neurons with aligned receptive fields, i.e. along the vertical axis of the visual field. The directional dependency of this outcome is also termed ‘anisotropy’.

The functional architecture of lateral connections was also studied electrophysiologically, e.g., by cross-correlating the spike responses of distant recording sites (e.g., Ts'o, Gilbert, & Wiesel, 1986; Gray & Singer, 1989; Hata et al., 1991). Ts'o and colleagues (1986) determined the orientation preference of a target cell (as marked with a star in Figure 1.12) and simultaneously recorded from other sites with the same or different orientation specificity. The authors then compared the incidents of simultaneous spikes, i.e. a measure of cortical activity, in a cross-correlogram (see Figure 1.12 far right column) where a center peak indicates a high coincidence. The results support the notion that iso-oriented sites are preferentially linked by lateral connections, even over longer distances.

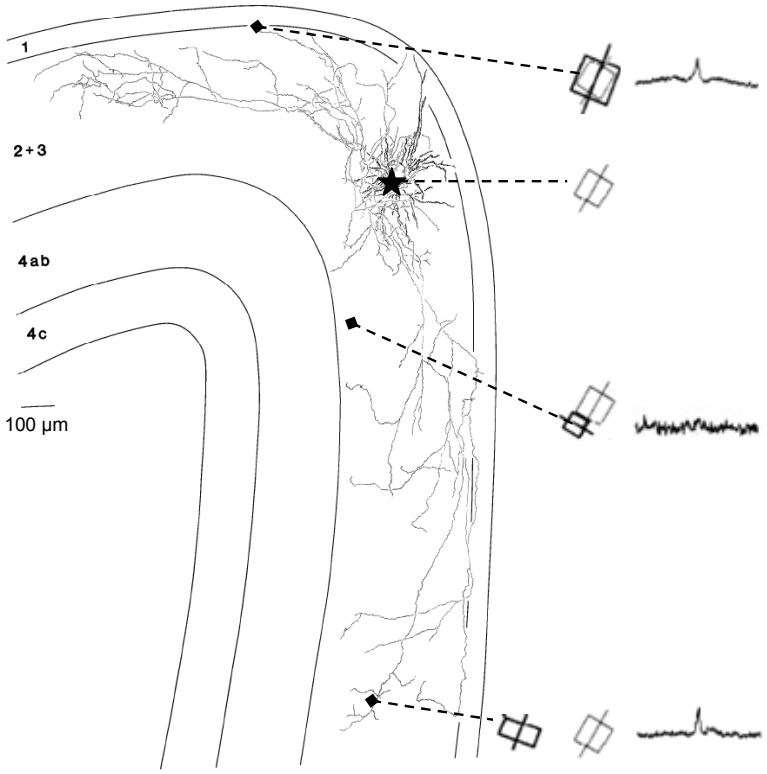

Figure 1.12 | Cross correlation of spikes between cells in V1.
Injection site of the anterograde tracer in to a layer II pyramidal cell is marked with a star. Axon collaterals project to distant sites in the same layer. The receptive field map and orientation preference of this reference cell is marked in light grey to the right. All other recording sites have their relative receptive field position and orientation preference marked in black. The cross correlogram on the far right side indicate the number of coincident spikes from both the reference cell and the respective text cell. A center peak (as in the top and bottom correlogram) indicates synchronous spiking activity, while a flat correlogram (middle one) indicates no joint spiking activity. The results show that recording sites of the same orientation preference, although they might have non-overlapping receptive fields, are linked with each other via lateral connections.
Image was composed after Gilbert & Wiesel, 1983; T'so, Gilbert, & Wiesel, 1986.

In order to study the function of lateral connections in V1, influences of stimulus context surrounding the receptive field of a cell in V1 were tested. This was done experimentally with electrode recordings from neurons in V1 (e.g., Gilbert & Wiesel, 1990; Sillito et al., 1995; Sengpiel et al., 1997; Polat et al., 1998; Mizobe et al., 2001; Akasaki et al., 2002; Chisum et al., 2003) or by imaging the cortical signal with an optical procedure (e.g., Chisum et al., 2003). See chapters 2.3 and 2.4 for a detailed description of these two neurophysiological recording methods.

In these studies different kinds of contextual stimuli were used, for example single bars, rectangular or circular gratings, or Gabor patches (two-dimensional sinusoidal luminance grating carrier weighted by a circular Gaussian envelope), see also Figure 1.13 A - E for illustration. In varying the stimulus properties such as size, relative orientation or contrast, results revealed facilitative or suppressive surround influences, supporting the understanding that neurons are influenced from outside their classical receptive field. In particular, Polat et al. (1998) described on the basis of their sample of recorded neurons in cat V1 (N = 83) that the facilitative effect of collinearly aligned surrounding flankers (Figure 2.13 D) was diminished as the contrast of the cell's RF stimulus element increased over a certain threshold. This change in effect due to contrast leveling was seen in 34% of their sample neurons, compared to 33% that only showed facilitation all along, as well as 19% with suppression effects alone, and 14% with no modulating effects. Interestingly, both facilitation and suppression from the surround onto RF activity is seen in the same neuron when changing stimulus parameters, e.g. stimulus contrast. On the other hand, when keeping stimulus parameters the same, both facilitation and suppression are seen in activity of different neurons across the sample. This indicates that there is no general effect of collinear surround influences on neurons in V1, instead both instances, facilitation and suppression are likely to be found. A later study tested for specific factors that might determine the variable effect across cells in V1 (Mizobe et al., 2001). However, they did not find any indicator such as cell type (simple vs. complex cells) nor cell location in any of the six laminar layers to explain the variability of surround effects.

A much more consistent result on collinear facilitation was reported in a study of the tree shrew primary visual cortex by Chisum and colleagues (2003). In electrophysiology recordings from 25 animals they gathered a sample of all together 35 cells and placed a single Gabor stimulus successively in each respective RF. Each

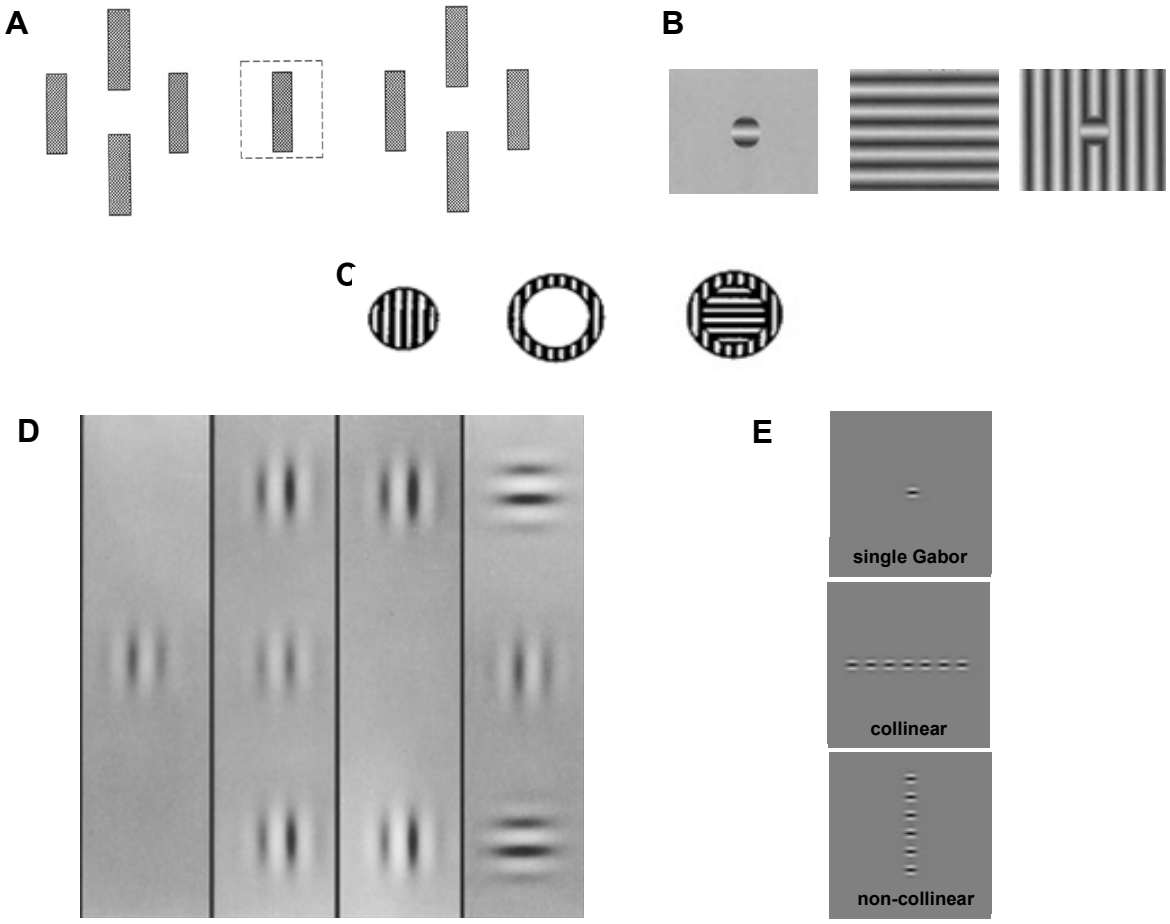

Figure 1.13 | Stimulus examples for studying influences from the cell's RF surround with extra-cellular recording in cat primary visual cortex.
(**A)** Effects of surround lines presented outside of a cell's receptive field (dotted line) varied from cell to cell: some were facilitated and some were suppressed by either configuration of alignment, i.e. end-to-end or side-to-side, (Gilbert & Wiesel, 1990).
(B) RF of a cell is indicated by the circle itself (first image). A uniform receptive field surround (middle image) predominantly suppressed cellular response, while a surround of orthogonal orientation (far right image) facilitated cellular response in some of the cells (Akasaki et al., 2002).
(C) The patch (first image, placed right on the cell's RF) at optimal orientation elicits a cell's response while the annulus (second image) yielded no response. Inner patch at orthogonal to optimal orientation and cross-oriented annulus (third image) yields strongest response (Sillito et al., 1995).
(D) A neuron's response to an optimally oriented but low contrast RF stimulus (first column) is enhanced when iso-oriented flankers are placed along the collinear axis (2nd column). There is no response to the flankers alone (3rd column) and diminished activity to orthogonally oriented flankers (4th column) along the collinear axis (Polat et al., 1998; Mizobe et al., 2001).
(E) For all cells (N = 35) recorded in V1 of tree shrews spiking activity was enhanced when RF stimulation with single Gabor (top) was surrounded by collinear elements (middle) but inconsistently diminished or even reversed in the presence of non-collinear stimulus surround. Results from optical imaging could confirm this finding in most of cases of the experiments (N = 9), (Chisum, Mooser, & Fitzpatrick, 2003).

cell was stimulated with its preferred orientation and the contextual surround was varied from collinear or non-collinear aligned Gabor elements or none. They reported that all of their sample cells showed a facilitation effect to the collinear surround and a diminished or suppressed response to non-collinear surround. They also applied an optical recording technique in 9 additional animals to reveal a pattern of cortical activity in response to the different stimulus conditions. In the recorded images they couldn't find any bias of elongated cortical activity evoked by either stimulus condition. Further they compared the differences in signal magnitude elicited by either stimulus condition which all had the single Gabor location in common. They analyzed the number and level of active pixels in the optical images separately for all nine experiments. For most of the experiements they observed greater activity for the collinear condition than for the non-collinear. However, their data only revealed significance when pooling data from all nine experiments gathered each over three experimental sessions with different inter-stimulus distances.

Mizobe et al. (2001) attempted to unify the findings from the different experiments as depicted in Figure 1.14. The image displays a cortical model of the spatial organization of facilitative and suppressive modulatory fields around the classical RF of a cell in V1. According to their model a suppressive surround field exists all around the RF while the facilitating surround is only located along the collinear axis of the cell's preferred orientation. This option of a suppressive *or* facilitative influence along the collinear axis might explain the different findings reported in the above studies.

The question arises what criteria might determine the kind of surround influence on classical RF responses. Cells in V1 carry an excitatory or inhibitory function depending on the cell type and what neurotransmitter they use to pass on information to the next cell. This functional anatomy was mainly accessed by pharmacological studies (e.g., Crook & Eysel, 1992; Girardin & Martin, 2009) or histological reconstructions of cells in V1 (Buhl & Singer, 1989; Kisvarday et al., 1997). Results revealed that the distribution of both functional cell types is about 3:1 in favor of excitatory neurons (Kisvarday et al., 1997). Direct application of GABA as an inhibitory neurotransmitter (e.g., Crook & Eysel, 1992) to the cortical region of interest it deactivates the inhibitory system in a broad surround. This makes it hard to study specific effects of surround influences for example only for the collinear stimulus axis. Further, pharmacological manipulations to study excitatory intra-cortical connectivity are difficult to interpret as they interfere strongly with the overall cortical activity itself. It

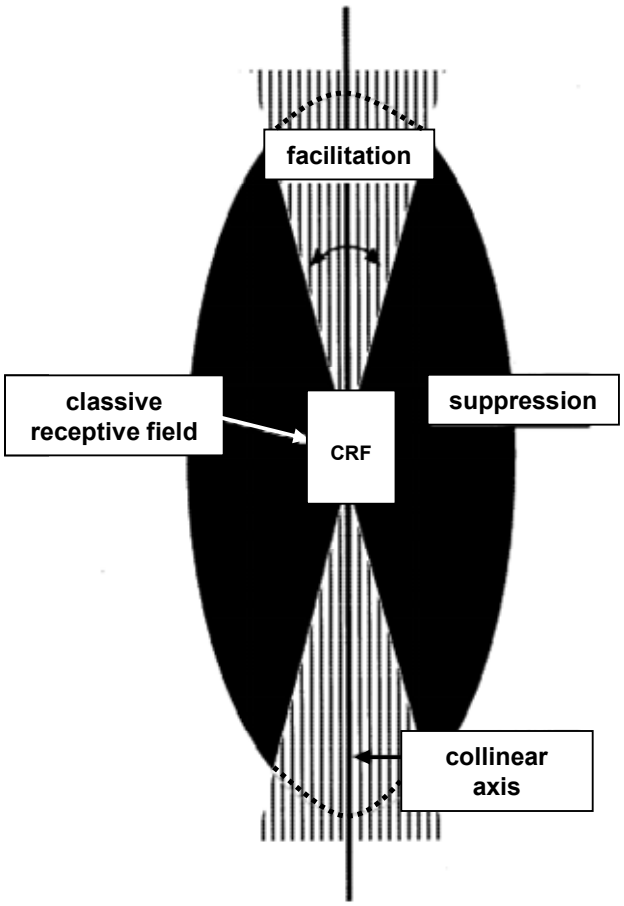

Figure 1.14 | A cortical model of the spatial organization of facilitative and suppressive modulatory fields around the classical RF of a cell in V1.
A suppressive modulating field surrounds the classical receptive field (CRF). Note the curve 'behind' the striped areas indicating a continuation of the black area all around. A facilitative modulating field is spanned along the optimal orientation axis of the receptive field (e.g. here vertical). Thus, by placing stimuli of the same local orientation along the collinear axis of optimally stimulated CRF, can lead to an facilitation of the cell's activity (or suppression for that matter). The suppressive modulatory field is reported to be distributed more diffusely and less selective for orientation. Thus, flanking stimuli on the orthogonal axis of the cell's optimal orientation modulates its response by suppression.
Graphic adopted from Mizobe et al. (2001).

can be concluded that by presenting different contextual stimuli and thus vary the kind of information available on either modulation axis of a cell's receptive field is a fair and common approach to study the function of lateral connections. However, it should be noted that the surround stimulus configurations like in Figure 1.13 B and C may provide a misleading view. In these cases surround stimulus content is present in all neighboring regions, on the collinear axis AND on the non-collinear axis. In fact, for studying collinear and non-collinear influences, stimulus configurations should be reduced to either axis for one stimulus condition, and then cortical activity compared over the different stimulus conditions.

Interestingly though, lateral connections intrinsic to the primary visual cortex share some of their characteristics with other connections within the visual system: callosal connections which bond together the visual information across the two hemispheres (Payne, 1994). They are much easier accessible to manipulation than intrinsic connections. Basic anatomical findings and physiological experiments thereon will be described in the following section.

1.4.4 Visual Callosal Connections

In the visual system of higher mammals, the left and right visual fields are represented in the respective contralateral hemisphere of the cortex. In this respect it is striking that our view of the visual world appears uniform without any noticeable interruption. The two hemispheres are connected via the corpus callosum, a bundle of axons spanning in between. Several anatomical and functional properties of callosal connections have been investigated in the cat primary visual cortex. For example, the cell type that is mainly involved in callosal sending is the pyramidal cell, and only about 5% are non-pyramidal (e.g., Buhl & Singer, 1992; Peters et al., 1990; refer to a later Figure 1.16 A). Physiological evidence suggests that pyramidal cells carry an excitatory function. On the other hand, neurons receiving callosal input from the respective contralateral hemisphere are both pyramidal (excitatory) and non-pyramidal (inhibitory) cell types. It has therefore been suggested, that depending on what cell type the callosal connections project to they either enhance excitatory or inhibitory neuronal activity in the contralateral hemisphere (Payne, Siwek, & Lomber, 1991). This functional attribute of callosal connections had already been demonstrated in studies that temporally deactivated the callosal sending zone in one hemisphere by cooling while simultaneously recording the activities of neurons in the callosal recipient zone in the other hemisphere (Choudhury et al., 1965; Blakemore et al., 1983; Payne, Siwek, & Lomber, 1991; Payne, 1994). The results revealed either an increase or decrease of visually driven activity in the sample of recording neurons.

Anatomical studies indicate that in the cat visual cortex the neurons of origin and termination of callosal connections are restricted to the border between area 17 and area 18 and that the vertical meridian of the visual field is represented thereon (e.g., Hubel & Wiesel, 1967). Figure 1.15 A visualizes in a coronal view the regions of neurons in the callosal sending (left) and callosal receiving (right) zones, both centered around the 17/18 border. Thus, the visual area close to the vertical meridian is

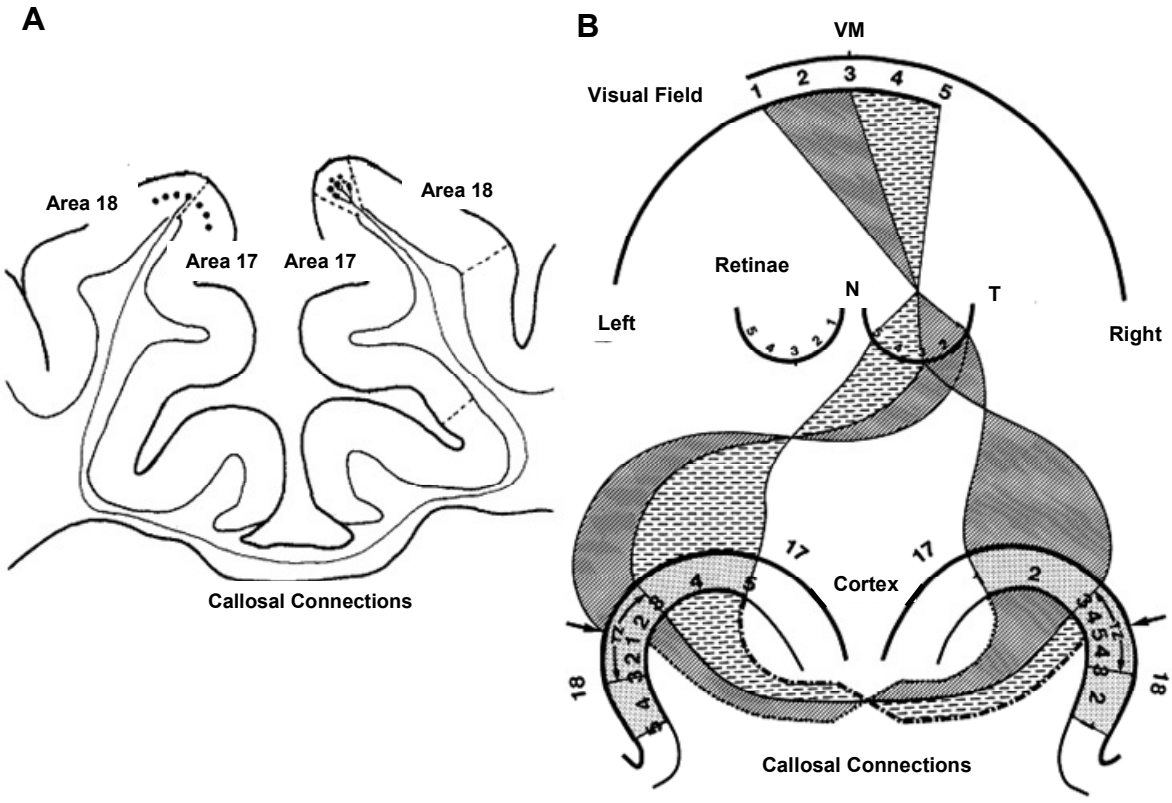

Figure 1.15 | Diagrams of callosal connections organization in cat primary visual cortex.
(A) The coronal view of the cat primary visual cortex shows the two hemispheres (left and right) connected by the callosal connections. The callosal sending zone (black circles left side) and the receipient zone of callosal neurons (small dots right side) are each centered on the respective border between area 17 and area 18. Image modified after Payne (1994).
(B) The sketch shows where information from the visual field is represented in either half of the primary visual cortex. For example, the numbers 3, 4, 5 in the right visual field are represented on the contralateral hemisphere in both area 17 and area 18 in a mirrored way. From there this '3,4,5' information is passed on via callosal connections to the transition zone (TZ) on the other hemisphere where it then represents the ipsilateral part of the visual field. This passing on of visual information via the corpus callosum is reciprocal and coextensive, it is linking cortical sites that are of retinotopic rather than anatomical correspondence. Image modified after Olavarria (2001).

not only represented in the contralateral hemisphere but also sent via callosal neurons over to the other hemisphere where it is transformed into an ipsilateral representation (Payne & Siwek, 1991). This concept of ipsi- and contralateral representation of the visual field in either hemisphere is illustrated in more details in Figure 1.15 B. Nevertheless, the functional organization of neurons involved in transcallosal

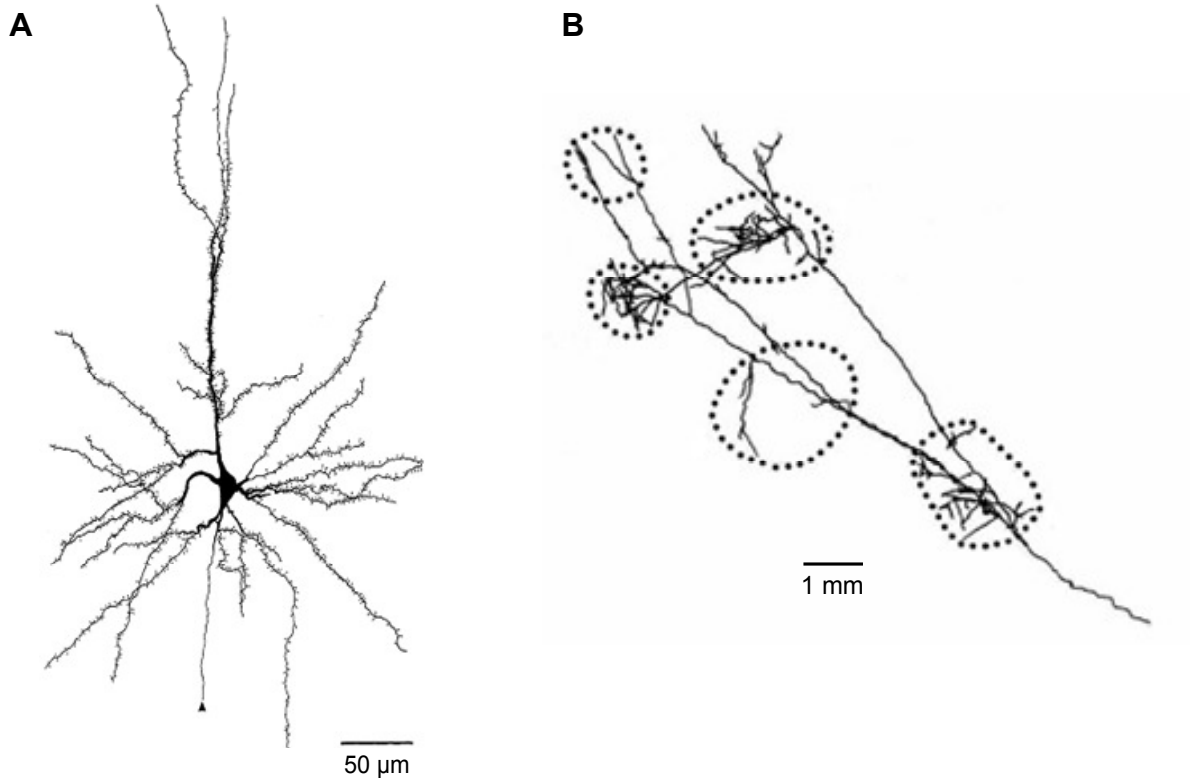

Figure 1.16 | Camera Lucida drawing of a callosal pyramidel cell (A) and computer-aided 3-D reconstruction of callosal axon arbors (B).
(A) The pyramidal cell has a characteristic triangular shaped cell body, an apical dendrite (towards the top), a single axon (towards the bottom, marked with a small arrowhead), and numerous basal dendrites with spikes. Image taken from Buhl & Singer (1989).
(B) As a callosal axon (here coming in from the right of the picture) projects to the opposite hemisphere it spreads into an arbor of axon collaterals which terminate in numerous clusters (encircled by dots). Image taken from Houzel, Milleret, & Innocenti (1994).

projections is still under debate. Houzel, Milleret, and Innocenti (1994) applied a tracer to visualize and reconstruct callosal axons and they found the axon terminals clustered in columns of about 300 – 600 µm diameter each with areas free of axon terminals in between (Figure 1.16 B). Consequently, several authors attempted to relate this finding to other functional organizations known in the cat primary visual cortex. For example, Olavarria (2001) reported to have found callosal axon terminals to occur primarily in the contralateral eye domains (Figure 1.17 A). Further, Schmidt et al. (1997a) and a recent study by Rochefort et al. (in press) showed that callosal axons connect columns of neurons with similar orientation preference (Figure 1.17 B). In addition, they could show that the distribution of callosal axon boutons was even elongated anisotropically along the corresponding retinotopic axis (here the vertical

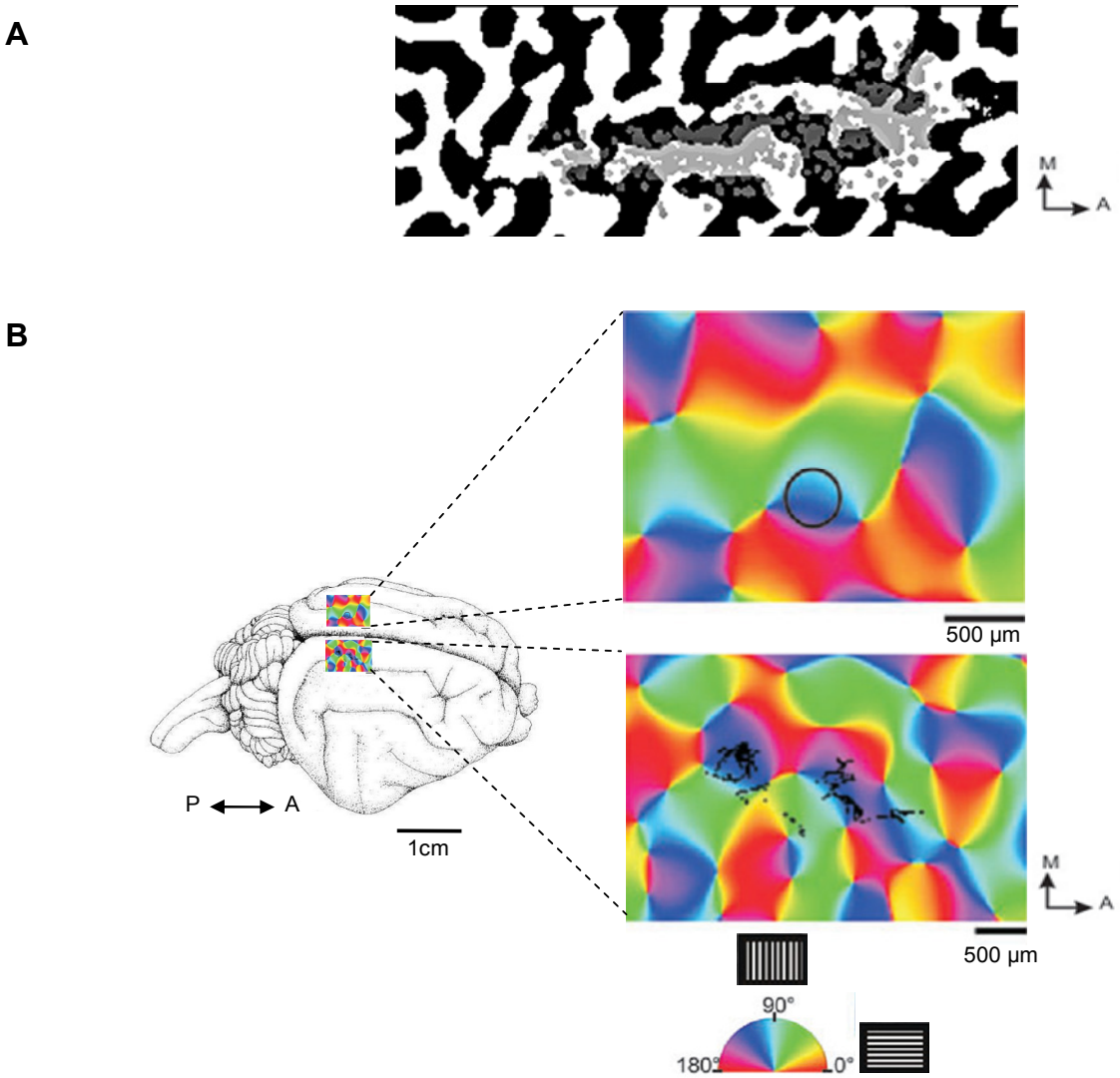

Figure 1.17 | Relating callosal axon terminals to underlying functional properties in the cat primary visual cortex.
(A) The pattern of axon terminals of visual callosal connections (light grey dots) was superimposed with the layout structure of ocular dominance columns (white areas for contralateral eye, black areas for ipsilateral eye). Callosal terminals are preferably located in ocular dominance columns of the contralateral eye. Image modified after Olavarria (2001).
(B) The drawing of cat cortex (taken from Tusa et al., 1978) indicates the location of where the two images were taken from. The top map demonstrates the side of tracer injection into V1 of the left hemisphere (circle). Colors in the map denote domains of neurons with particular orientation preference. The reference color scale is shown down below. The lower map shows the axon terminals (small black dots) in relation to the orientation preference domains in V1 of the right hemisphere. Results indicate a consistency in orientation attribution of both injection side (top) and axon terminals (bottom). Further, the distribution of the later is elongated along the retinotopic axis of their orientation preference (here vertical, thus from posterior (P) to anterior (A)). Images modified after Rochefort (in press).

axis in Figure 1.17 B). As ocular dominance columns and orientation columns are known to be spatially related these two findings do not contradict each other.

In summary, callosal axons display a highly specific organization in the visual areas 17 and 18 by linking topographically corresponding cortical regions across the two hemispheres (visuotopic organization). They connect cortical regions across the two hemispheres that have the same orientation preference and link ocular dominance columns serving the same eye. It has been suggested that callosal connections fulfill similar functions across the midline as intrinsic lateral connections within one hemisphere and that they serve to unify the visual percept distributed in two hemispheres (Hubel & Wiesel, 1967; Payne, 1994; Innocenti et al., 1986; Kennedy et al., 1991).

It is to be assumed that the cortical representation of visual stimuli crossing the vertical midline depends on the interaction of both hemispheres via callosal connections. The cortical representation of collinear and non-collinear contextual stimuli which continue from one into the other visual hemifield ought to be studied in this regard. Because of their exposed anatomy, interhemispheric connections are easier to access than intrinsic connections, e.g. by cutting the corpus callosum or by cooling the contralateral hemisphere (Choudhury et al., 1964; Blakemore et al., 1983; Payne, Siwek, & Lomber, 1991; Carmelli et al., 2007; Makarov et al., 2008). Given their functional similarities to lateral connections within one hemisphere it might be reasonable to draw conclusions on the function of both by studying the interhemispheric pathway.

1.5 Summary of Research Hypotheses

The work described in this thesis aimed to increase our understanding in how far the primary visual cortex reflects the perceptual advantage of a collinear over a non-collinear line, as the Gestalt law of collinearity proposes. In order to address this question two common methods in systems neurophysiology, i.e. extra-cellular recording and intrinsic optical imaging, were applied to gather information on the neuronal activity in the cat primary visual cortex, while visually stimulating with collinear vs. non-collinear context. Further, by temporarily deactivating half of the primary visual cortex by cooling we addressed the question of what role callosal connections play in forming one coherent image of the visual field, in particular in the context of collinearity.

Based on anatomical and functional properties described in the cat primary visual cortex so far, it is hypothesized that neuronal activity therein varies as visual stimuli of collinear vs. non-collinear context are presented. As both directions of effects have been reported in V1 neurons, i.e. facilitation and suppression by collinear surround (e.g., Polat et al., 1998) the direction of effect is not specified in this study's proposition. An explorative approach of how cortical activity depends on stimulus context was chosen.

Further, it is hypothesized that by temporarily deactivating V1 activity in one hemisphere by cooling the representation of contextual lines crossing the vertical midline (when recorded on the contralateral side) will be affected. Assuming that neuronal activity is influenced across the two hemispheres via callosal connections especially from and along their collinear axis of preferred orientation (Rochefort, in press), it is proposed that neuronal activity on collinear stimuli is more affected than to non-collinear stimuli.

2 MATERIALS AND METHODS

Scientific discovery and scientific knowledge have been achieved only by those who have gone in pursuit of it without any practical purpose whatsoever in view.

- Max Planck, Where is science going?, 1932 -

This section will describe the experimental procedures of recording cortical activity from the cat visual cortex and the experimental design developed for this study. First, it will be explained what animals were used for the studies and how surgery procedures were carried out. Second, the independent variables of this study will be introduced, i.e. what variations in the experimental settings were chosen to study their effect on cortical activity. Third, the two neurophysiological recording methods will be introduced successively. The recorded signals derived from each method will serve as the dependent variables. Finally, a demonstration of post-experimental histology work will be provided for a descriptive and demonstrative purpose. This chapter will conclude in a summary of this study's experimental design to address the proposed research hypotheses.

2.1 Animals & Surgery

Eight adult cats aged 12 to 48 months from the cat colony of the Max Planck Institute for Brain Research in Frankfurt were used as experimental animals for this study. These animals were part of other research projects involving the same methods and similar stimuli. Experiments were carried out one at a time for about five days each (night and day). All surgeries in the experiments were carried out by colleagues holding a legal authorization for animal experiments at the Max Planck Institute for Brain Research. All procedures were in accordance with the German legislation on animal care, approved by the ethical committee of the local authorities and in agreement with the global guidelines for animal research of the Society for Neuroscience.

For this research project data were analyzed from three animals tested with an electrophysiological method only, two animals tested with intrinsic optical imaging method only, and three animals tested with both, electrophysiology and intrinsic opti-

cal imaging methods successively. Both recording methods will be described in later sections of this chapter.

On the first day of the experiment, the cat was initially anesthetized intramuscularly with 10mg/kg bodyweight ketaminhydrochloride (Ketamin® 10%) and 1mg/kg xylazinhydrochloride (Rompun® 2%). The animal underwent tracheotomy and was then artificially ventilated via a tracheostoma. The anesthesia was maintained with a mixture of either halothane (~0.6%) or isoflurane (~1%) and N_2O (~70%) and O_2 (~30%) over a period of about five days. The values correspond to percentage of total air volume. Table 2.1 provides an overview of experimental methods, age of the animals and anesthesia used. Note that despite the different anesthesia used in this study, there is no methodological relevance for this study.

General life support was provided to the animals around the clock throughout the experiment. This included artificial ventilation by a respiration pump and constant monitoring of exhaled CO_2 (3%) and breathing pressure. The body temperature was kept constant at 37.5°C with a heating pad and controlled by a rectal thermometer.

Every couple of hours the animals received intravenous (i.v.) injections of glucose (10%) and Tutofusin® K 10 (Baxter, Germany) to compensate for loss of electrolytes and fluids. The animals' bladder was emptied manually every couple of hours. To prevent eye movements the animals were paralyzed by continuous administration (0.3 mg/h) of the muscle relaxant Pancuroniumbromide (CuraMED Pharma GmbH, Germany). The pupils were dilated with drops of atropinsulfate (1%, Atropin®, Ciba Vision, Germany).

Atropinsulfate was also given i.v. every twelve hours for prevention of circulatory disturbances and reducing secretion in bronchi and in the respiratory tract. To stabilize the respiratory tract and prevent swelling of tissue a daily dosage of 1mg Dexamethason-21-isonicotinat (Voren®, Boehringer Ingelheim, Germany) was given to the animal. Post-experimentally, the animal was put to death with a lethal intravenous injection of 200mg/kg pentobarbital sodium (Narcoren®, Merial, Germany).

Table 2.1 | Overview of Experimental Methods, Animal Characteristics, and Anesthesia Used (OI = Optical Imaging; Ephys = Electrophysiology).

Recording method	Experimental code	Animal gender	Animal age	Anesthesia during recording
Ephys	121107	female	3 years	isoflurane
Ephys	021808	male	3 years	isoflurane
Ephys	040308	male	1 year	halothane
Intrinsic OI	091608	female	2 years	halothane
Intrinsic OI	100608	female	2 years	halothane
Intrinsic OI / Ephys	011009	female	2 years	halothane
Intrinsic OI / Ephys	021609	female	2 years	halothane
Intrinsic OI / Ephys	033009	female	2 years	halothane

Note that for all experiments recording of cortical activity was on the left hemisphere except for experiment 021808 (right hemisphere).

The nictitating membranes, that is a duplication of the conjunctiva additionally covering the eye in some animal species such as the cat, were retracted with phenylephrinhydrochloride (Neosynephrin-POS®, Ursapharma, Germany). With a refractometer one could then determine the refractive condition of the animal's eyes. Black contact lenses of the correcting value with an artificial pupil of about 3mm were inserted in both eyes.

Both recording methods in this study, electrophysiology and intrinsic imaging (refer to the next section for a more detailed technical description), require the opening of the animals' skull. After tracheotomy the head of the animal is fixated in a stereotactic frame in order to position the openings over the border of area 17 and area 18. According to the American Heritage Medical Dictionary 'stereotaxy is a medical surgical technique that allows to precisely locate an anatomical site in a three-dimensional system'. The primary visual cortex of the cat is located around zero of the anterior-posterior (AP) coordinate axis to both sides of the central commisure (Horsley & Clarke, 1908). Figure 2.1 A shows a skull model of the cat, indicating in shaded gray the portion of the cat's skull that was removed by craniotomy. Figure 2.1 B shows for a graphic of the cat cortex – corresponding in size to Figure 2.1 A – indicating the cortical area visible after removing the bone material. The two openings gauged an area of less than half a square centimeter each. A bridge of bone was left between the two openings, both for stabilization of the recording setup and to keep the dura-bone adhesion above the interhemispheric cleft intact as thermal isolation.

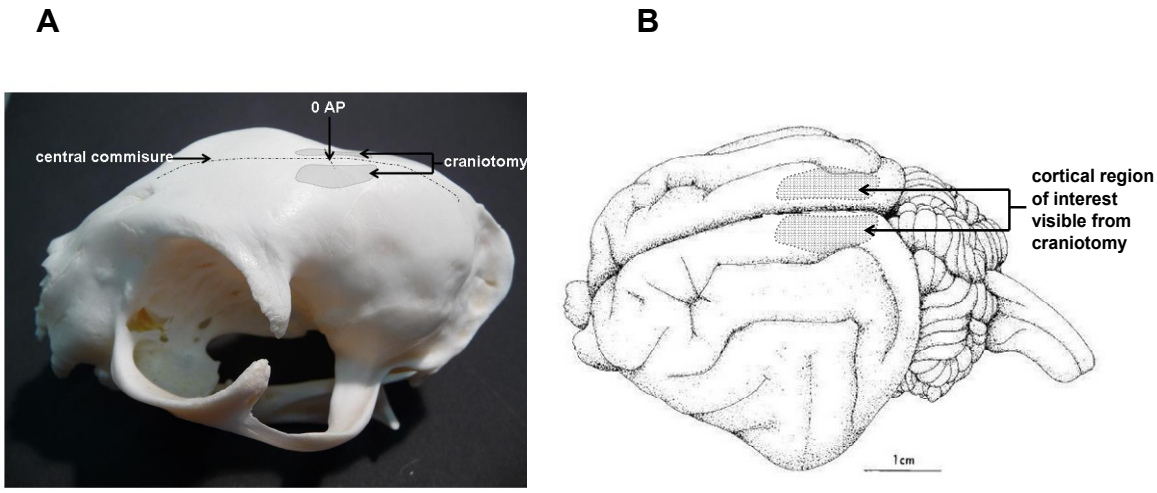

Figure 2.1 | Anatomical coordinates for experiments in the cat primary visual cortex.
(A) Photographed cat skull with indication of central commisure, zero anterior-posterior (0 AP) coordinate after Horsley & Clarke (1908), and outlined craniotomy location over V1 of both hemispheres. **(B)** Graphical display of cat cortex with the areas that are accessible after craniotomy here shaded in gray, separated in between by the medial bank and to either side by the first lateral gyrus. (Modified after Tusa et al., 1978).

The dura mater, a fibrous membrane covering the brain and lining to the inner surface of the skull, was opened above the exposed area for both hemispheres. For optical imaging experiments a custom-made stainless steel chamber of 1.5 mm inner diameter was glued onto the bone surrounding the opening of the recording hemisphere (Figure 2.2 A). The chamber was fixed onto the skull with dental acrylic (Paladur®, Heraeus Kulzer GmbH, Germany) and sealed from inside with bone wax. The chamber was then filled with silicone oil (DS Fluid, Boss Products, USA), and sealed with a round cover glass. For electrophysiology experiments, instead of a recording chamber a small wall of dental acrylic was drawn up around the skull openings and, after insertion of the electrodes, dilled with agarose. In three of the experiments both of the recording methods were applied successively. For these cases the electrodes had to be placed within the frame of the opened imaging chamber. Further, in all experiments a metal cryoloop (see Figure 2.2 B on the left, but for more detailed technical description and usage see section '2.2 Independent Variables') of approximately 10mm x 4mm diameter was placed in the craniotomy on the other hemisphere. We aimed to position the probe specifically on the area topographically corresponding to the contralaterally exposed area visible in the recording chamber.

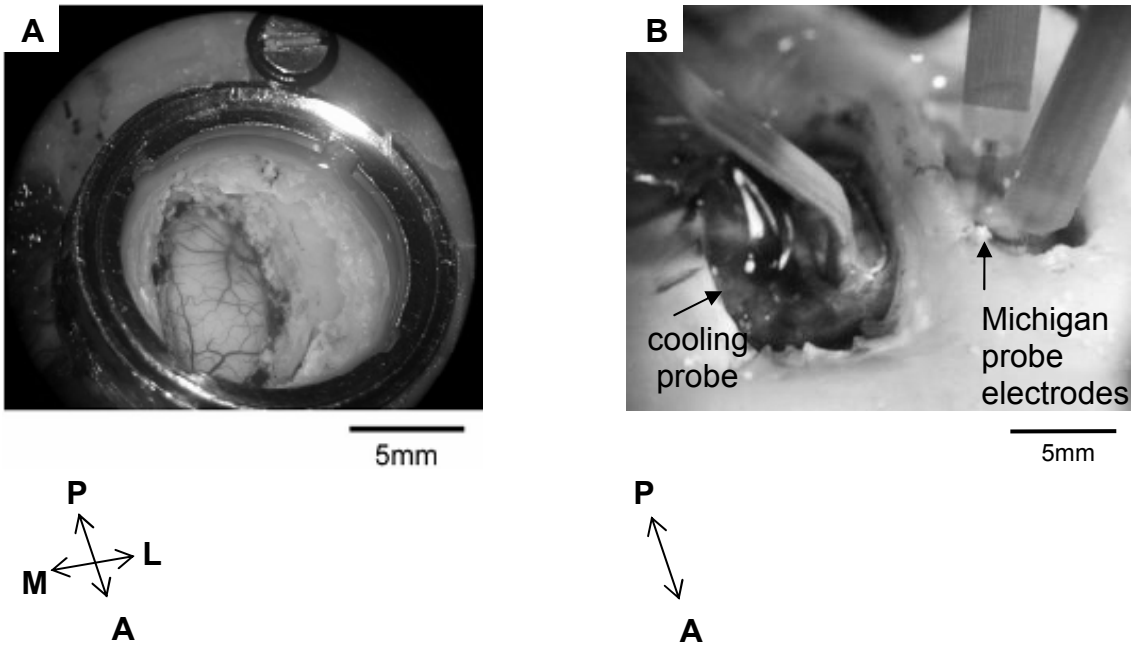

Figure 2.2 | Experimental recording setup.
(A) Photograph of a metallic chamber set up over the first gyrus of the left hemisphere. **(B)** Photograph of an electrophysiology experimental setup with two Michigan probe electrodes inserted into the first V1 gyrus of the left hemisphere, and a cooling probe placed onto the surface of the first V1 gyrus of the right hemisphere. P-Posterior, A-Anterior, M-Medial, L-Laterals.

2.2 Independent Variables

Two independent variables (IVs) were defined to address the two research questions of this study. The first question was whether neuronal activity in the primary visual cortex already reflects the perceptual advantage of a collinear line over a non-collinear line of oriented elements, as the Gestalt law of collinearity proposes. This question was investigated by varying the stimulus conditions (IV1) to either form a figure obeying collinearity or not and by measuring the cortical activity under each condition. The second research question was what role the intact connection between the cortices in both hemispheres plays in reflecting the advantage of a collinear over a non-collinear line of elements. This question was tested by thermally deactivating (IV2) the primary visual area on the contralateral hemisphere (as opposed to the ipsilateral hemisphere where the recordings were made).

The following sections will describe the two IVs of visual stimulus conditions, and thermal deactivation in more detail.

2.2.1 Visual Stimulus Conditions

Visual stimuli for this research project were a number of locally oriented elements aligned to either form a collinear line or a non-collinear line. The elements were cosine gratings weighted with a Gaussian function, a so called Gabor. The Gabor transformation – named after the Hungarian physicist Dennis Gábor – is a special Fourier transformation (see Figure 2.3). Using a Gabor instead of a regular grating for visual stimulation holds a certain advantage. A regular cosine function of finite size consists of multiple local frequencies. The conversion of the signal into a Gabor function removes all local frequency information. They are void of sharp contours and are thus ideally suited to stimulate a RF locally without confounding border artifacts and Fourier components. Further, also psychophysically they turned out to be the most effect stimuli in tasks involving precise spatial localization (e.g., Field et al., 1993; Westheimer, 1998).

The diameter of each Gabor patch was five degrees of visual angle. At 57 cm viewing distance between animal and stimulation monitor one degree of visual angle corresponded to one centimeter on the monitor. The spatial frequency of each Gabor patch was chosen to be 0.5 c/° (cycles per degree of visual angle). This spatial characteristic describes simply how much of a black-white cycle of the Gabor fit in one degree of visual angle. The Gabor pattern was chosen to cycle at a temporal frequency of 4 °/s (degrees per second). Moving stimuli crossing the RF are known to elicit a more pronounced cortical response (e.g., Müller et al., 2001; Albrecht et al., 2002).

The direction of Gabor cycling is always orthogonal to its orientation, i.e. for a horizontal Gabor the black and white bar appear to sweep up or down within the given Gabor location; for a vertical Gabor element (as in the example in Figure 2.3) the sweeping direction appears to the right or the left within the given Gabor location. The combination of spatial and temporal frequency results in a velocity of 2 Hz (0,5 c/° x 4 °/s = 2 Hz). The spatial and temporal frequency of the Gabor elements were chosen to match the response properties of neurons in the primary visual cortex (e.g. Movshon, Thompson, & Tolhurst, 1978). Note that neurons in both area 17 and area 18 differ in their preferences for spatial and temporal stimulus properties. Neurons in A17 of the primary visual cortex preferably respond to stimuli of high spatial and low temporal frequency, i.e. 0,5 cycles per degree and 4 degrees per second, and neurons in A18 preferably responding to stimuli of low spatial and high temporal

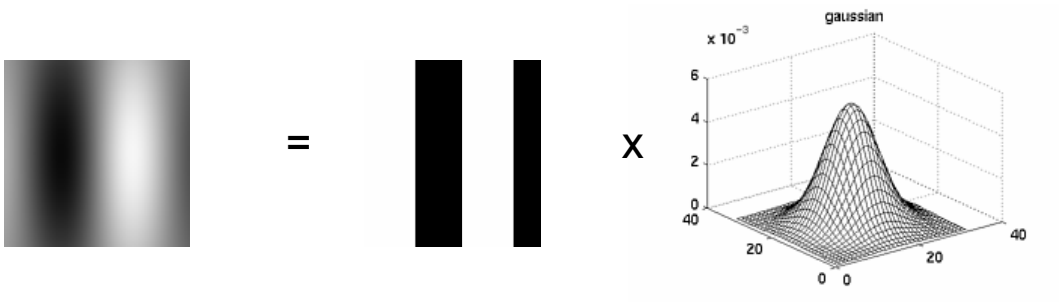

Figure 2.3 | Schematics of the physical properties of a Gabor patch.
A regular square wave grating is weighted with a three-dimensional Gausian function. The resulting Gabor function is free of any local frequency information.

frequency, i.e. 0,15 cycles per degree and 16 degrees per second. Nevertheless, when choosing stimulus properties which are best for A18 stimulation, they will also elicit activation in A17, but not the other way round. This results from the fact that in cat cortex, A17 receives neuronal input from both y- retinal cells that have large receptive fields and x-retinal cells that have small receptive fields, while on the other hand A18 receives input only from y-retinal cells.

It was decided to use only stimuli of 100% contrast because they evoke the strongest neuronal population response in primary visual cortex (e.g., Albrecht et al., 2002). Nevertheless, there seems to be some critical remarks on using high contrast stimuli for RF stimulation. Researchers (e.g., Polat et al., 1998) have reported that a desired contextual effect on RF stimulation is most prominent when the receptive field stimulation is at lower contrast than the flankers surrounding it. Nevertheless, it has not been reported that using full contrast stimulation would abolish the effect. Stimulus protocols used for both recording methods will be presented successively in the following.

Stimuli for Electrophysiology Recording

The stimuli were programmed in Labview (Laboratory Virtual Instrumentation Engineering Workbench).

The stimulus protocol for electrophysiology recordings contained six stimulus conditions. For each of the two local orientations, horizontal (Figure 2.4 A+B+C) and vertical (Figure 2.4 D+E+F), there was a Single Gabor condition, a collinear line con-

dition, and a non-collinear line condition. The two single Gabor conditions (Figure 2.4 A+D) were by themselves not considered to form any Gestalt figure, but rather served as a stimulus control for RF stimulation only. The two lines of collinearly aligned Gabor elements (Figure 2.4 B+E) and the two lines of non-collinearly aligned Gabor elements (Figure 2.4 C+F) were considered to form a line figure. A set of Gabor elements was considered collinear if their local orientation corresponded to their global axis of alignment. A group of Gabor elements were considered non-collinear if they were arranged along the global axis orthogonal to their local orientation, i.e. side-by-side. All line stimuli had the local position of the Single Gabor condition in common, i.e. the center Gabor. As described in Gestalt Psychology a set of collinearly arranged elements are considered a 'better' Gestalt (Wertheimer, 1923). A set of non-collinearly arranged elements also forms the percept of a line, but it has been described to be recognized much more slowly in psychophysics experiments (e.g., Polat & Sagi, 1994) and elicit diminished spiking activity in some of the recorded cells in V1 (Polat et al., 1998).

The program for constructing the aligned Gabor elements was based on a grid pattern with numerous squares to fill in the stimulus elements. This only allowed local elements of horizontal or vertical orientation to be aligned with the same inter-element distance. If elements of local oblique orientation had been used for stimulus construction their inter-element distance along an oblique axis would have been much larger than for the vertical and horizontal versions (due to Pythagoras rule). Thus, only stimulus elements of locally vertical or horizontal orientation were constructed and used for stimulation in electrophysiology experiments.

Interestingly, a predominance of cells preferring stripes of cardinal orientations in the central visual field has been described for both cats (Pettigrew et al., 1968; Orban & Kennedy, 1981; Payne & Berman, 1983) and macaque monkeys (Mansfield, 1974). This is also in accordance with the well described psychophysical "cardinal effect" – that there is a higher visual acuity for cardinal contours than for oblique contours.

In fact, prior to the electrophysiology experiments two different sets of six stimulus conditions had been prepared. The two sets differed in the cycling direction for the Gabor elements, i.e. the first set was the combination of all horizontal Gabors cycling upwards and all vertical Gabors cycling rightwards, and the second set was the combination of all horizontal Gabors cycling downwards and all vertical Gabors

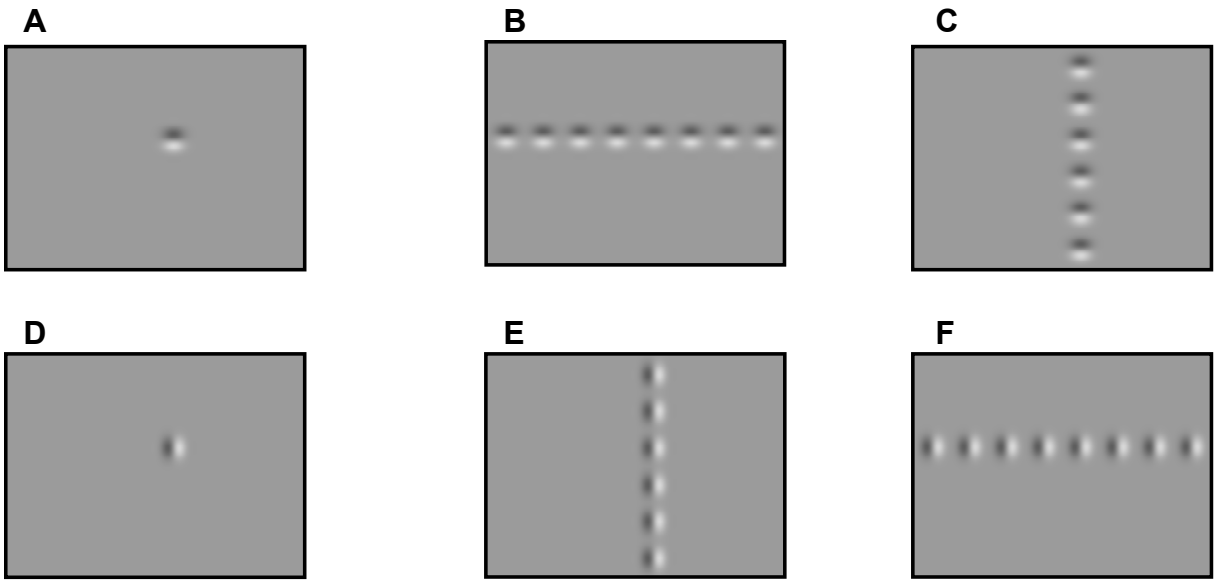

Figure 2.4 | Gabor stimuli used in electrophysiology experiments.
Stimulus conditions are either a single Gabor (A+D), collinearly aligned Gabors (B+E), or non-collinearly aligned Gabors (C+F). A group of Gabors is considered collinear if their local orientation corresponds to their global axis of alignment, and considered as non-collinear when the local orientation and the global arrangement are orthogonal to each other. The local orientation of the Gabor elements was either horizontal (A+B+C) or vertical (D+E+F).
The characteristics of a Gabor patch are defined as follows. Each patch is of 5° visual angle in diameter (1° = 1cm). The spatial frequency is 0.5c/° and the temporal frequency is 4.0°/s (refer to the text for more details on these parameters).

cycling leftwards. Depending on the recorded neurons' direction preference, this or the other set of conditions was chosen for stimulation. This issue will be addressed more thoroughly in a later section 'Recording preparations'. In brief, prior to stimulation the recording units (one electrode picks up signals from many neurons = 'unit') were assessed for their receptive field location as well as stimulus orientation and direction preference. Depending on the preference of the majority of units we then decided which stimulus protocol version was to be used for stimulation in a given recording session.

It is important to note that the distance between the individual Gabor patches for collinear and non-collinear conditions was chosen according to recommendations described in the literature (e.g. Polat & Sagi, 1993), that is in multiples of the wavelength, λ, of the Gabor i.e., λ = 1/spatial frequency. The distance between two Gabor centers was therefore chosen to be 2.5λ, that is 5°, so that two adjacent Gabor patches (each 5° in diameter) are right next to each other (see again '1.2 Psychophysical Studies on Collinearity').

Stimuli for Optical Recordings

For optical imaging experiments a set of 24 Gabor stimuli was prepared prior to the experiment (see Figure 2.5; note that there are only 12 stimulus conditions displayed; but both cycling directions were presented in one set, thus making up 24 conditions). Compared to the electrophysiology recordings there were some additional stimulus conditions for optical imaging, i.e. obliquely oriented stimuli. Optical Imaging experiments were performed later in the course of the study than the electrophysiology ones. Consequently, using a different program (Matlab) that is not based on a grid pattern (remember Pythagoras problem described earlier) lines of oblique orientation with the same inter-element distance as the horizontal or vertical ones could be designed. However, all characteristics of the vertically and horizontally oriented Gabor patches were kept the same for electrophysiological and optical recordings.

Figure 2.5 displays the Gabor stimuli used for optical recordings. Stimulus conditions were a single Gabor (A+D+G+J), a line of collinearly aligned Gabors (B+E+H+K), or a line of non-collinearly aligned Gabors (C+F+I+L). The local orientation of the Gabor elements was either horizontal (A+B+C), vertical (D+E+F), oblique -45° (G+H+I), or oblique +45° (J+K+L). All conditions shared the position of the center Gabor element.

In intrinsic signal imaging it serves a methodological purpose to stimulate the primary visual cortex with various orientations/directions, i.e. here four orientations with two possible directions each. A more detailed description of the optical imaging technique will be presented in a later section ‘2.3.5 Optical Imaging Data Processing’. In brief, optical imaging maps the functional organization of a cortical area with good spatial resolution. This includes for example, what orientation of a visual stimulus neurons preferably respond to. Neurons are grouped into orientation domains in a patchy manner (see section ‘1.4.2 Orientation selectivity of neurons in V1’ for a more detailed description). In contrast to electrophysiological recordings, where a single electrode only picks up signals from nearby neurons sharing the same orientation preference, optical imaging captures a wider cortical area covering a wide range of orientation preferences. Therefore, when stimulating repeatedly with many different oriented stimuli, it is assured that all cortical areas in view of the recorded image will be preferentially stimulated by some stimulus orientation. Against intuition, this resulting ‘cocktail blank’ (i.e. the sum of all pictures recorded with each stimulus

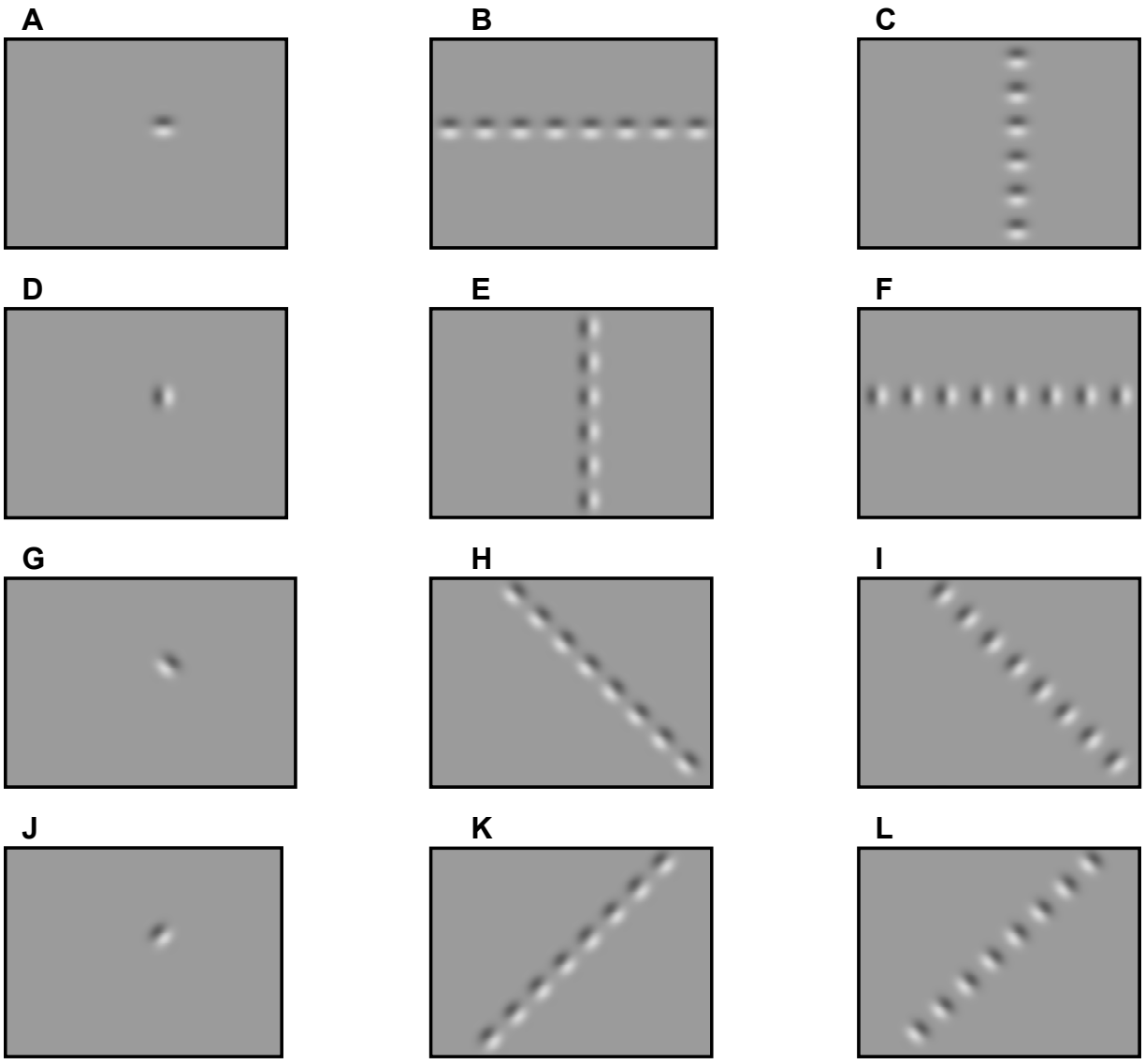

Figure 2.5 | Gabor stimuli used for optical imaging recording.
Stimulus conditions are either a single Gabor (A+D+G+J), or collinearly aligned Gabors (B+E+H+K), or non-collinearly aligned Gabors (C+F+I+L). The local orientation of the Gabor elements are either horizontally (A+B+C) or vertically (D+E+F) or oblique -45° (G+H+I) or oblique +45° (J+K+L). The characteristics of a Gabor patch are the same as for the stimuli used in electrophysiology recording.

orientation) serves as a better reference to normalize the signal than a recording with a blank stimulus screen.

For experimental variation the stimulus conditions constitute the independent variable of 'context' with two levels: 'collinear' and 'non-collinear'. The single Gabor was used as a reference stimulus for normalizing visually driven activity of the two line conditions. This will be explained in more detail when the dependent variables derived from the two recording techniques have been introduced.

2.2.2 Thermal Deactivation

The second independent variable of this study was the deactivation of the primary visual area on the contralateral hemisphere (opposed to the hemisphere where we recorded from) by cooling the cortical tissue. Thermal deactivation is temporary and applicable multiple times and therefore allows repeated application of this manipulative variable within one experimental procedure (Payne & Lomber, 1999). Cooling deactivation serves to address the research question of what role the intact primary visual cortex plays in integrating visual information across the two visual hemifields, in particular with regard to the cortical representation of a Gestalt figure.

The following text will describe the cooling method (see also section '1.4.4 Visual Callosal Connections') as well as how its application can be divided into steps of an independent variable.

The cooling system consists of a bended metal loop, connected to Teflon tubes, and a thermo sensor (see Figure 2.6 A and B). The tubing circuitry is filled with methanol, and connected to a pump. The tubes themselves are placed within an ice bath of methanol that can be cooled to -70°C by adding dry ice. When activating the pumping mechanism, the now chilled methanol within the tube gets passed through the tubing system, and the metal loop at the tip of the system reaches a temperature of about 2±1°C. The metal loop is placed on the cortical surface (refer back to Figure 2.2 B and section '2.1 Animals and Surgery Procedures') cooling the surrounding tissue in about 3 mm radius (Vanduffel et al., 1997; Lomber, 1999), which includes the depth of all six cortical layers. The question arises what happens to cortical functioning when the tissue gets cooled so far beyond normal temperature. In general, every chemical process is dependent on temperature. Cooling cortical tissue affects the membrane potential of the cell which causes the cell metabolism to slow down, thus disrupting the generation of action potentials and synaptic transmission (McCullough et al., 1999). Nevertheless, the brain can tolerate cold more readily than it can tolerate heat (Mark et al., 1961), and by terminating the cooling process and letting the cortex re-warm, neural activity returns. The cooling effect is reversible (Lomber et al., 1999). In previous studies, there was no correlation found between the number of cooling cycles and strength of effect (e.g. Hupé et al., 2001). Therefore, cooling cortical tissue is a practical variable to study how well other brain regions can maintain the behavior in the absence of a deactivated region (Lomber, 1999).

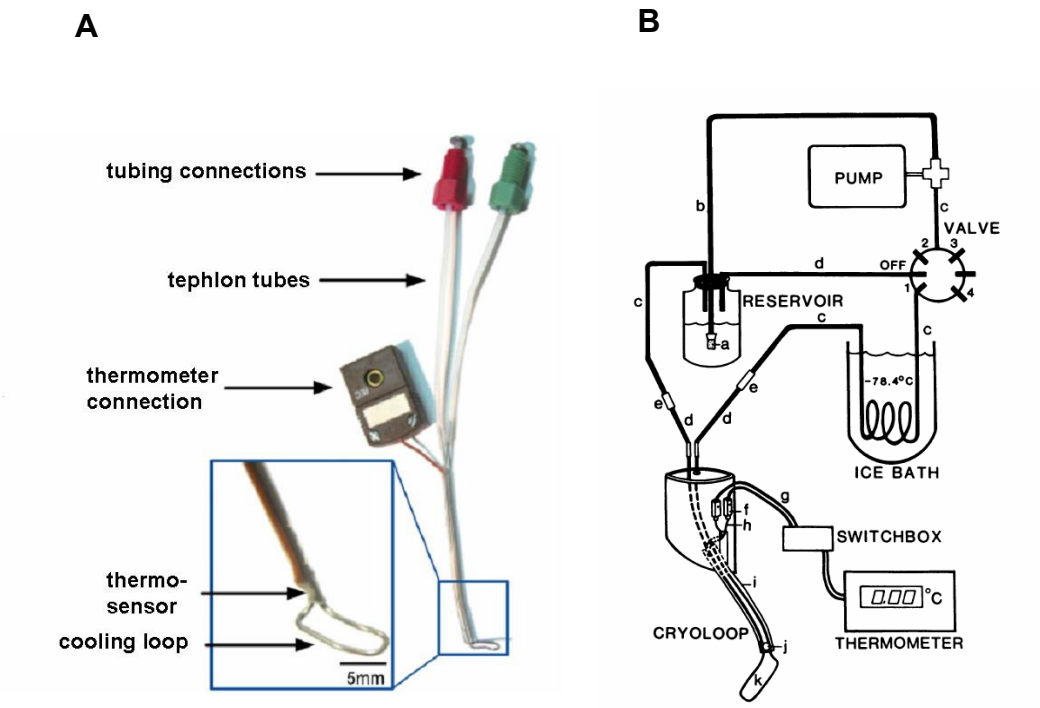

Figure 2.6 | The experimental cooling system.
Cooling System in photograph (A) and in graphic (B) modified after Lomber et al., 1999. The cooling system consists of a metal loop bended to conform the lateral gyrus, connected to Teflon tubes, and a thermo sensor. The tubing circuitry is filled with methanol, and connected to a pump. The tubes themselves are placed within an ice bath of methanol that can be cooled to -70°C by adding dry ice. When activating the pumping mechanism, chilled methanol within the tube gets passed through the tubing system, and the metal loop at the tip of the system reaches a temperature of about 2±1°C.

The deactivation variable consists of three experimental steps: recording of cortical activity taking place 1) before the deactivation ('baseline'), 2) during the deactivation ('cooling'), and 3) after the deactivation ('recovery'). In between these three states there was enough time to let the cortex cool down to 2±1°C or re-warm to 33.7°C, respectively. Temperature values were controlled via a thermo sensor placed close to the cooling loop.

For experimental variation this cooling technique constituted the independent variable of 'state' with two levels: before cooling, i.e. 'baseline' and 'cooling'. In the time period after cooling, i.e. 'recovery' recording of cortical activity was also performed. This served as a control to certify that brain activity eventually returned to normal for the next session of 'baseline' recording.

2.3 Experiments Using Optical Imaging of Intrinsic Signals

The following section will describe the recording technique Intrinsic Optical Imaging. This description will eventually lead to an understanding of the dependent variable derived from the signal recording, and what analysis is planned for comparing the signal in dependence of the stimulus variation and the thermal deactivation of the contralateral primary visual cortex (both independent variables were described in the previous section).

The description for the Optical Imaging method is divided into five subsections covering the following topics: 1) The subsection on the *setup* will describe the recording system and materials. 2) The subsection on the *principle of the recorded signal* will give an understanding of the underlying biological mechanism. 3) The subsection on *data acquisition* will outlay the time course of the stimulus protocols including number of trials and repetitions, as well as other specified settings. 4) The subsection on *data processing* will describe any post-experimental storing and conversion of the raw data into analysis capable data format. 5) The subsection on the *dependent variable derived from Optical Imaging* will describe the kind of variable and structure of the data that is studied in dependence of the proposed independent variables. A later chapter '2.5 Experimental Design and Statistical Modeling' will describe the statistical analysis performed for both recording methods electrophysiology and optical imaging.

2.3.1 Optical Imaging Setup

In the 1980s Optical Imaging of Intrinsic Signal was still in its infancy but ever since then numerous studies have been conducted using this technique. The name of Amiram Grinvald, a Neuroscientist at the Weizman Insitute of Science in Israel, is in every case repeadetly cited or even himself part of the group of authors. It was Grinvald and his colleagues (1986) who first found this relatively slow optical signal of cortical activity useful for studying the functional architecture of the cortex in-vivo, i.e. in the living organism.

Optical recording in our lab is performed according to the standards of Grinvalds methodological descriptions (e.g. Bonhoeffer & Grinvald, 1996). A high resolution CCD camera ('charge coupled device') was positioned in close distance

over the exposed cortex (refer to Figure 2.12 for a model). The cortex was illuminated with light, and controlled by the 'Imager 3001' recording system. The camera acquired pictures of the cortex while at the same time the animal was visually stimulated. Refer to Figure 2.8 for a schematic visualization of our laboratory setup for Intrinsic Optical Imaging.

A computer digitized the acquired images and saved them in a common data format. One pixel of the recorded image corresponds to 12 x 12 μm^2 cortex area. For each recording session we set a region of interest (ROI) from that we wanted to record the optical signal. This ROI is commonly chosen to about 300pixel (anterior-posterior extension) by 100pixel (medial-lateral extension), corresponding with a 2 x 2 binning of information to 7.2 mm x 2.4 mm cortical area.

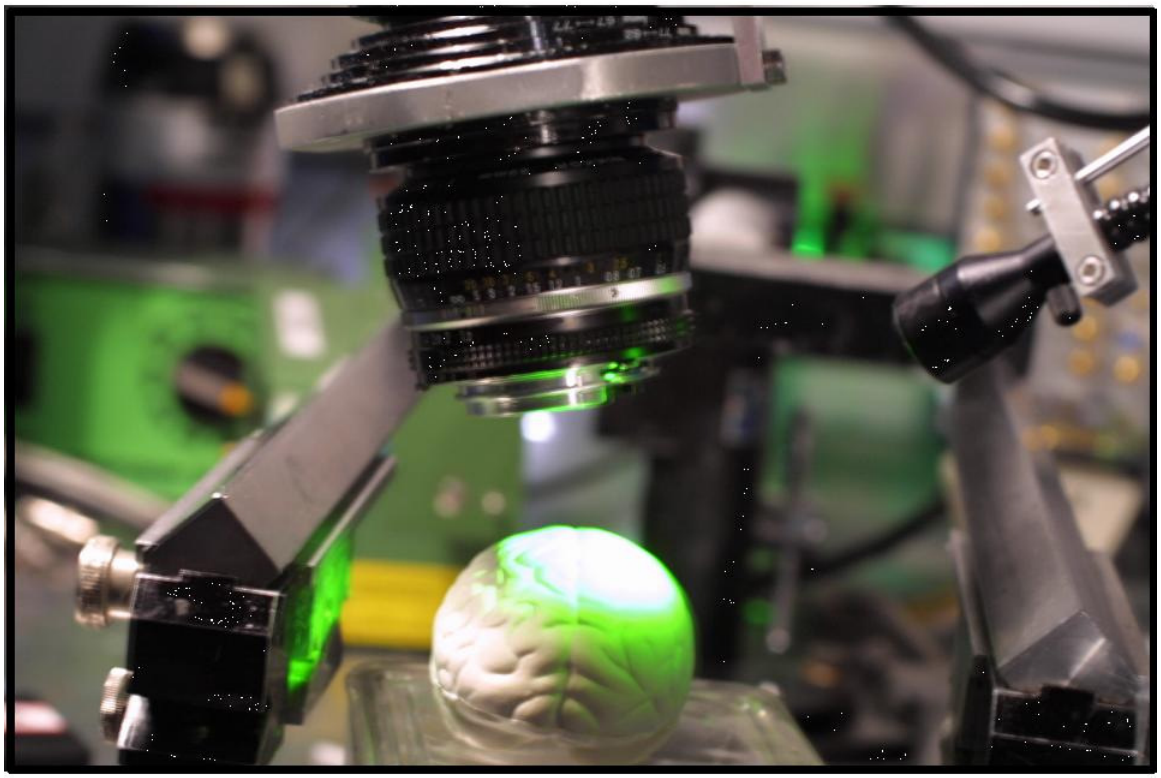

Figure 2.7 | Re-enacted optical imaging recording situation.
Optical imaging camera positioned over plastic model of cat cortex. Light (right side of the picture) from an external source is illuminating the surface.

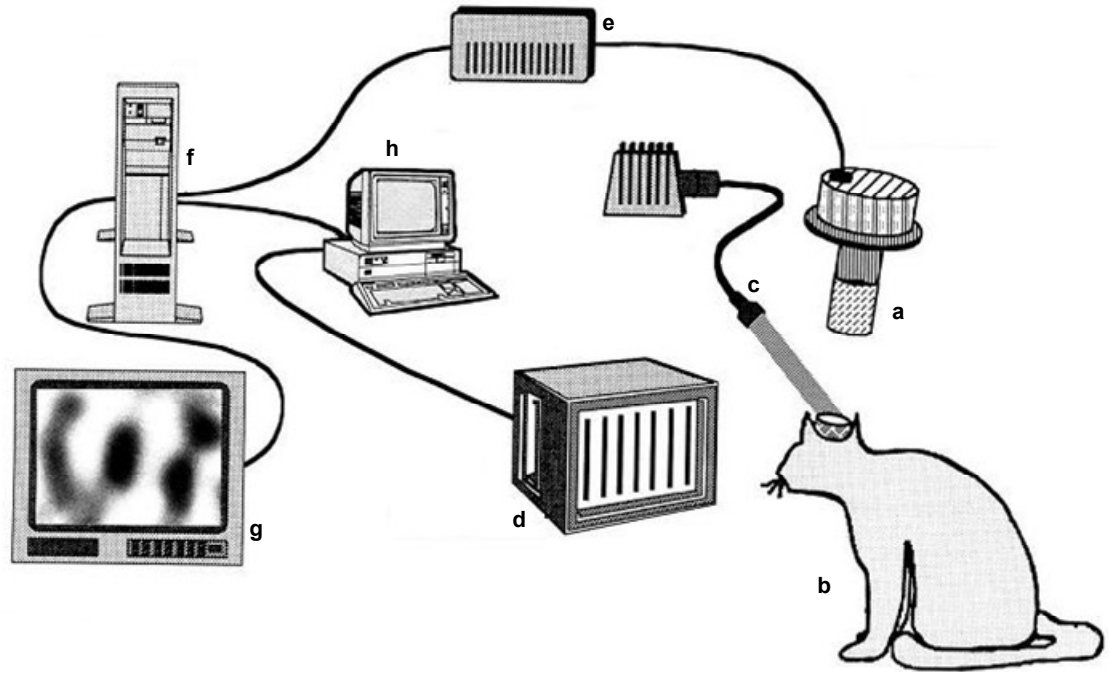

Figure 2.8 | Schemata of optical imaging laboratory setup.
A high resolution CCD camera (a) is positioned over the recording chamber implanted on the animal's skull (b). Light (c) is illuminating the cortical surface and a Imager 3001 recording system acquires pictures of the cortex while at the same time the animal is visually stimulated (d). The acquired images are digitized (e) and saved on a computer (f). A winmix software analysis program allows to view the resulting activation map of the cortex online (g), where dark regions correspond to cortical regions that respond to an in this case vertical stimulus and bright regions that are unresponsive to this stimulus condition. The acquisition computer (f) is the 'master' in this system sending out the trigger signal to the stimulation computer (h) as well as starting the acquisition of the camera frames. (Image modified after Bonhoeffer & Grinvald, 1993)

2.3.2 Principle of the Intrinsic Optical Signal

The term 'intrinsic' refers to the fact that the optical signal we record is internally generated and by nature part of the brain. The signal is principally based on three components: oxygen saturation of cortex tissue, cerebral blood volume, and light diffusion (Frostig et al., 1990). For a basic understanding of this method for our experimental purpose the following description is limited to the aspect of oxygen saturation. In brief, the intrinsic signals is based on the fact that cortical domains driven by visual stimulation contain more deoxygenated blood than non-active sites and thus absorb more light of a certain wavelength. Neurons depend on oxygen for their active cell metabolism, thus the red blood cells bind oxygen molecules on hemoglobin. Active cortical regions make instant use of this oxygen supply leaving the hemoglobin 'deoxygenated'. Figure 2.9 displays the absorption spectra of light in different

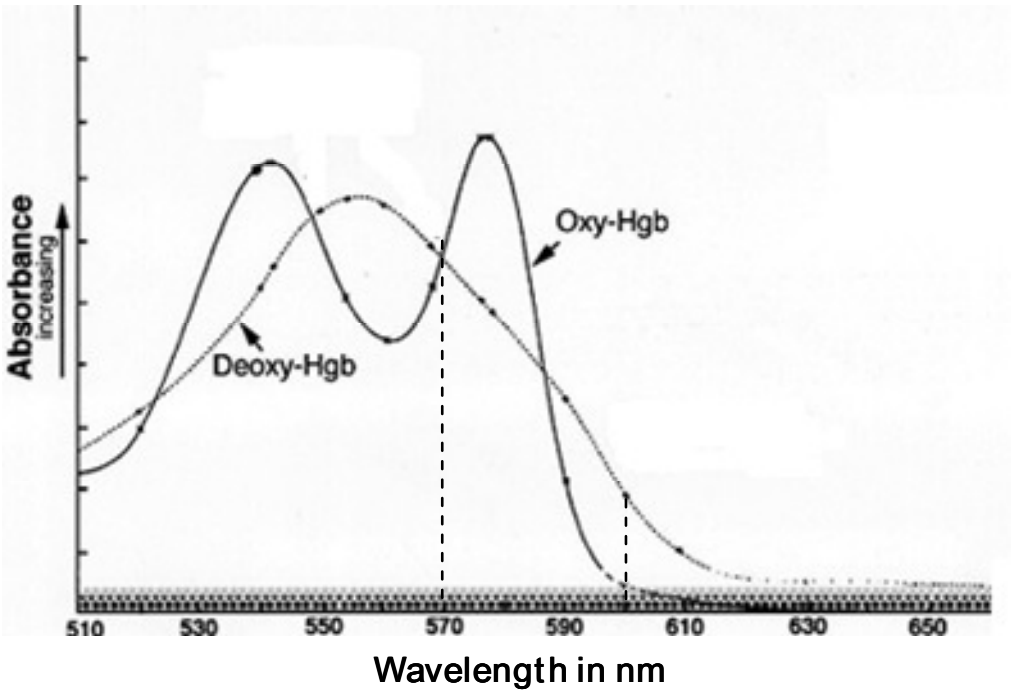

Figure 2.9 | Light absorption of oxygenated and deoxygenated hemoglobin under different wavelengths.
Absorption of light as a function of wavelength for oxygenated and deoxygenated hemoglobin. Note that at 570nm (first dashed line) the absorption is relatively high for both curves, while at 605nm (second dashed line) the absorption values for both can be well differentiated. (modified after www.medsource.com)

wavelengths as a function of hemoglobin bound with oxygen (Oxy-Hgb) and hemoglobin without bound oxygen (Deoxy-Hgb). At a certain wavelength of light, for example 570 nm, the light absorption for both Oxy-Hgb and Deoxy-Hgb is relatively high. Recording an image under this light condition shows a clear layout of blood vessels (Figure 2.10 A + B) which serves as a good reference for locating cortical positions. Nevertheless, in order to distinguish between areas that contain deoxygenated or oxygenated blood, respectively, i.e. to tell apart non-active from active cortical domains, images are optimally recorded under a light situation that both hemoglobin functions differ in, for example 605nm (as it is used in our lab). This is an optimal wavelength for recording because the function for Oxy-Hgb is almost zero, thus no light is being absorbed, while in contrast the Deoxy-Hgb absorbs light to a certain extent. Figure 2.10 C+D shows the same cortical region as in Figure 2.10 B but recorded under reddish light of 605 nm, while presenting a visual stimulus of vertical orientation (Figure 2.10 C) or horizontal orientation (Figure 2.10 D). Those patches in the image that appear dark refer to active cortical sides, i.e. those

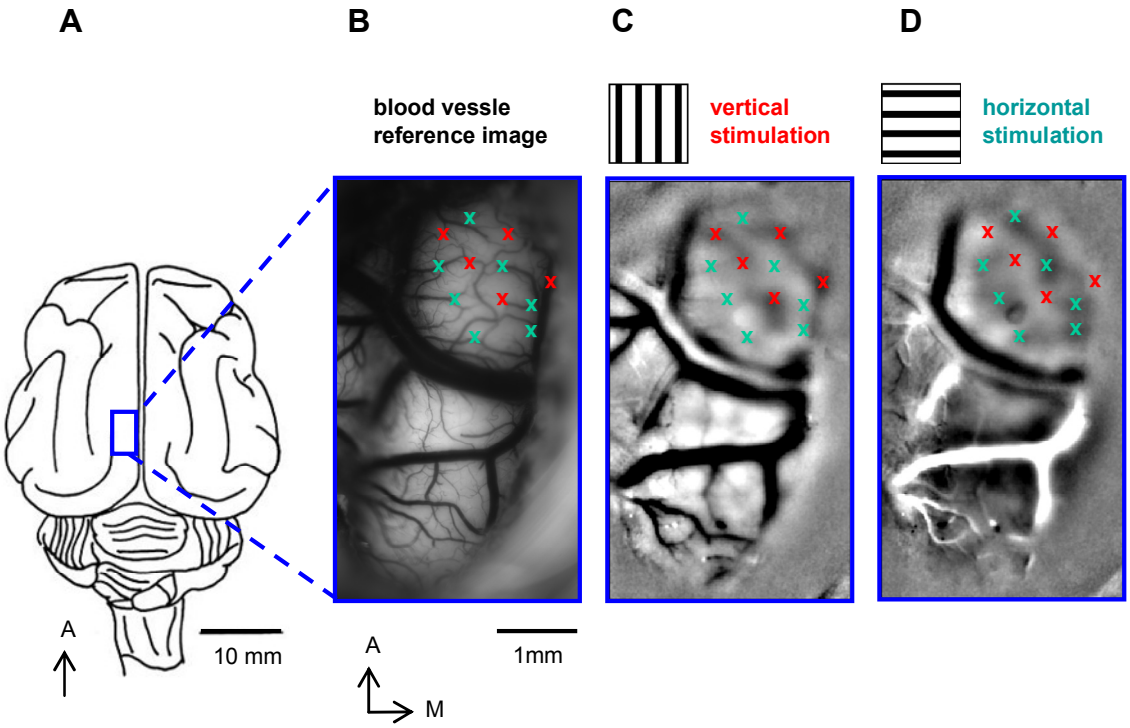

Figure 2.10 | Principle of optical recording.
(A) Schema of the cat brain viewed from above. A=anterior. The small blue square indicates the region of cortex that is being imaged. Enlargements of this area are given in **(B-D)**.
(B) Camera focused on cortical surface. Image is taken under greenish light (570 nm) where hemoglobin absorbs much of the light, so that the blood vessels can be seen. **(C)** Camera is focused approximately 600µm below surface, this blurs out the big surface vessels. Image is taken for the same cortical region as in **(B)** but now under redish light (605 nm) while simultaneously presenting a grating stimulus of vertical orientation. At this light deoxygenated hemoglobin absorbs more light than oxygenated one. Those patches in the image that appear dark (marked with red crosses) refer to active cortical sides, i.e. those domains which are responsive to vertical stimuli. In contrast, those patches in the image that appear white refer to non-active cortical sites, i.e. those which are non-responsive to vertical stimuli (marked with green crosses).
(D) The same content as in **(C)** but here for horizontal stimulation. Note active cortical regions for horizontal stimulation are marked with green crosses.
Note that orientation domains from vertical and horizontal stimulation appear complementary to each other.

domains which are responsive to vertical stimuli (Figure 2.10 C). In contrast, those patches in the image that appear white refer to non-active cortical sites, i.e. those which are non-responsive to vertical stimuli. A more detailed description of how these signals are acquired and processed will follow in the next section.

2.3.3 Optical Recording Preparations

Before any recordings of cortical responses could be performed, two preparatory questions needed to be answered: a) Are the optical axes of the eyes aligned? To answer this first question one is looking for the area centralis and the optic disc of both eyes and therewith estimating the vertical and horizontal midline positions in the animal's gaze. b) Where in the visual field should we place the stimulus to arouse a response in that cortical area we are recording from? The visual field is basically 'scanned' with moving light bars in time-matched correspondence to cortical activity. Both preparations will be explained in more detail in the following text.

Vertical and Horizontal Midline Positions

As described in the 'animals and surgical procedures' section the animal had dilated pupils covered with spheric contact lenses of such value that a stimulus screen at 57 cm distance from the cat was in clear focus. Recall that at this distance one centimeter on the stimulus monitor corresponds to one degree of visual angle on the retina. The monitor was centered in front of the cat's nose. In order to test for the visual center to be 'straight ahead', i.e. that the cat's gaze was not tilted to either side, the eyes were checked with a Fundus Camera (Zeiss, Jena). This is a microscope designed to look onto the interior surface of the eye, for our purpose to find the optic disk ('blind spot') and the area centralis ('yellow spot') on the retina (see '1.3 The Visual System – An Overview'). In brief, the 'blind spot' corresponds to the area on the retina that doesn't contain any photoreceptors but where the optic nerve leaves the eye towards inlaid brain regions. The 'yellow spot' corresponds to the area on the retina that contains the highest density of photoreceptors and is thus also referred to as the 'point of best focus'. Once either spot has been detected in the eyes a light projects back (reverse optics) in the direction of the observer, i.e. pointing to a certain location on the stimulus monitor. See Figure 2.11 A for a photograph of the human retina showing the blind spot and the area centralis. The corresponding locations projected back onto the stimulus monitor, documented with a sheet of paper, are shown in Figure 2.11. Thereafter, the stimulus monitor was centered on the estimated vertical midline, i.e. the projected location of the area centralis, or the center position between the blind spots of both eyes. Note that in anesthetized and paralyzed cats the eyes move, i.e. drift to the side, and this modifies the location of the vertical meridian. Therefore, the optic discs and area centralis were mapped regularly

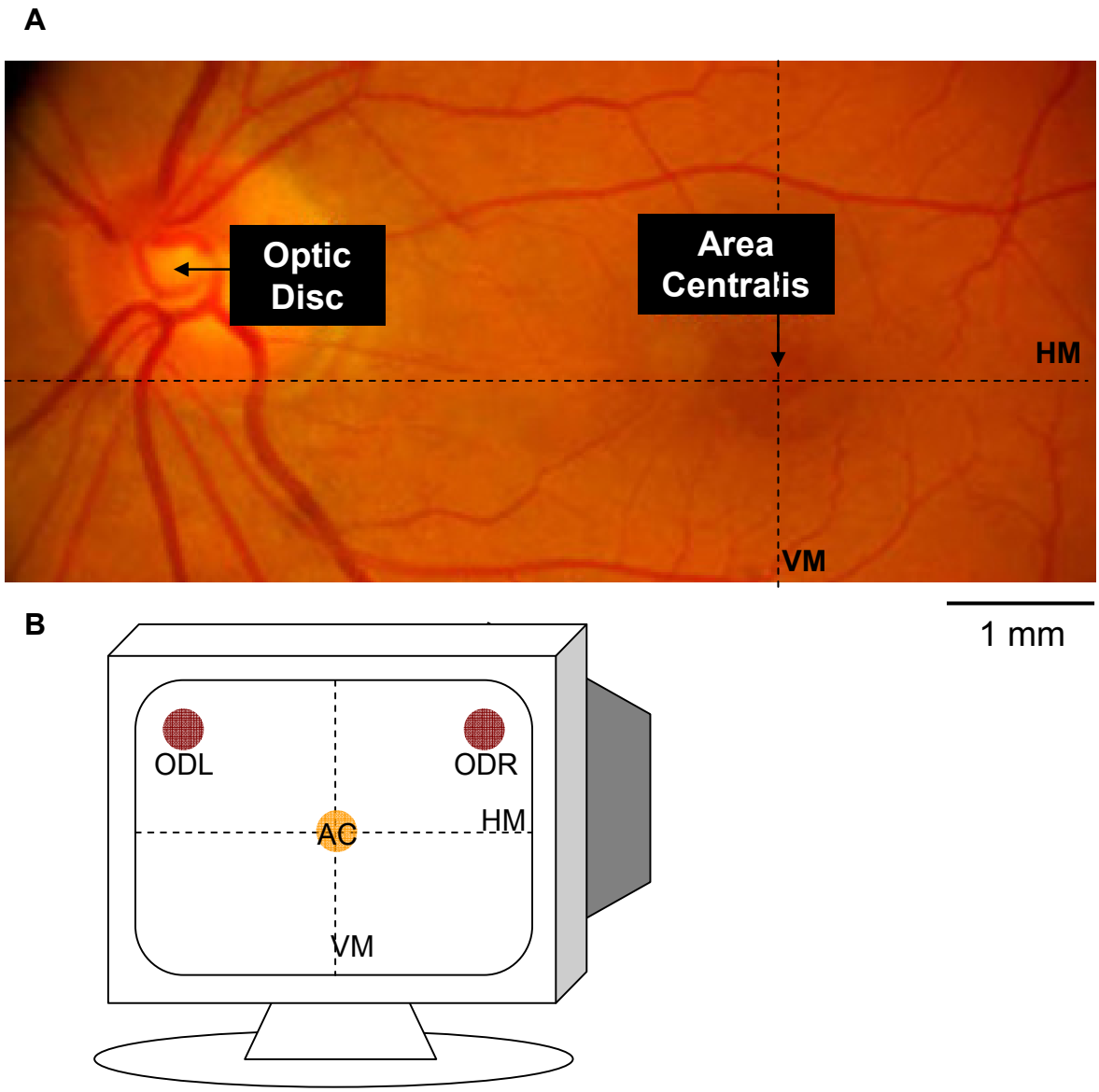

Figure 2.11 | Estimating positions of the vertical and horizontal midlines.
(A) A photograph taken (exemplarily) from a human retina in the left eye (graphic modified after www.eyetec.net/group5/M23S1.htm). The area centralis is the retinal area devoid of blood vessels, but with a very high density of photo receptors for a high acuity in vision of the central visual field. In contrast, the optic disk (black circle) is the point where the optic nerves exits the back of the eye and retinal blood vessels enter and spread over the inner eye surface.
(B) The corresponding representation of the areae centrales (AC; orange circle) and the optic discs (OD; dark redish circles; L = left exe, R = right eye) as it is during animal experiments projected onto the stimulus monitor right in front. Projections are documented on a sheet of paper covering the stimulus monitor that is positioned in front of the animal. The vertical midline is defined as the axis crossing vertically through the area centralis projection. The horizontal midline is defined as that axis crossing horizontally through the areae centrales projection.
Note that the projections of the area centralis from both eyes should optimally fall on top of each other. Further, in the cat retina the optic disc is rather positioned slightly below the horizontal axis running through the area centralis, thus resulting in a visual field representation above the horizontal midline axis as shown in **(B)**.

over the course of the experimental days and the monitor position corrected if necessary.

Representation of Visual Field on Recorded Cortical Area

In optical imaging experiments activity from many neurons at a time is recorded. Not all of V1 is exposed by surgery, in fact a great part of the primary visual cortex lies hidden to our accessibility in the medial bank or inside the first lateral sulcus (refer again to the introduction section to Figure 1.7 A + B). Therefore, it requires some careful examination to find the corresponding area in the visual field, i.e. on the stimulation monitor, that is represented on the cortex visible by the recording camera setup. The cortical area visible from craniotomy is approximately 15 mm x 10 mm in size, and it is even less in the frame captured by the imaging camera. This relatively small cortical area is represented on a stripe of about 5 ° x 15 ° visual angle (in our setup 1 ° = 1 cm) on the stimulus monitor, referring to anatomical studies in the cat primary visual cortex (e.g., Tusa et al 1978; or see again Figure 1.7 B+C in the 'introduction' section).

Figure 2.12 A-C describes in detail how the corresponding position in the visual field was determined according to the imaged cortical area. One after another a vertical and a horizontal moving bar sweep back and forth over the stimulation monitor. For each moment when the bar is located at a specific position on the monitor, the coincidental cortical activity was recorded, and both information then coded relatively to each other (Figure 2.12 A+B). Finally, a Matlab program set off both pieces of information against each other resulting in a spatial scratch of cortical representation (Figure 2.12 C). This mapping method was introduced by an imaging study in mouse visual cortex (Kalatsky & Stryker, 2003). Note that the scratch of representation in Figure 2.12 C does not outline a nice square or circular location but it is rather an overlaid sample of different trials. This emphasizes the slight variability in gathering the cortical activation patterns time locked to the position of the bar on the stimulation monitor and in performing the necessary calculations. Nevertheless, it serves as a sufficient approximation of visual space location to position the visual stimulus.

Let me emphasize again the importance of knowing what position in visual space the imaged cortical area corresponds to. It was the aim of this research project to study the cortical activity in response to different stimulus conditions. Thus, one needs to make sure that the stimulus location in visual space is in fact aiming at

stimulating the corresponding cortical area which one is recording from. After data acquisition the images have to be 'searched' for the exact patch of cortical area that responds to the stimulus center. This procedure of post-processing the recorded images will be explained in more detail in the next section.

Figure 2.12 (following page) | Locating the position in the visual field (on the stimulus monitor placed in front of the animal) that corresponds to the imaged cortical area.
(A + B) The imaged cortical area (left column) is of approximately 3 mm x 5 mm in size. While one after another a vertical and a horizontal moving bar sweep back and forth over the stimulation monitor, the positions that elicit a cortical response can be determined (compare the color code left and right column). Note that for a vertical bar crossing the visual field it is only within the range of approximately 7 cm on the stimulus monitor that elicit a cortical response **(A)**. For a vertical bar crossing the visual field it is only the range of approximately 11 cm that elicits a cortical response **(B)**.
(C) When combining the spatial information gathered from the vertical and horizontal mapping a representation of cortical correspondence in the dimension of the stimulation monitor (30 x 40 cm) can be calculated via a Matlab program. Note that the scratch of representation does not outline a nice square or circular location but it is rather different trials of the mapping overlaid, emphasizing that it is an as-good-as-it-can-be approximation of the visual space corresponding to the imaged cortical area.
Note. A=Anterior, P=Posterior, M=Medial, L=Lateral

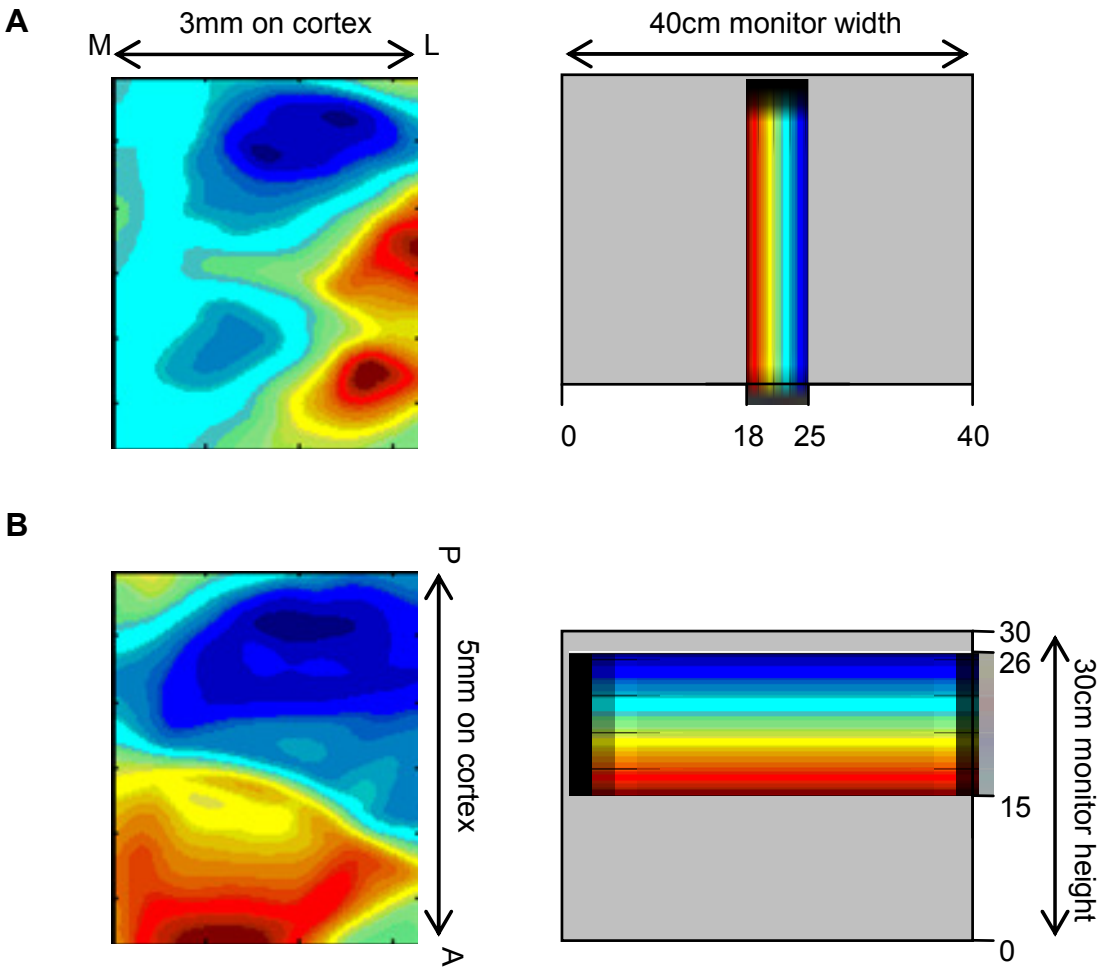
A
3mm on cortex
M
L
40cm monitor width
0
18
25
40
B
P
5mm on cortex
A
30
26
15
0
30cm monitor height
C
30cm monitor height
40cm monitor width
0
5
10
15
20
25
30
35
40

2.3.4 Optical Imaging Data Acquisition

A high resolution camera (Imager 3001) acquires pictures of the reflected light from the cortical surface. The spatial resolution of the camera is as fine as 12 µm cortex represented in one pixel of the camera image. With a 2 x 2 binning of information the cortical area was commonly captured in an image of about 6 x 10 mm in size (for example, refer back to Figure 2.12 A+B, left column).

In optical imaging experiments all of the 24 stimulus conditions (see section '2.2.1 Visual Stimulus Conditions') were presented 20 times each in a pseudo-random sequence. Each stimulus condition was shown for 4000 ms but recording started 1000 ms prior to stimulus onset for a uniform grey (blank) screen and lasted until the condition disappeared. This so called 'blank' recording serves to have a relative comparison between spontaneous activity and stimulus driven activity, and was used for judging whether a unit was stimulus responsive or not. Between subsequent recordings of each condition a 1500 ms inter-stimulus-interval paused the recording. Figure 2.13 visualizes the timing for stimulation and recording in optical imaging experiments. Note that the 5000 ms recording previously mentioned is, to be more specific, a recording of 25 frames with 200 ms frame duration each.

Note that for the optical imaging protocol of Gabor stimuli it took about 100 minutes to present and record 20 times 24 conditions of 5 seconds recording time and 1.5 seconds inter-stimulus interval each. This 100-minute recording session was then repeated under application of thermal deactivation (cooling) of the corresponding visual area on the contralateral hemisphere, and once more for a 100-minute recovery period after turning off the cooling and letting the cortex rewarm again. These three recording sessions (baseline, cooling, recovery) added up to an approximately 5 hour long experimental round; note that the animals were also used for other research projects involving the same methods and similar stimuli, so the commonly five days experiment time was divided up between all experimenters.

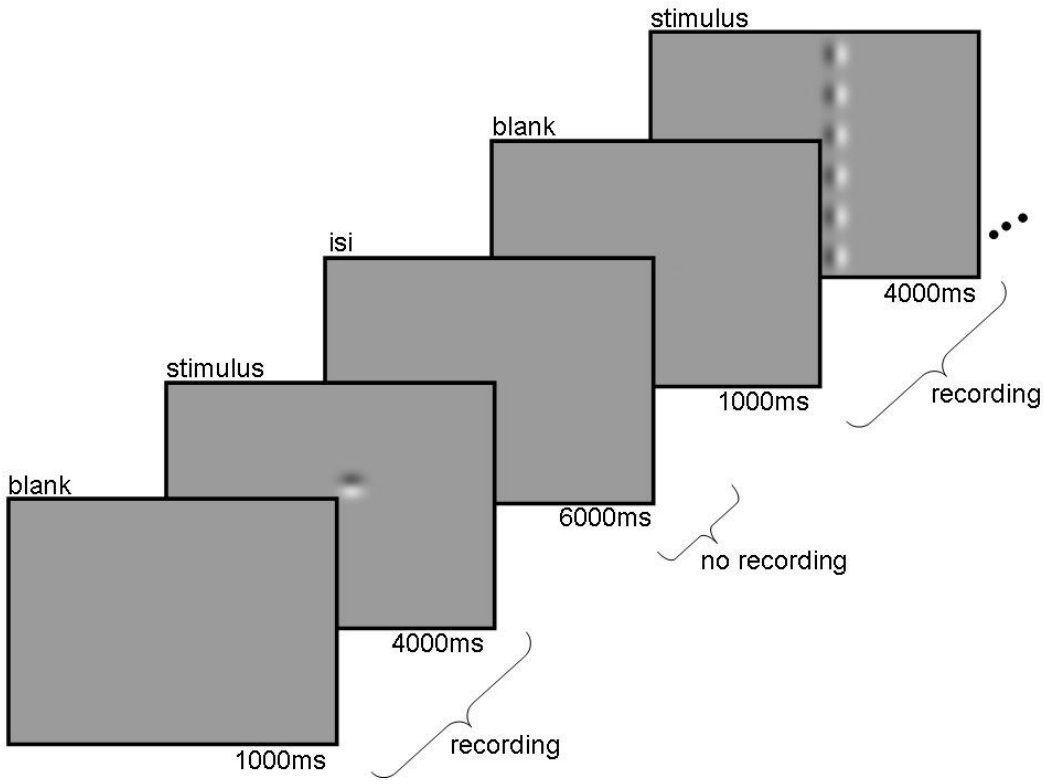

Figure 2.13 | Timing of stimulation and recording in optical imaging.
Each stimulus condition was shown for 4000 ms but recording started 1000 ms prior to stimulus onset with a uniform grey (blank) screen and lasted until the stimulus disappeared. Between subsequent recordings for each condition a 6000 ms inter-stimulus-interval (isi) during which a grey monitor screen (blank) was presented paused the acquisition.

Figure 2.14 A - D visualizes examples of images derived from intrinsic optical imaging. Cortical responses were imaged over an area of approximately 3 mm x 5,2 mm (Figure 2.14 A - D). As mentioned in the introduction section '1.4.2 Orientation Selectivity of Neurons in V1', neurons in primary visual cortex are grouped together in domains (looking onto the cortical surface) according to their preference for stimulus orientation. This patchy pattern is constant in depth throughout the six (laminar) layers, therefore the term 'orientation column' has been introduced (Hubel & Wiesel, 1962). The surface of such an orientation column spans about 300µm in diameter. Thus an image that is acquired while stimulating with a particular oriented stimulus contains many different domains of that orientation preference (marked by a white crosses in Figure 2.14 C; note the resemblance between Figure 2.10 A – C and Figure 2.14 A - C). In order to optimally stimulate the entire cortical area captured in the recording of an image, a variety of stimulus orientations have to be applied suc-

cessively. Later when the imaging data are processed, one depends on all images that were recorded under different stimulus orientations in order to study them relative to each other, resulting in a so called ‘angle map’ (Figure 2.14 D). This map allows to code all of the visible cortical surface with the orientation preference revealed by cortical activity recorded with the camera. For example, cortical areas that are active when stimulated with vertically oriented stimuli (colored blue in Figure 2.14 D and marked with white crosses) are not active when stimulated with horizontally oriented stimuli (colored green in Figure 2.14 D). This complementary behavior of cortical areas according to orthogonally oriented stimuli plays a key role in all optical imaging data analysis. As an example for complementary activation for vertical and horizontal stimulation refer again to Figure 2.10 in the section ‘Intrinsic Optical Imaging’.

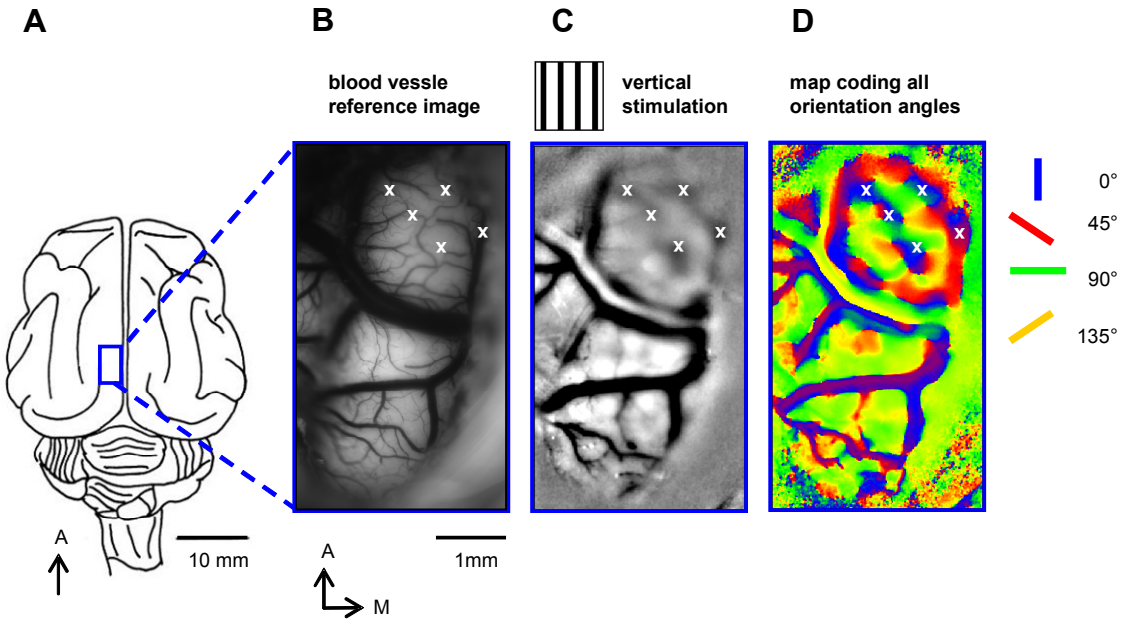

Figure 2.14 | Orientation columns in a region of the cat primary visual cortex.
(A) Schema of the cat brain, with direction A=anterior on the top. The small blue square indicates the region of cortex that is being imaged. Enlargements of this area are given in **(B – D)**, with direction A = anterior on the top and M = medial to the right of each.
(B) As previously described the camera is focused on the cortex surface. Image is taken under greenish light (570 nm) where hemoglobin absorbs much of the light, so that the blood vessels can be seen in a clear layout. White crosses mark locations described in **(C)**
(C) Camera is focused approximately 600 µm below surface, this blurs out the big surface vessels. Image is taken for the same cortical region as in **(B)** but now under redish light (605 nm) while simultaneously presenting a grating stimulus of vertical orientation. Under this light deoxygenated hemoglobin absorbs more light then oxygenated one. Those patches in the image that appear dark (marked with white crosses) refer to active cortical sides, i.e. those domains which are responsive to vertical stimuli. Note that it might take some experience to distinguish stimulus induced orientation columns from artifacts due to blood vessels.
(D) All images of cortical activity that were acquired while presenting stimuli of different orientations (for example for vertical stimulation in **(C)**) are then accumulated to result in a so called 'angle map'. Each color codes an orientation according to the schema to the right of the figure. White crosses mark same vertical orientation columns as in **(C)**.

2.3.5 Optical Imaging Data Processing

Subsequent analyses of the optical images including a) averaging, b) filtering, and c) contrast enhancement served to optimize image quality and normalization for further statistical analyses. Another two steps in data processing had to be conducted and will also be described in this section, i.e. d) 'cocktail blank' division, and e) finding the center Gabor representation on the imaged cortical region. The final section of this chapter will describe the dependent variable derived from optical imaging.

The process of 'averaging' refers to the reduction of the data dimensions, i.e. 25(frames) x 20(trials) x 24(conditions) x 446 (number of pixels on ROI y-axis) x 246 (number of pixels on ROI x-axis). (Note the ROI size of 446 x 246 pixels is taken from the image example of Figure 2.10 B-D). First, the data matrix was reduced by averaging over those image frames that were recorded while the cortex was stimulated, i.e. thus excluding frames taken during the 'blank' stimulation. Averaging over the number of frames holds the logic that whatever location on the cortex bears a stimulus driven activation will remain so in all frames. In contrast, those cortical areas not driven in stimulus activation will vary in activation, and this variance is averaged "out", resulting in a much better signal to noise ratio. The same kind of averaging logic applies for reducing the dimension of 20 trials. In this case, trials are commonly looked at one by one, and in case of any distorting artifact – which can have any reason such as an air bubble floating through the recording chamber within one trial – 'bad' trials are not included in the averaging. This leaves three dimensions of data, namely 24 (conditions) x 446 (number of pixels on ROI y-axis) x 246 (number of pixels on ROI x axis) – to refer back to the above example.

The process of 'filtering' further reduces recording artifacts and is performed with a digital high and a low-pass filter (similar to smoothing photos). A high-pass filter balances gross distortions in the image, for example due to irregular illumination of the curved cortex surface. A low-pass filter is adjusting for every pixel its surrounding pixel values therefore eliminating high-frequency noise. For the data of this study, the images were high-pass filtered at 40 pixels and low-pass filtered at 3 pixels.

The process of 'contrast enhancement' or 'clipping' refers to the correction of image values, i.e. grey values. In fact, the stimulus driven signal represents only 0.1% of the overall recorded signal. Therefore, the range of grey values is 'clipped' below and above the stimulus-driven signal, and the remaining range is extended to 256 grey values (8 bit) again. For the data of this study, the images were all clipped

well beyond the signal i.e. ± 4 x 10^{-3} so as not to loose any information. Thus, the range of pixel values was from - 4 x 10^{-3} until + 4 x 10^{-3}.

Further, when processing the recorded images the focus was laid on the stimulus conditions where the center Gabor element was of vertical or horizontal orientation. The reason to do so was to allow a comparison of results to data obtained from electrophysiology recording where only these two local Gabor orientations were present in the stimulus conditions. Nevertheless all other stimulus orientations were of importance for qualified data processing, which was performed in the following way: For the example of the two single Gabor conditions (two because of both cycling directions), both individual camera images were averaged in their pixel values. Next, the resulting average was normalized by dividing it by the summed pixel values of all eight Single Gabor conditions together (also called 'cocktail blank', Bonhoeffer & Grinvald, 1996). This processing is based on the assumption that all eight stimulations uniformly activate the cortex at that location where the Single Gabor is represented. Thus, when dividing the pixel values of an image by the 'cocktail bank' of all conditions, any artifacts resulting from blood vessels or irregular illumination of the cortex surface will be 'cancelled out'.

Finally, the 446 x 246 pixel camera image (as in the previously described example) had to be searched to find the area which represents the center Gabor stimulus that all stimulus conditions (single Gabor, collinear line, non-collinear line) had in common. The section '2.3.3 Optical Recording Preparations' described a procedure of placing the stimulus monitor at the correct height and center in front of the animal to assure, that the stimulated area in the visual field was actually represented in that cortical region of interest the optical imaging camera is taking pictures of. See Figure 2.15 for a theoretical cartography of the imaged cortical area in correspondence to the center Gabor position on the stimulus monitor. Once the experiments were run, the images of cortical activity taken for all stimulus conditions were fed into a similarity matrix program (Kriegeskorte et al., 2008). Therein the (empirical) imaged cortical activation maps in response to each stimulus condition were correlated with a theoretical matrix model resulting in an 'activation spot' (see Figure 2.16 A - C) that all stimuli conditions had in common: the center Gabor. Any following analyses were limited to that region of the image, where the center Gabor stimulus had its representation – Gabor Region of Interest (Gabor ROI), see Figure 2.16 C.

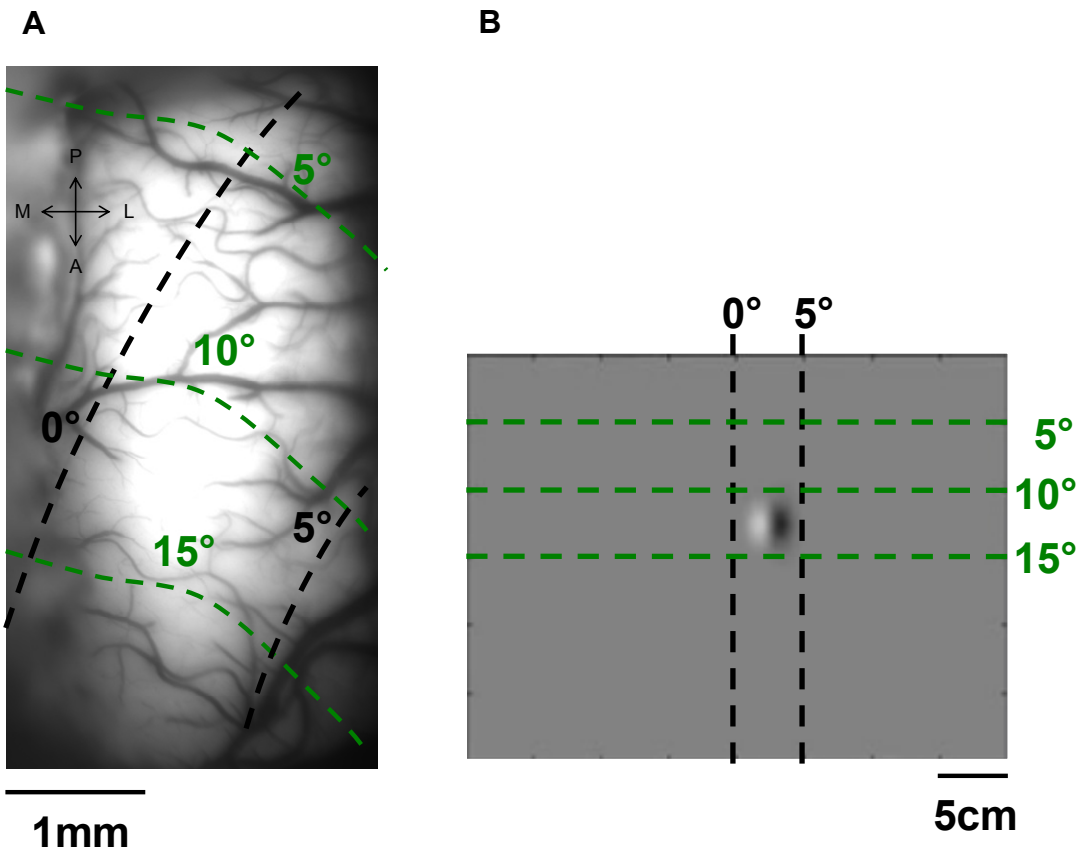

Figure 2.15 | Retinotopy in correspondence to center Gabor location.
(A) Camera is positioned over the cortical region of interest to be studied, the surface blood vessels are clearly visible. The image was overlaid with retinotopic coordinates (black & green) based on an approximation from anatomy literature (e.g., Tusa et al., 1978). The top of the image represents P = posterior on the cortex. As one moves further down in the picture (green coordinates), which is more A = anterior in cortical coordinates, the cortical representation correspond more and more to the lower visual field **(B)**. The left of the image is M = medial on the cortex. The (black) 0° marking line represents the 17/18 border or vertical midline in the visual field. As one moves further to the right in the picture (black coordinates), which is more L = lateral in cortical coordinates, the cortical representation corresponds is more in the periphery in the contra-lateral visual field. The cortical recording is performed in the left hemisphere, therefore the representation in the visual field is on the right side.

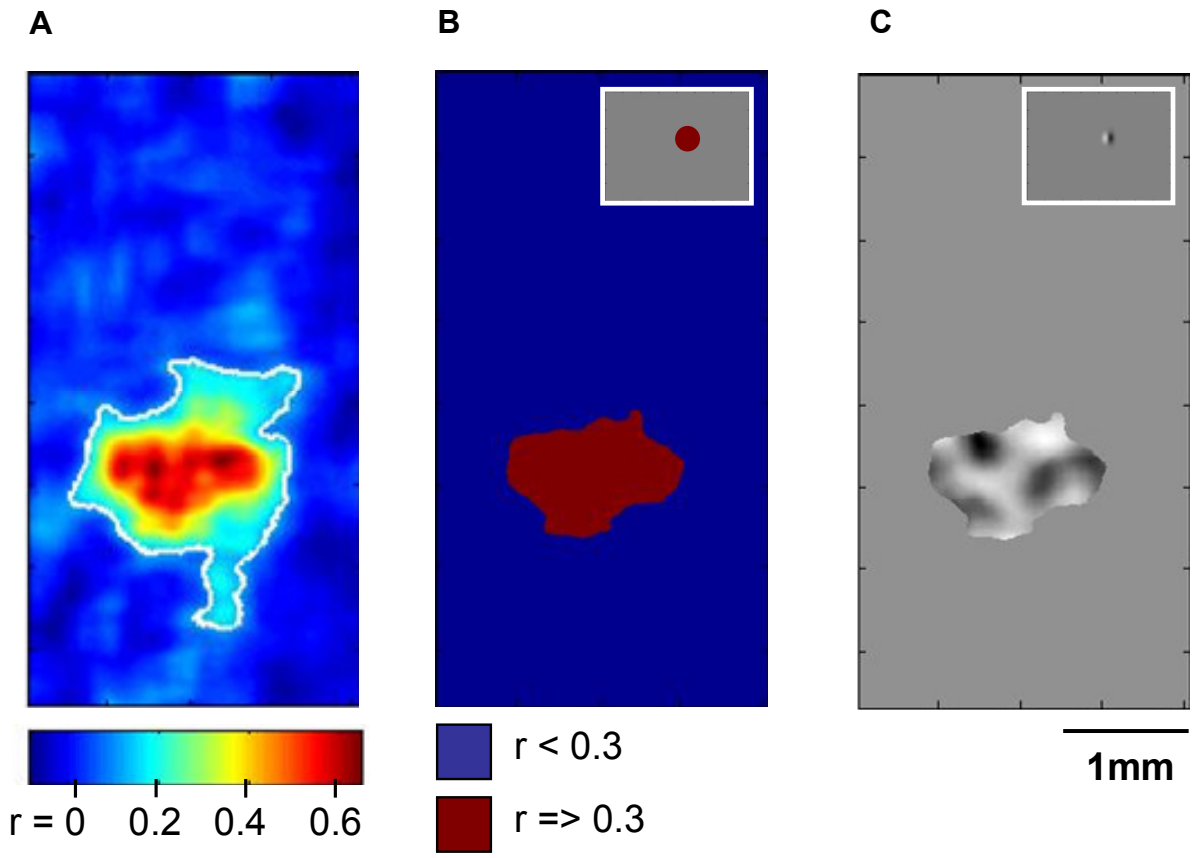

Figure 2.16 | Similarity matrix program determines specific cortical area that corresponds to the center Gabor location on the stimulus monitor.
The images **(A – C)** represent the same cortical region as Figure 2.15 A.
(A) The imaged cortical region is color-coded as a correlation result derived from the Similarity Matrix Program. As all stimulus conditions are fed into the program the resulting 'activation spot' indicates the cortical area that was stimulated by the center Gabor - the stimulus element which all conditions have in common.
(B) The imaged cortical region is colored in red for that region which revealed a correlation of equal or larger than 0.3, and blue for those correlation values below. This Gabor-ROI (region of interest) will be used for all further data analyses, so that any activation values are always limited to a specific area. Of course, for the different experiments this Gabor-ROI differs. But the Gabor-ROI of all experiments will be displayed in the 'result' section.
(C) An example activation map for a vertically oriented single Gabor stimulus that cycled leftwards, limited to that cortical area that was determined by the Similarity Matrix program to represent the center Gabor location. As explained previously, dark areas in the image correspond to cortical regions that were activated by the vertical stimulus, brighter areas in the image indicate cortical regions that were not activated by the vertical stimulus.

2.3.6 Dependent Variable derived from Optical Recording

Optical imaging was performed in five animal experiments. In four animals one recording session each was performed. In one animal (experimental code 091608) two recording sessions were performed. Together, six recording sessions made up the sample for optical recordings.

The resulting dependent variable from each recording was a vector of pixel values derived from the different images taken under the various experimental conditions. The region of cortex studied was reduced to the 'Gabor ROI' described previously. The pixel values of an image indicate the strength of activation for cortex locations in the given pixel resolution, as is exemplarily shown in Figure 2.16 C. The range of grey values in each image was normalized in the computerized image processing to values between 0 (dark grey; very high strength of cortical activation) and 8 (bright grey; very low strength of cortical activation).

It was decided for the frame of this thesis to describe optical imaging data qualitatively for each of the six optical recordings and thus give an unbiased overview of experimental outcomes. The basic experimental design will be explained in more detail in section '2.5 Experimental Design'.

2.4 Experiments using Electrophysiology Recording

The following section will describe the recording technique of electrophysiology. This description will eventually lead to an understanding of the dependent variable derived from the signal recording, and what analysis was carried out for comparing the signal in dependence of the stimulus variation and the thermal deactivation of the contralateral primary visual cortex (both independent variables were described in the previous section).

The description of the electrophysiology method is divided into five subsections covering the following topics: 1) The subsection on the *setup* describes the recording system and materials. 2) The subsection on the *principle of the recorded signal* will give an understanding of the underlying biological system. 3) The subsection on *data acquisition* will lay out the time course of the stimulus protocols including number of trials and repetitions, as well as specified settings for the respective recording setup. 4) The subsection on *data processing* will describe any post-experimental storing and conversion of the raw data into analysis capable data format. 5) The subsection on the *dependent variable derived from electrophysiology recording* will describe the kind of variable and structure of the data that is studied in dependence of the proposed independent variables. The last subsection '2.5 Experimental Design' will finally explain in more detail what type of statistical analysis was conducted.

2.4.1 Electrophysiology Setup

Our lab has been using three different kinds of recording electrodes: Tungsten 4 x 4 matrix electrode arrays with 400 µm inter-electrode distance (Figure 2.17 A), Tungsten 4 x 4 matrix electrode arrays with 200 µm inter-electrode distance (Figure 2.17 B), and Michigan Probe electrodes (Figure 2.17 C) with four electrode contacts on each of four flat shanks with 200 µm distance among each. For the Tungsten matrix with 400 µm inter-electrode distance, the matrix covers a cortical area of about 1200 µm x 1200 µm. For the Tungsten matrix with 200 µm inter-electrode distance, the matrix covers a cortical area of about 600 µm x 600 µm. For the Michigan Probe

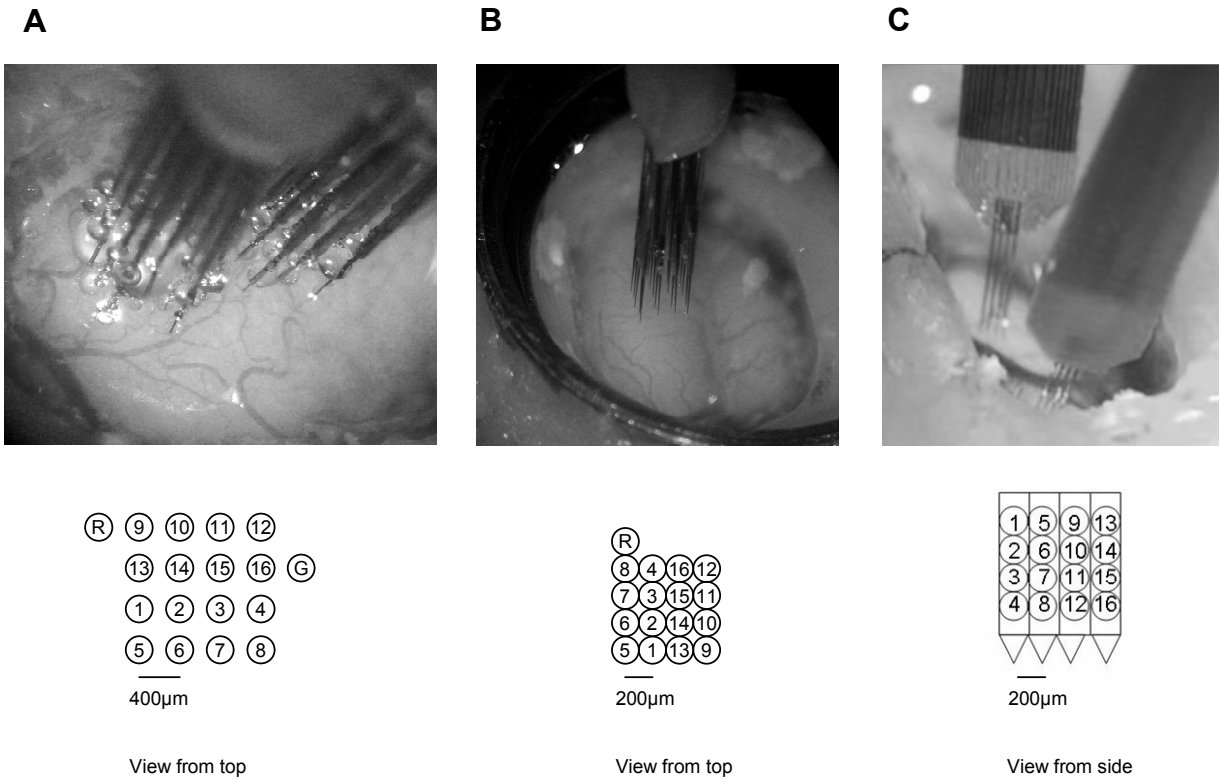

Figure 2.17 | Electrode setups used for this research project.
(A - C) The top row gives three photographed examples of each electrode setup. The bottom row graphically displays the pattern of electrode penetrations resulting from the layout of the electrode alignment. The scale of each graphic corresponds to the above photo in terms of the inter-electrode distance. R = Reference Electrode, G = Ground Electrode.
(A) Two Tungsten Matrix electrodes with 400 µm inter-electrode distance are placed over the primary visual cortex. Below the photo the penetration pattern of one of the matrix electrodes is displayed as if viewed from the top onto the cortex surface.
(B) One Tungsten Matrix electrode with 200 µm inter-electrode distance is placed over the primary visual cortex. A second matrix was placed after this photograph was taken. Below the photo the penetration pattern of one of the matrix electrodes is displayed as if viewed from the top onto the cortex surface.
(C) Two Michigan Probes with four shanks of four electrode contacts each are placed over the primary visual cortex. Below the photo the outlay pattern of the electrodes as if viewed from a cross section through the cortex. The inter-electrode distance sideways and stacked is 200 µm each.

the electrodes with a spacing of about 200 µm the four flat shanks (similar to the teeth of a fork) span a distance area of approximately 700 µm.

For recording, the electrodes are inserted into the cortex by less than 2 mm. The primary visual cortex of the cat is only about 2000 µm in depth measured from the pia at the surface through six cortical layers all the way to the white matter (refer to section '2.4.6 Histological Post-' for an image of the cortical layers from histological processing of the cortical tissue). For experimental recording the electrodes were lowered into the cortex in 100 µm steps at a time until acquisition of a signal. In the first two experiments we used two sets of Tungsten matrix electrodes with 16 channels each and 400 µm inter-electrode distance. In the third experiment we first used two Microprobe electrodes with 16 channels each, but when one of them was accidentally bent over in the cortex and broke we had to replace it with a matrix set of Tungsten electrodes with 400 µm inter-electrode distance. In the fourth, fifth, and sixth experiment of electrophysiological recording we used two sets of Tungsten matrix electrodes with 16 channels each and 200 µm inter-electrode distance. Note that for these last three experiments electrophysiological recording was preceded by two days of voltage-sensitive dye imaging. Whether to expect any influences from this experimental variation on the outcome of the data recording will be discussed more thoroughly later on.

In placing the electrodes in the cortical region we aimed at positioning at least one set of electrodes in the close vicinity of the vertical meridian, i.e. 17/18 border (refer back to the introduction section on 'Anatomical properties of the primary visual cortex' for further explanation). This placement was commonly done by the best guess we had on anatomical references from literature or prior optical recordings, but subsequent data analysis allowed a more specific judgment. The second set of electrodes was placed somewhat farther away in the periphery of either A17 or 18 depending on the experiment. The distinction of A17 from A18 was of major interest for other research projects carried out in the same experimental animals, and thus is only mentioned here briefly. Figure 2.18 A - F shows photographs of all the cortical areas of all six experiments, overlaid with the pattern of electrode penetrations of the employed electrode setup. Note that it was always checked very carefully through the microscope where the electrodes had been placed in reference to the layout of the blood vessels. Nevertheless, it is only an approximation (for example liquid on the cortical surface can distort the view). The cortical tissue from the first three electro-

physiology experiments was processed post-experimentally in an attempt to support localizing the electrode tracks in relation to the 17/18 border. The procedure of this post-experimental histological processing will be described in the respective section. However, despite the very careful and detailed histology work it was not possible to reconstruct all electrode tracks from the experimental recording.

Figure 2.18 | (on the following three pages) | Image protocols of electrode placements from all six electrophysiological experiments.
Each of the six graphics **(A -F)** indicates the experimental code in the upper right corner, for example 121107, and an indication whether recording was performed in the left cortical hemisphere (LH) or the right cortical hemisphere (RH). The top left corner contains a thumbnail graphic of the cat cortex, with the front (A = Anterior) to the right. A little red square indicates the location that was made visible by craniotomy. A close up of the area within the red square is given below. The polar positions in the graphic and in the photo are in correspondence.
In the first two experiments **(A + B)** two sets of Tungsten matrix electrodes with 400 µm inter-electrode distance were used. In the third experiment **(C)** data was collected from one set of Tungsten Matrix electrodes with 400 µm inter-electrode distance and one set of Michigan Probes with 200 µm inter-electrode distance. The fourth, fifth and sixth experiment **(D + E + F)** included each two sets of Tungsten Matrix electrodes with 200 µm inter-electrode distance each.
Note, that the electrode positions are judged through a microscope placed over the experimental setup and is an approximation of about 20 µm accuracy.

A

121107 LH

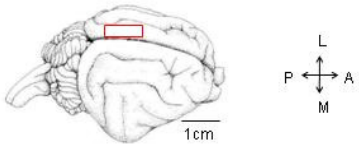

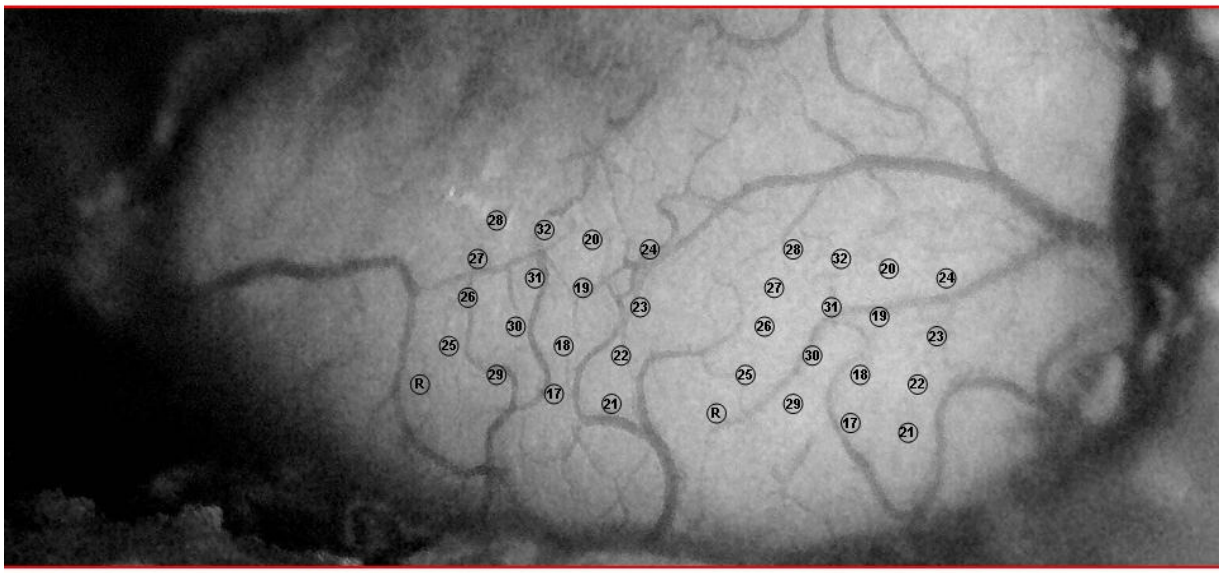

1mm

B

021808 RH

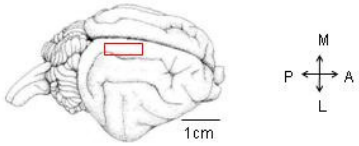

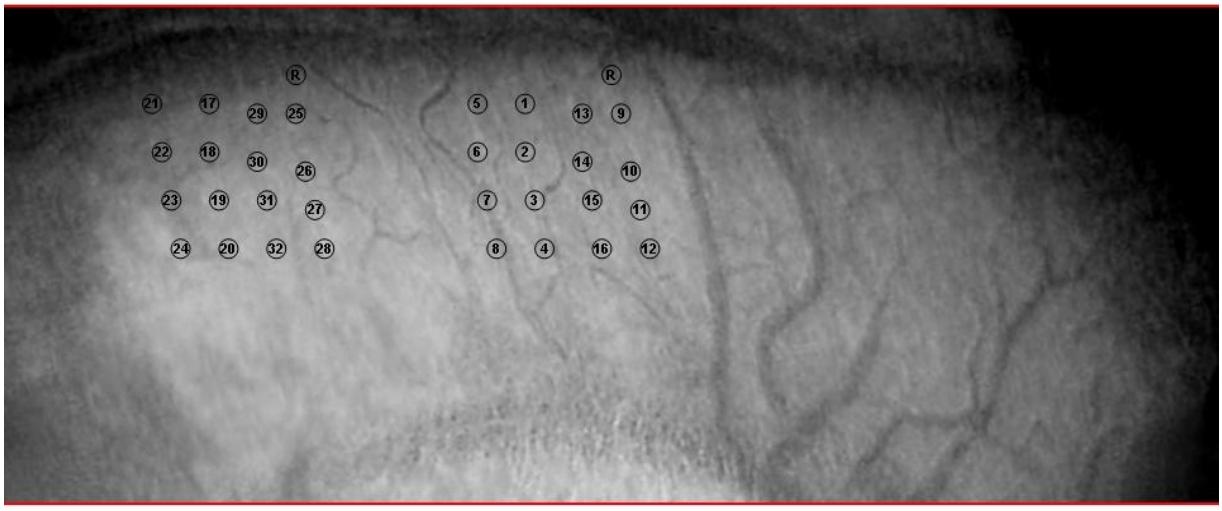

1mm

C

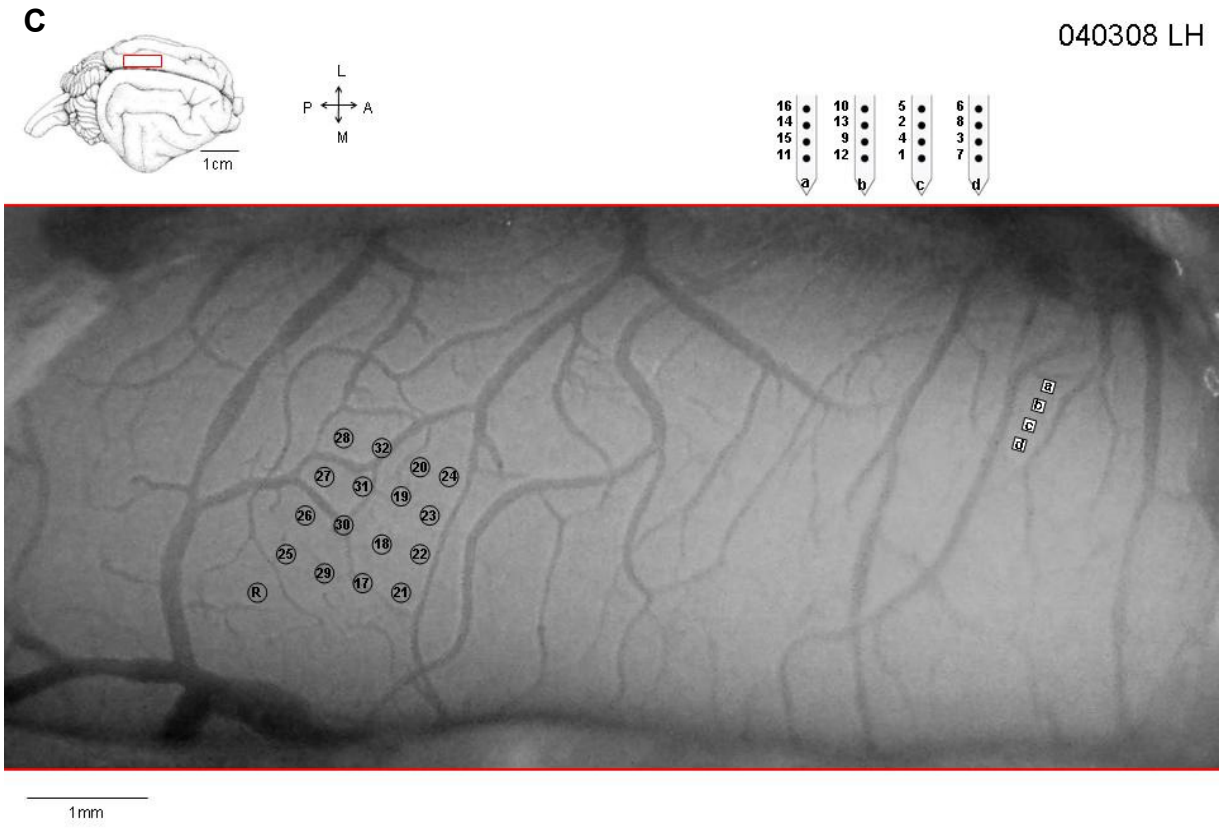
040308 LH
L
P
A
M
1cm
16 14 15 11
10 13 9 12
5 2 4 1
6 8 3 7
a
b
c
d
28 32 20 24 27 31 19 26 30 23 18 25 22 29 17 21 R
1mm

D

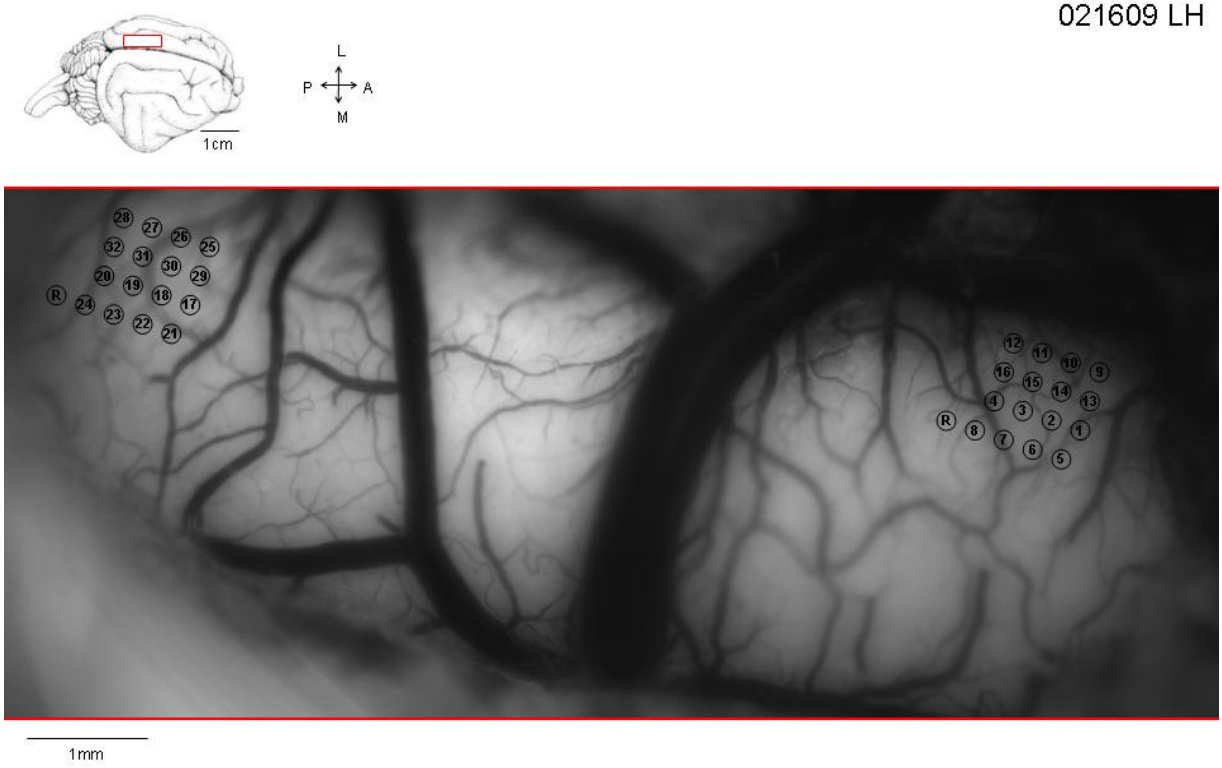
021609 LH
L
P
A
M
1cm
28 27 26 25 32 31 30 29 20 19 18 17 R 24 23 22 21
12 11 10 9 16 15 14 13 4 3 2 1 R 8 7 6 5
1mm

E

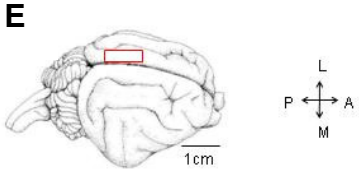

011209 LH

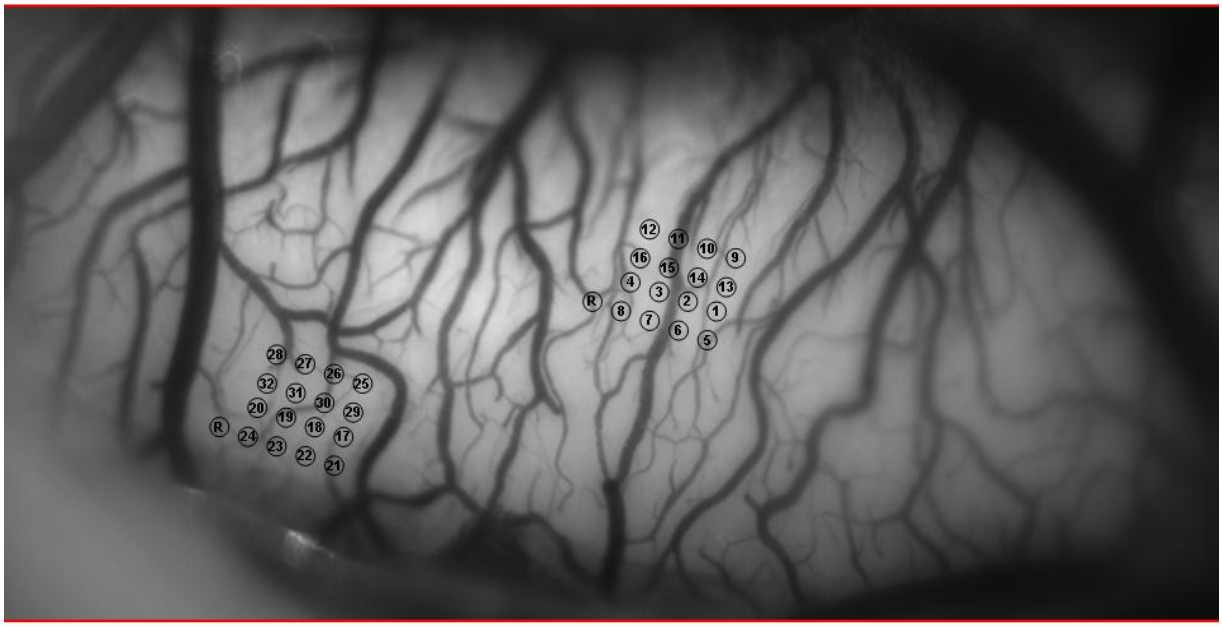

1mm

F

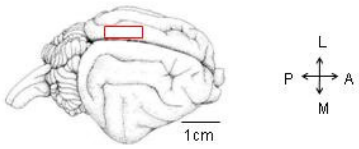

033009 LH

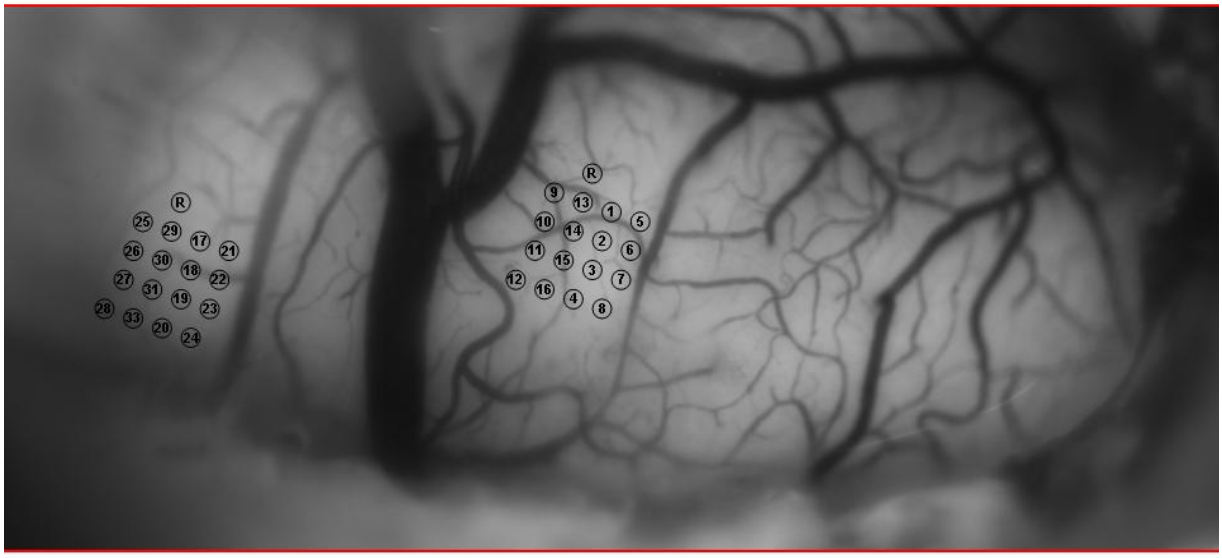

1mm

2.4.2 Principle of Electrophysiological Recording

The following part will describe in brief what happens on a biological level when we perform electrode recordings from the cortex. The content is based on general and text book knowledge, as for example Kandel, Schwartz, & Jessel (2000), and Birbaumer & Schmidt (1996). When the electrodes are inserted into cortical tissue they get placed in the vicinity of many different neurons. This principle of 'extra-cellular' recording is displayed graphically in Figure 2.19.

In electrophysiology the signal that one is recording from the cortex is the change in membrane potential resulting from an action potential of an active cell. The membrane potential is the difference between the inside and outside voltage of the membrane of a cell. In order to record the potential as a signal one needs a reference point. As we place our recording electrode in the extra-cellular space, i.e. in between many different neurons, another electrode farther away - but also extra-cellular - is used as the reference signal (see Figure 2.18 A - F where the circle containing an 'R' refers to the reference electrode in an electrode setup). Is a cell inactive, the membrane potential is at rest ('resting potential'); bio-chemically that means that there are more negative ions inside the cell membrane than outside of it. When an action potential arrives, commonly 'traveling' from the soma of a cell down its axon, for a brief moment the membrane becomes permeable for positive ions to flow inside the cell. For an instance the potential sharply increases inside the cell membrane and thus decreases outside the cell membrane; this is called 'depolarization'. Following is a phase where the potential overshoots its resting value, the 'hyperpolarisation' before coming slowly back to its resting state, also referred to as 'repolarisation'. Thewhole cylce from resting state to action potential and back to resting state takes less than a millisecond. One can imagine that for one second of recording an extracellular signal hundreds of these action potentials can arise. This very fast frequency in rising and falling amplitude of the potential can be framed in a threshold, in that whenever the amplitude of the signal crosses over the threshold a time stamp is marked – and a 'spike' event has occurred. Refer to the section of '2.4.5 Electrophysiology Data Processing' for a more detailed description of 'spikes'.

While the frequency of the 'spike' is very high, there are of course also slower frequency components in the changing signal of membrane potentials which can be

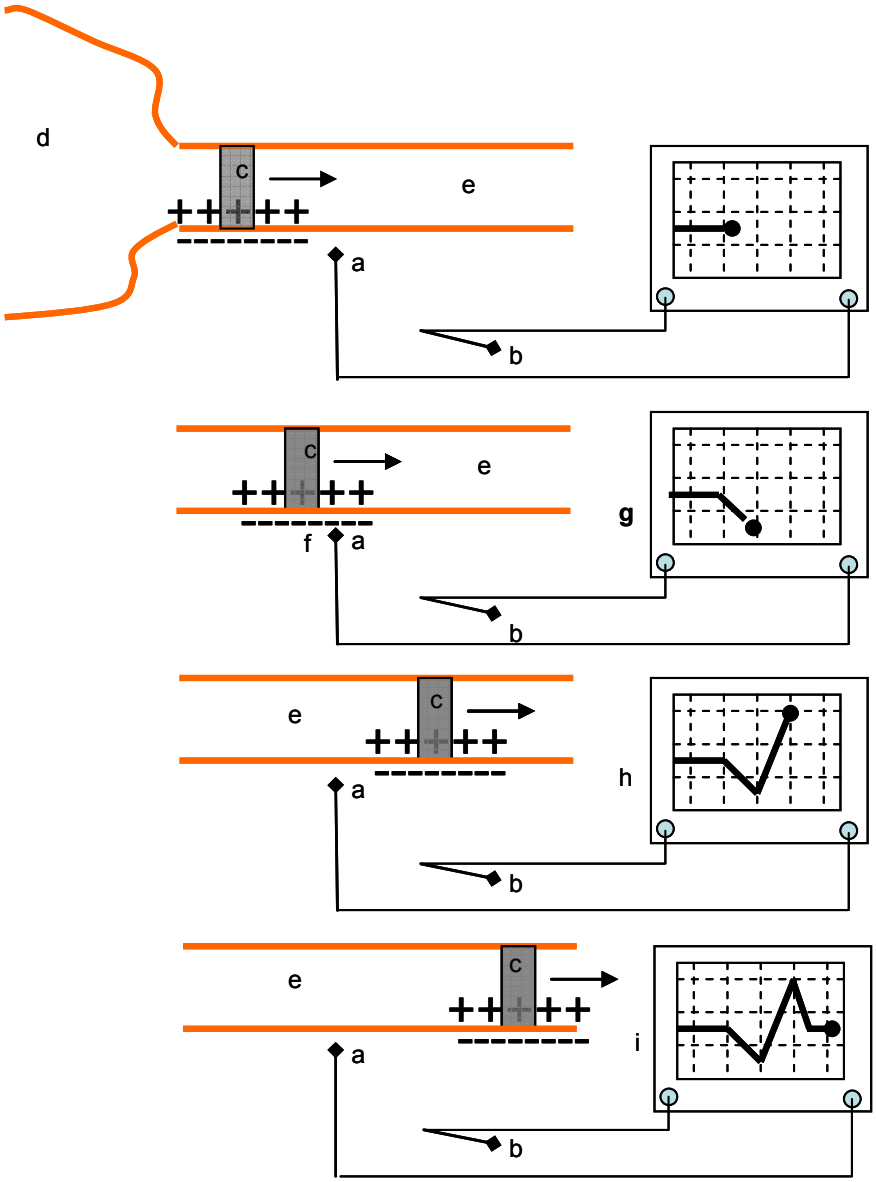

Figure 2.19 | Schemata of principle of extra-cellular recording.
From top to bottom the graphic shows four stages of extra-cellular recording (a + b), for example visualized on an oscilloscope (black box on the right), while an action potential (c) is traveling down the axon (e) of a neuron.
We place our recording electrode (a) in the extra-cellular space, i.e. in between many different neurons, another electrode (b) farther away but also extra-cellular is used as the reference signal. When an action potential (c) arrives, commonly 'traveling' from the soma (d) of a cell down its axon (e), the resting state of a cell is broken for a brief moment and membrane becomes permeable for positive ions to flow inside the cell resulting in the outside to be 'more' negative than the inside (f). For an instance the potential sharply increases (inside the cell membrane) and decreases (outside the cell membrane, g) – 'depolarization'. This is followed by a phase of the potential to overshoot (h) over its resting value - 'hyperpolarisation' - before coming slowly back - 'repolarisation' - to its resting state (i). This whole happening from resting state to action potential and back to resting state takes less than a millisecond. Graphic was modified after www.biochemtech.de.

recorded from much farther sources. This broader signal is termed local field potential, 'LFP', and is defined as the net activity of many cells. It is in some way reflecting the sum of action potentials of cells of approximately 50 - 300 µm (e.g. Gray et al., 1995; Katzner et al., 2009) away from the electrode. Other than that, the underlying biological principle of the 'LFP' is equivalent to that described above for the 'spike' signal.

2.4.3 Recording Preparations for Electrophysiology Experiments

In electrophysiology experiments it is also of great importance to determine the vertical and horizontal midline positions and place the stimulus monitor at the right height and center in front of the animal. The procedure to do so is exactly the same as in optical imaging experiments, refer back to section '2.3.3 Optical Recording Preparations' for a detailed description. Further, two other questions need to be addressed prior to recording with an electrophysiology setup with regard to the proposed research questions: a) Where in the visual field should we place the stimulus to arouse a response in the units off neurons which we are recording from? To answer this question the visual field is basically 'scanned' with moving light bars in timing correspondence to cortical activity. b) What stimulus characteristics should we use to optimally elicit cortical responses in our recording position? This question is only essential in an experimental setup with electrode recording – not so in optical imaging recording – because stimulus orientation is going to be chosen according to what a certain 'unit' (group of neurons) preferentially responds to.

Representation of Cortical Area in the Visual Field

In contrast to an optical imaging recording, in electrophysiology experiments one needs to determine the representation of the studied cortical area in the outside visual field in more detail. Namely, one has to determine the receptive field (RF) of neurons in the primary visual cortex. This term had been introduced in the introduction section '1.3 The Visual System – an Overview'. In brief again, the RF is defined as a restricted area in the visual world from which a neuron receives sensory information. Neurons that are close together in the cortex will have nearby if not overlapping receptive fields. When one records extra-cellular, i.e. in the inter-space between different neurons, the signal that gets picked up by an electrode is commonly that of multiple neurons together. Depending on the impedance of the electrode this number can

vary from two to hundreds of neurons. In our setup we recorded the response signal from a group of approximately ten neurons which is referred to as ‘unit’. As these neurons are very close together one can assume that there is no variation in receptive field location or any other characteristics. Thus when talking about a ‘unit’, we literally refer to a unity of neuronal properties. Note that we recorded with 32 electrodes simultaneously, so that we needed to determine 32 receptive field locations of these 32 units.

For locating the RFs, a computer generated light bar swept over the stimulation monitor in different orientations, always covering in length the full monitor size. For example, a vertical white bar would start from the left side of the monitor and move on a black background orthogonal to its orientation all the way to the right side of the monitor. Next a horizontal white bar would start from the top of the monitor and move downwards all the way to the bottom of the monitor, and so on. The speed of the bar movement was the same for all orientations, i.e. 20°/sec. The electrode recording of cortical activity has a high temporal resolution. A recorded unit will indicate stimulus driven activity when the light bar crosses its receptive field location. For all moving bars one can therefore determine that moment in time, i.e. distance it had traveled on the stimulation monitor that elicited a unit’s activity. Given bars of four different orientations with two directions of movement each (back and forth), the optimal response positions for all eight bars will cross in a single point (see the encircled red colored area in Figure 2.20 A): the receptive field of this unit. Thus, the stimulus monitor position could be adjusted (up or down and to the left or to the right) to place the center Gabor within the receptive field of a unit of interest, as for example shown in Figure 2.20 B.

Testing for preferred stimulus orientation

In electrophysiology recording, one electrode tip has a diameter of approximately 10 µm. Depending on which matrix of 4 x 4 electrodes was used, the inter-electrode distance was either 200 µm or 400 µm, in any case the span of all electrodes together included more than just one orientation column. In order to optimally stimulate a unit of neurons at one of the 32 specific electrode locations (in all experiments we always used two of those 4 x 4 matrices) one needs to find out what orientation that unit prefers. As a matter of fact, a unit might not respond at all or very little if stimulated with not optimally oriented stimuli. In order to get this information of orientation preference

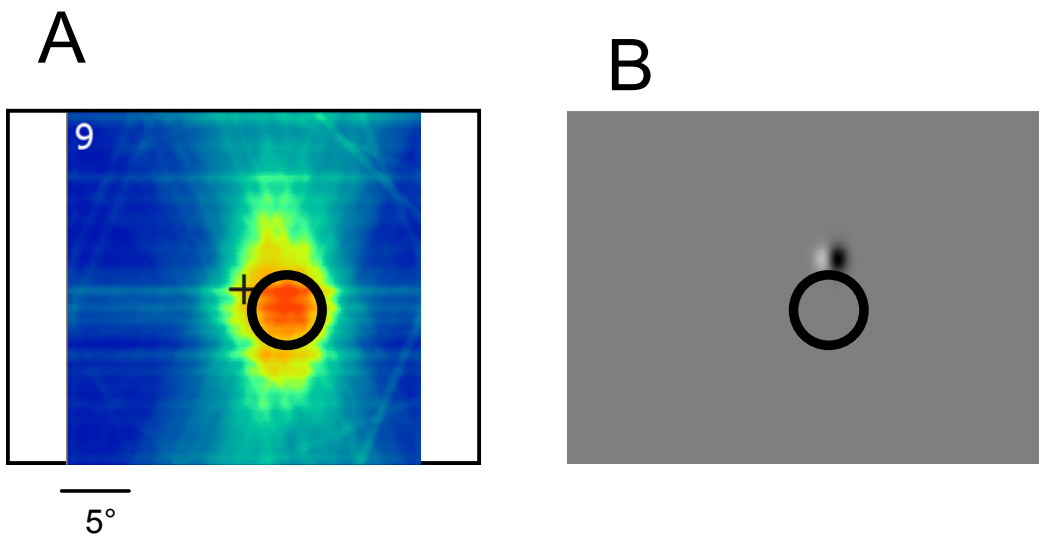

Figure 2.20 | Locating a receptive field in electrophysiology experiments. (here exemplary unit 9 out of a random experiment)
(A) The black square outline represents the stimulus monitor of 30x40 cm size, the black cross indicating the monitor center. The blue square represents the extension of the mapping program. Light bars of different orientations were swept over a black background across the stimulus monitor. For a given electrode unit a response signal was recorded whenever a bar crossed it's receptive field. In combining the response information of all bar orientations a common cross-point could be calculated: the receptive field (red coloring). Note that some faint 'blue-yellowish' lines are still visible indicating the full length of the stimulus bar in that given orientation. Overlaid for demonstration a black circle indicating the receptive field location after filtering the data to a more strict criterion
(B) The position of the center Gabor of all stimulus conditions is always the same, i.e. 2,5 cm above the horizontal center line of the monitor, and 2,5cm to the right of the vertical center line of the monitor. In this example of the receptive field location in **(A)** the monitor had to be moved downward to place the center Gabor stimulus inside the receptive field of momentary interest.

for the unit at each electrode position we recorded cortical activity while stimulating with whole field gratings (Figure 2.21) of varying orientations and directions of cycling movement. As these gratings cover the whole stimulation monitor it doesn't matter where the receptive field positions of each of the 32 units is at, they will be stimulated anyway. Note that all 32 receptive fields are for sure within the range of the monitor width and height, because electrodes were positioned in the representation of the central visual field. As a result one can plot orientation tuning curves (see Figure 2.22 for two examples) for all 32 units and choose those for the experimental sample that match the necessary requirements.

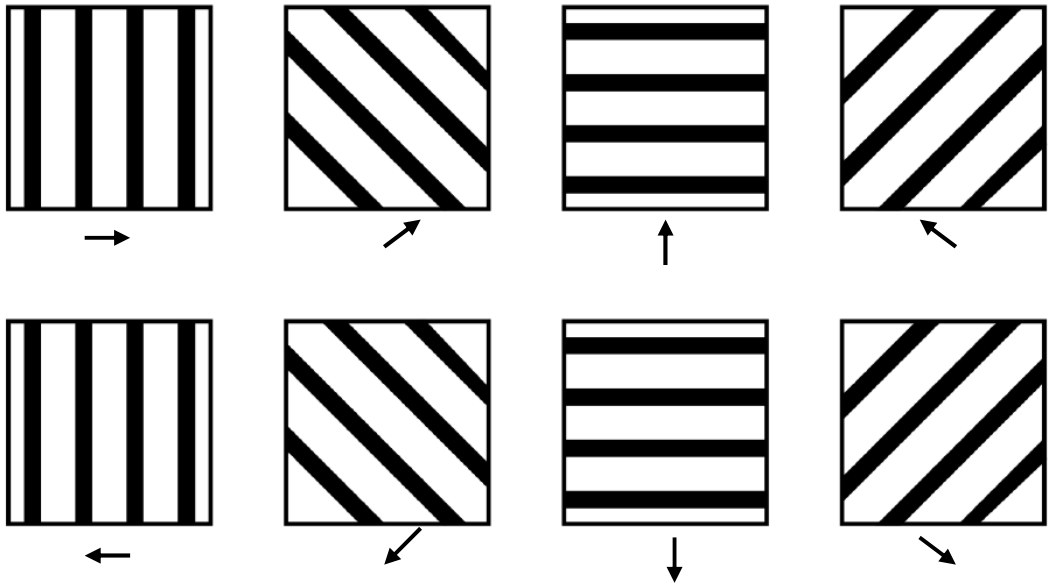

Figure 2.21 | Grating stimuli for determining a unit's orientation preference
Whole Field Grating Stimuli for four orientations and two directions of 'cycling' each. Note that 'cycling' refers to the observed appearance that the bars of the grating are moving in the direction, indicated by the arrow (→), and any part of the grating getting out of sight at the end of the monitor is added again on the opposite site.

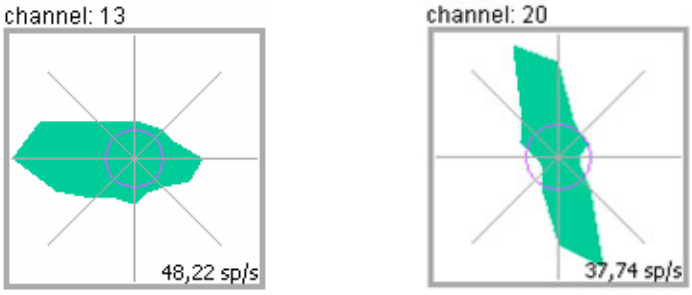

Figure 2.22 | Visualization of a unit's orientation preference: Tuning curves.
Two examples of tuning curves derived from multi-unit activation to eight whole field stimuli of different direction movement. Grey bars indicate direction of movement for grating stimuli, always oriented orthogonal to movement direction. Electrode channel 13 is direction selective for a vertical stimulus moving to the left. Electrode channel 20 is direction unselective, it responses equally well for stimuli of horizontal orientation moving up- or downwards. The value in the lower right corner of the graph indicates the maximal number of spiked recorded in either direction of the eight whole field gratings. The violet circle indicates the amount of non-stimulus driven spiking activity.

2.4.4 Electrophysiology Data Acquisition

Once the electrodes were inserted into the cortex, the cortex surface was covered with Agar, a gel-like substance, to stabilize the brain from natural pulsation (due to heart rate and breathing). Later in the experiment the electrodes were pushed deeper into the cortex tissue but spatially they remained in one position at all times.

Before recording was started some preparations had to be taken care of, for example where to place the stimulus monitor. These recording preparations will be described in a later section as their content depend on the understanding of this description of recording technique, data acquisition and processing.

In electrophysiology experiments all 6 stimulus conditions (see section '2.2.1 Visual Stimulus Conditions') were presented 20 times each in a pseudo-random sequence. Each stimulus condition was shown for 2000 ms but recording started 500 ms prior to stimulus onset with a uniform grey (blank) screen and lasted until the condition disappeared. This so called 'blank' recording serves to have a relative comparison between non-stimulus driven activity and stimulus driven activity, and will be addressed closer in the results section. Between the subsequent recordings for each condition a 1500 ms inter-stimulus-interval paused the recording. Figure 2.23 visualizes the timing for stimulation and recording in electrophysiology.

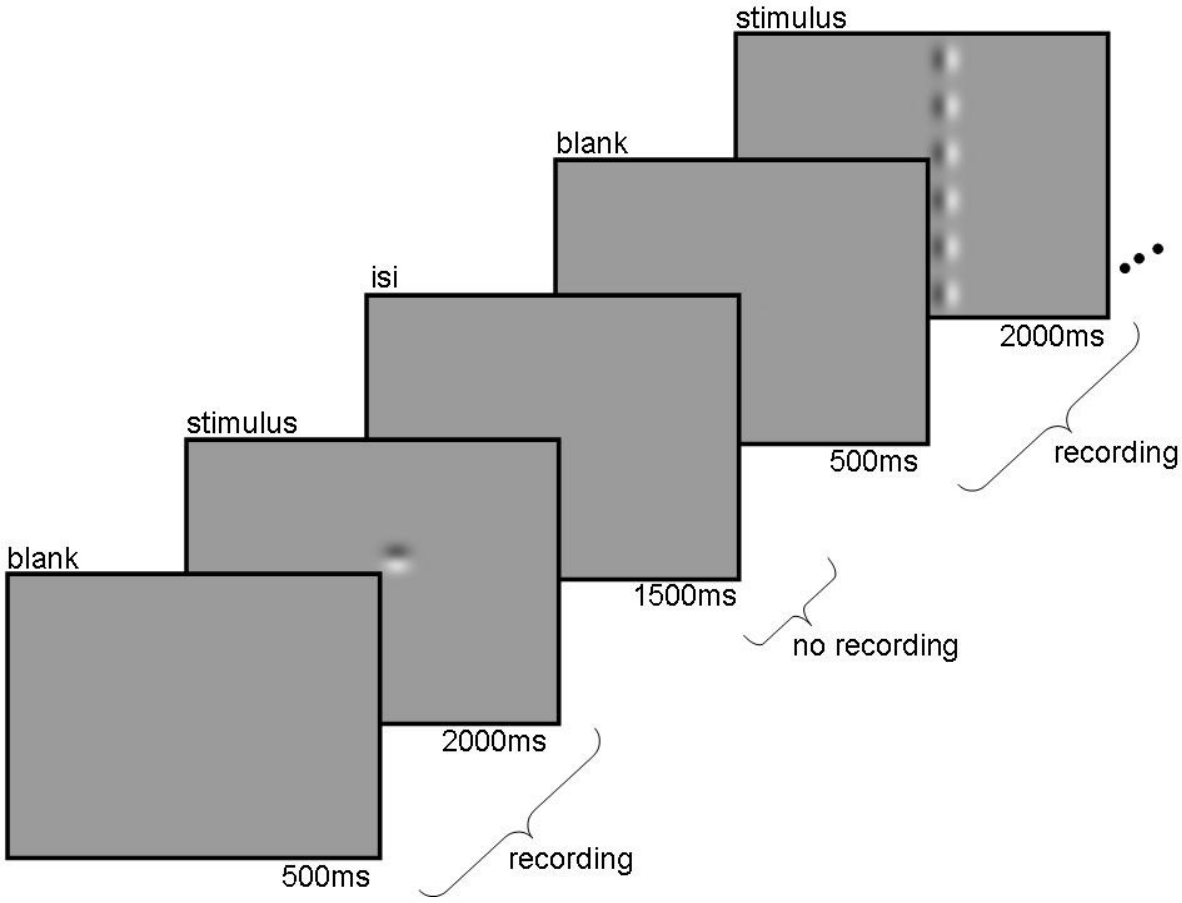

Figure 2.23 | Timing of stimulation and recording in electrophysiology.
Each stimulus condition was shown for 2000 ms but recording started 500 ms prior to stimulus onset on a uniform grey (blank) screen and lasted until the one stimulus condition disappeared. Between the subsequent recordings for each condition a 1500ms inter-stimulus-interval (isi) paused the recording, and was then continued for the next stimulus condition.

As mentioned earlier, the recording electrode was placed in the vicinity of many neurons. The recorded signal was from more than one neuron and thus was called ‘multi-unit’ recording. In some studies it is essential to do ‘spike sorting’, that is the sorting of the spike with regard to different neuronal sources according to similarities in their shape, for example their rising and falling slope. It is a very challenging work, there are many different methods on the market, and sorting is always subjective. For the frame of this study it was therefore decided to use the ‘multi unit’ signal. Neurons which are in reach of an electrode are considered to have very similar re-

sponse properties and therefore serve as a reliable estimate of the average single-unit (e.g., Super & Roelfsema, 2005).

Considering this signal over time, it contains a variety of frequencies ranging from very slow frequencies of 1 Hz (= s^{-1}) to very fast frequencies in the kilohertz range. Commonly, the signal is hardware filtered during recording in order to reduce the immense amount of data and also to focus the analysis on a defined frequency range. A low pass filtered signal, i.e. 1 Hz - 100 Hz, is called Local Field Potential (LFP). If one applies a high pass filter to the signal, i.e. only looking at the range of 700 Hz – 3 kHz, so called spiking activity can be detected. Note that the recorded signal is commonly very weak and thus is amplified to a 20 x 50 fold strength in our hard-ware system. For the latter frequency range, i.e. spiking activity, we set by hand an amplitude threshold for each electrode channel that is well above noise level, but still in range to include the amplitude of a potential spiking event to cross this threshold. 'Noise' in this case is referred to a stimulus independent ongoing voltage change usually in a range of +/- 10mV. For further analyses, a computer program stores the time stamps for spikes for each time when the amplitude of the rising voltage change crossed the amplitude threshold.

2.4.5 Electrophysiology Data Processing

Not all electrode recordings during an experiment could be included in the data sample. This might partly be due to an electrode simply showing no signal at all or due to some restrictions on receptive field positions and orientation preference characteristics. Taken together from all experiments using electrophysiological recording N = 78 units were selected as 'valid' and thus included in the data sample.

For each unit included in the data sample the number of spike events that occurred in a certain time frame were drawn from the recording. The number of spikes, i.e. time stamps from when a spike occurred and crossed the amplitude threshold, can be visualized in a post-stimulus-time-histogram (PSTH). Figure 2.24 displays such a PSTH for number of spikes in each ms summed over 20 trials for a random stimulus condition. The number of spikes that occurred in a specific time frame, for example within one second, were then averaged across that one second recording time and also across trials. The time window that is chosen for averaging the number of spike events was set between 800 ms and 1800 ms. It is common to choose a starting time somewhat after stimulus onset (which was at 500 ms in our

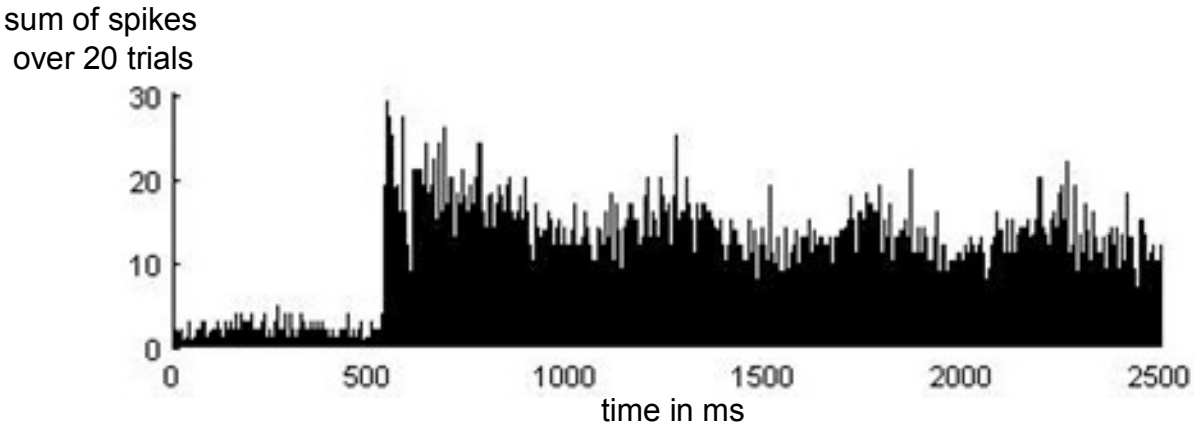

Figure 2.24 | Example Post-Stimulus-Time-Histogram (PSTH).
For visualization number of spike events are summed over 20 trials for a random stimulus condition. Stimulus onset was at 500ms and lasted for 2000ms until the end of the recording cycle. There are very few spike events before stimulus onset, mainly originating from ongoing spontaneous activity. There is an increased number of spikes once the stimulus presentation has started and there appears to be some 'waveform' in the course of the spike-sum with two peaks of these waves within one second, e.g. at 1250ms and at 1750ms. This complies a 2Hz rhythm which is in accordance with the cycling frequency of the presented stimulus (refer back to the section on stimulus conditions for a more detailed explanation).

experimental settings) as the stimulus onset, i.e. sudden bright light input, can cause recording artifacts. Thus, the resulting value of average number of spikes per second (sps) was calculated for each condition of the stimulus protocol and stored for further analyses. Note that there appears to be a 'waveform' in the course of the spike-sum PSTH (Figure 2.24) with two peaks of these waves within one second, e.g. at 1250 ms and at 1750 ms. This complies a 2Hz rhythm which is in accordance with the cycling frequency of the presented stimulus, which is exactly what would be expected (refer back to section '2.2.1 Visual Stimulus Conditions' for a more detailed explanation).

2.4.6 Histological Post-Processing

The brain tissue from the first three animals of electrophysiology recording, was used for further histological examination. The purpose of this work was to determine the electrode paths relative to cortical area 17 and 18 of cat V1, and relative to cortical layers. As mentioned before this was a very extensive and time consuming work and unfortunately did not deliver the desired information. Nevertheless, the best example of detected electrode paths will be presented in this section to give an idea of what the histology work looks like. These histological images also serve to visualize the different cortical layers as it has been referred to in previous sections of this writing.

Figure 2.25 A shows a graphic of the cat cortex overlaid with marks of where coronal sections that were taken post-mortem. Figure 2.25 B shows one example of a coronal section of the cat brain. The coronal sections had been stained with Nissl tincture, which is known to stain the cell bodies in the brain tissue, so that all areas of dark violet color indicate neuronal cell bodies. Figure 2.25 C shows an enlargement of the (green) marked region in Figure 2.25 B, overlaid with a graphical marking of the different cortical layers. Note that there are two of these markings, the one in the left half of the image indicate the layers of area 18, the marking in the right half of the image indicates the layers of area 17. Note the most prominent difference between the two, in that A18 had a wider cortical layer III, while A17 had a wider cortical layer IV.

Figure 2.26 shows three of those enlargements similar to the one in Figure 2.25 C. Here the first enlargement was taken from cut number 311 starting from the posterior end of the cortex, with each cut being of 60 µm thickness – this adds up to a distance of 18660 µm from the posterior end of the cortex. Note that it is nearly impossible to perform the coronal sectioning parallel to the electrode tracks, so that electrode lesions can only be found on subsequent sections. In this example one can see marks of electrode tracks, encircled in red. This is one of the few examples where the histology sections were of such good quality to actually find the electrode ‘holes’. If one could find all 32 electrode tracks, and knowing what cutting distance they are from the posterior end of the cortex, then one could protocol position and depth of all electrodes. But as the low quality of the histology work does not allow to gather all necessary information for a full analysis of the planned inquiry, this section on histology will only serve as a brief description of the technique without any further implications on the results of this project.

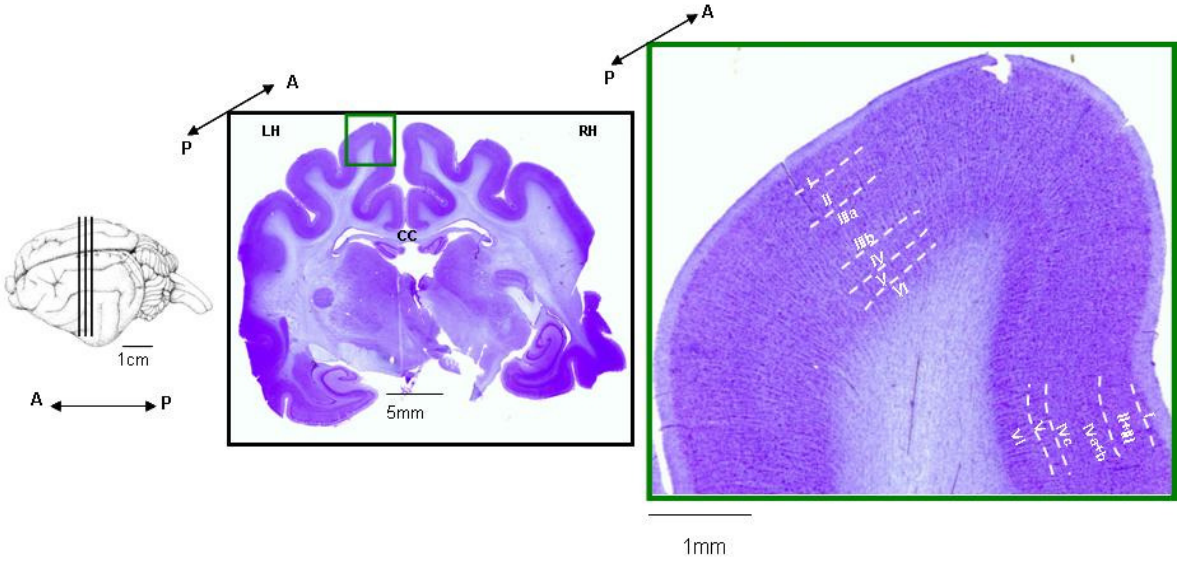

Figure 2.25 | Coronal section of the post-mortem cortex, stained with Nissl.
(A) Graphic of the cat cortex overlaid with marks of the coronal sections that were taken post-mortem. A = Anterior, P = Posterior
B) Example of coronal section from **(A)**, stained with Nissl. All areas of dark violet color indicate neuronal cell bodies. CC = Corpus Callosum
(C) Enlargement of the green marked section in B), overlaid with with a graphical marking of the different cortical layers. Note that there are two of these markings, the one in the left half of the image indicate the layers of area 18, the marking in the right half of the image indicates the layers of area 17. Note the most prominent difference between the two, in that are 18 has a wider cortical layer III (a + b), while area 17 had a wider cortical layer IV (a + b).

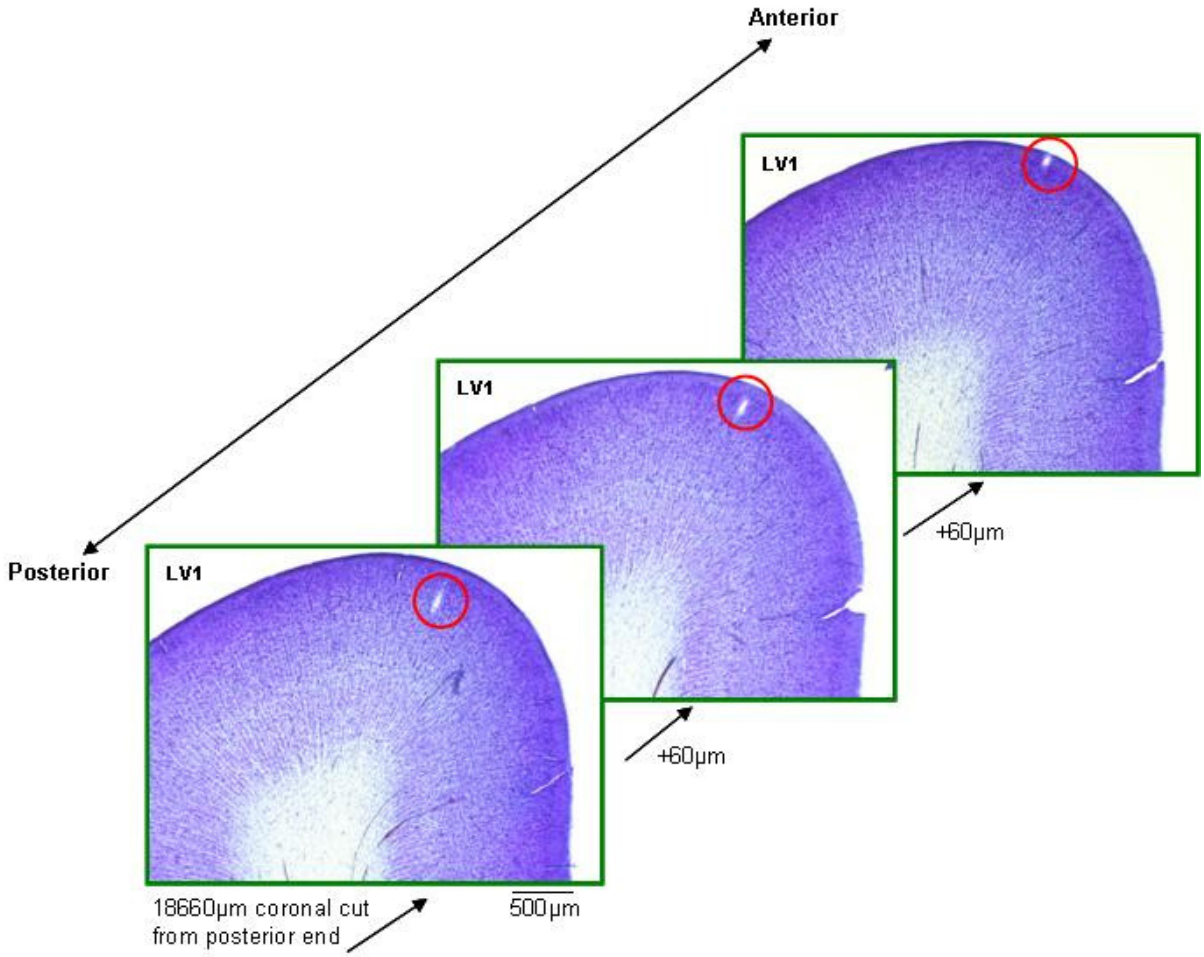

Figure 2.26 | Attempt to find electrode tracks in coronal sections of the cat primary visual cortex.
Three enlargements similar to the one in Figure 2.25 C. Here the first enlargement was taken from cut number 311 starting from the posterior end of the cortex, with each cut being of 60 µm thickness – this adds up to a distance of 18660 µm from the posterior end of the cortex. Every further section is another 60 µm further anterior in brain coordinates. Note that it is nearly impossible to perform the coronal sectioning parallel to the electrode tracks, so that electrode lesions can only be found on subsequent sections. In this example one can see marks of electrode tracks, encircled in red. LV1 = Left Primary Visual Cortex

2.4.7 Dependent Variable Derived from Electrophysiology Recording

The data collected from electrophysiology recording is the spike rate (SR). This value represents the intensity of neuronal activity recorded locally at different electrode positions, averaged over the time period of one second and over different trials. The SR data value is naturally very variable between electrode units due to electrode properties. For example, averaged over time and trials at one unit the mean spike rate per second (sps) could be 10 sps while for another unit the value could be 100sps, a large numerical difference without any meaning with regard to content. Therefore, the SRs from different electrode units cannot simply be averaged across the sample. Instead, for each electrode unit the SRs derived while stimulating with the respective stimulus conditions were put in comparison. A similar procedure was undertaken in a study by Chisum et al. (2003) in the tree shrew using similar stimuli. In their study they subtracted spiking activity (P) to a collinear line stimulus by spiking activity under non-collinear line stimulation and divided this difference by the sum of the two, and named the resulting value 'Facilitation Index':

$$\text{Facilitation Index} = (P_{collinear} - P_{non\text{-}collinear}) / (P_{collinear} + P_{non\text{-}collinear})$$

In doing so they normalized their data to values in the range from -1 to 1 with negative values being in favor of spiking activity under non-collinear line stimulation and positive values indicating a greater spiking activity under collinear line stimulation.

In the frame of this research project it was decided to normalize spiking activity to both lines separately from each other by using the spike rate to the single Gabor condition as a reference for each. This allowed to study the influence of RF surround context separately for the two line variations in contrast to RF stimulation only. Thus, for each electrode unit the SR during RF stimulation with surrounding collinear context (SR_coll for collinear line) was subtracted from the SR during Single Gabor stimulation (SR_SG), and the resulting difference was then divided by the sum of the two respective variables. Along this line the same calculation was performed for the SR during RF stimulation with surrounding non-collinear context (SR_nc for non-collinear line). This calculation normalized the SR differences to values in the range between -1 and 1. Depending on which context was considered in the formula the resulting value can be considered as a spike rate index for collinear context (F.1) or a

spike rate index for non-collinear context (F.2). Thus, this index value, here under two different conditions, defines the dependent variable derived from electrophysiology recording.

‘Collinear spike rate index’ = (SR_coll –SR_SG) / (SR_coll + SR_SG) (F.1)

‘Non-collinear spike rate index’ = (SR_nc –SR_SG) / (SR_nc + SR_SG) (F.2)

2.5 Experimental Design

The following section will introduce the experimental variables and planned analyses applied to the data from both recording methods. While the dependent variable for electrophysiology recording is the spike rate index, the dependent variable for optical imaging is an pixel activity index.

The differentiation between collinear versus non-collinear arrangement of context elements serves as the first independent variable of the experimental design. Recording different stimulus conditions was performed also while cooling the contralateral hemisphere. Thus, comparing the above defined index values before cooling, i.e. baseline, and during cooling serves as the second independent variable of the experimental design. Figure 2.27 visualizes the two factors with two levels each.

In animal physiology research with electrode recording it is common to gather various data points within each animal and then merge the data points together across all animals, in some way ‘pretending’ all data was collected in one animal only. Thus, in electrophysiology experiments the sample of different recordings across animals is treated like a sample of random data points. Data were collected from 6 cats. Spike rate activity was recorded from different electrodes within each animal and then merged across all other animals into one common sample of N = 89 units. In Optical Imaging experiments data were collected from 5 cats, in one of them two recordings were carried out. Thus, the sample size was N = 6 randomly sampled optical recordings.

On the basis of the proposed research questions there is no evidence from prior studies to differentiate between neurons of different orientation preference. Nevertheless, due to the methodological fact that two different population of neurons (horizontal vs. vertical orientation preference) were addressed and each optimally stimulated during experimental recording, this factor of ‘orientation’ suggests itself to be included in the statistical analysis. Adding a third factor to the design may improve the chance to reduce more error variance (Maxwell & Delaney, 2005). Figure 2.28 A visualizes the three-factorial design after adding the factor ‘orientation’ to the previous version shown in Figure 2.27. All three factors have two levels of action, while the levels of ‘context’ and ‘state’ are repeated measures, the ‘orientation’ factor

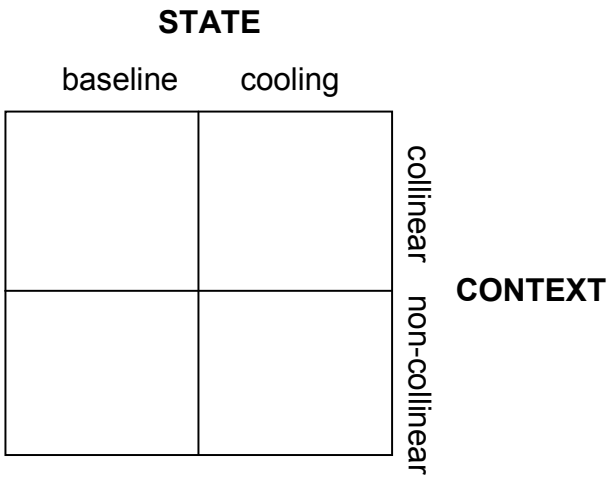

Figure 2.27 | The two factors of this study, state and context.
The first factor 'context' consists of two levels (collinear and non-collinear), the second factor 'state' also consists of two levels (baseline and cooling). Note that both factors are repeated measures because for each sample case data are collected across all levels of the defined variables.

is a between-subject factor as the two levels describe statistically independent populations.

The separate levels of the factor 'orientation' was also made possible for optical imaging data. Here, both types of local stimulus orientations, horizontal and vertical, had been used for stimulus presentation as well. Each image recorded while stimulating with a stimulus of either orientation is defined by pixels. These pixels can be sorted according to the orientation preference assigned to the underlying orientation columns. Thus, in the imaged cortical region, pixels assigned to horizontal vs. vertical preference will be averaged separately. Within each image these two groups of pixels are non-overlapping.

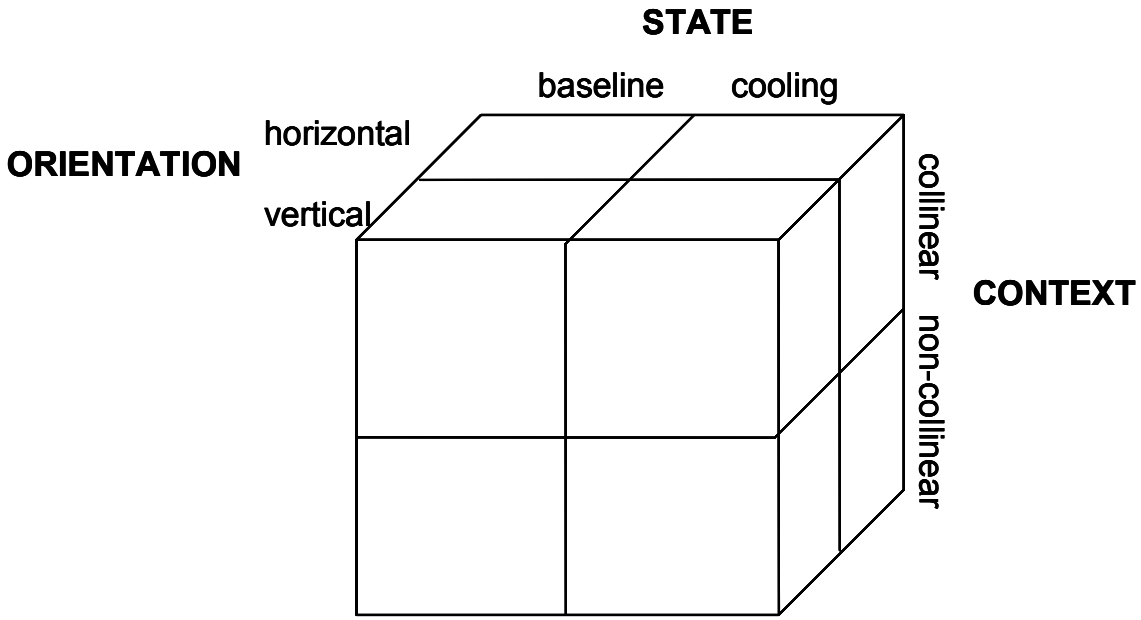

Figure 2.28 | The extended experimental design: the three factors of this study
The distinction between neurons of vertical versus horizontal orientation preference is taken up as an additional factor into the experimental design. The design now consists of three factors with two levels each: ‘state’, ‘context’, and ‘orientation’. Refer to the text for more detailed explanation.

3 RESULTS

Science cannot solve the ultimate mystery of nature. And that is because, in the last analysis, we ourselves are a part of the mystery that we are trying to solve.

- Max Planck, Where is science going?, 1932 -

3.1 Results from Electrophysiology Experiments

The means and standard deviations for the units' spike rate indices under different conditions are presented in Table 3.1. By definition, the possible indices ranged from -1 to 1. The total sample of 89 units were divided into 33 units with horizontal orientation preference (h-units) and 56 units with vertical orientation preference (v-units).

In the baseline state, the mean index value for the h-units was smaller for the collinear context (M = -.036) compared to the non-collinear context (M = 0.58), while for the v-units it was vice versa (M = .064 for collinear vs. M = -.004 for non-collinear). The same pattern of mean indices was found in the cooling state with h-units having a smaller mean collinear index (M = -.094 vs. M = .059 for non-collinear index) and v-units vice versa (M = .106 for collinear vs. M = -.019 for non-collinear).

From the baseline to the cooling state the collinear index for h-units decreased (from M = -.036 to M = -.094) while it increased for v-units (from M = .064 to M = .106). For the same change in state the non-collinear index for h-units increased (from M = .058 to M = 0.59) while it decreased for v-units (M = -.004 to M = -.019).

Further, it appears noteworthy that the standard deviations for v-units are overall larger with the smallest value at SD = .316 compared to those for the h-units with the largest value at SD = .190 with both SD values derived from the respective baseline collinear condition.

Table 3.1 | *Mean Spike Rate Indices and Standard Deviations for Units of Horizontal and Vertical Orientation Preference*

		baseline		cooling	
		collinear	non-collinear	collinear	non-collinear
horizontal	M	-.036	.058	-.094	.059
	SD	.190	.123	.187	.127
	n	33	33	33	33
vertical	M	.064	-.004	.106	-.019
	SD	.316	.318	.322	.348
	n	56	56	56	56
	N	89	89	89	89

3.1.1 Context Effect on Recorded Spiking Activity

To address the first research question in how far neuronal activity in the primary visual cortex already reflects the perceptual advantage of a collinear line over a non-collinear line of oriented elements, as proposed by the Gestalt law of collinearity on a phenomenological level, an analysis of variance (ANOVA) was performed to reveal the effect of 'context' on the spiking activity recorded in cat primary visual cortex. For this purpose, the analysis was focused on recordings performed during baseline state only. It was hypothesized that neuronal activity in V1 varies as visual stimuli of collinear vs. non-collinear context are presented. To improve the chance of explaining error variance in the analysis, the between-subjects factor of 'orientation' was included in the design. This additional factor distinguished between neurons of horizontal orientation preference vs. units of vertical orientation preference. As the factor of 'context' was a repeated measures variable with two experimental levels, collinear vs. non-collinear, a 2 x 2 mixed-design ANOVA was used for this analysis.

Before calculating the ANOVA it should be noted that this analysis holds certain assumptions about the population that the given sample was drawn from. One of the assumptions is that the data is normally distributed. In the given sample of this

study this is not the case. However, at large sample size (here N = 89) the ANOVA is robust if the assumption of normal distribution is not met (a large sample size is indicated as N = 30 and more, Maxwell & Delany, 2005). Another assumption for a repeated measures design is that of sphericity, i.e. that the variance of differences between all levels of a factor is equal. However, if a repeated measures factor has only two levels then the assumption of sphericity is automatically met (Maxwell & Delany, 2005).

Results revealed no significant main effect for the factor 'context' ($F(1,87) = .355$, $p = 553$, $\eta^2 = .004$). There was also no significant main effect for the factor 'orientation' ($F(1,87) = .119$, $p = .730$, $\eta^2 = .001$). However, the interaction between these two factors 'context' x 'orientation' was found to be significant ($F(1,87) = 14.073$, $p < .05$, $\eta^2 = .139$). For h-units, the mean spike rate index was positive and higher in value for the non-collinear stimulus context (M = .058, SEM = .021) than for the collinear stimulus context (M = -.036, SEM = .033). In contrast, for v-units the result was vice versa with higher mean spike rate in response to collinear stimulus context (M = .064, SEM = .042) compared to non-collinear stimulus context (M = -.004, SEM = .042). The ANOVA results are summarized in Table 3.2 and the interaction effect between the two factors is visualized in Figure 4.1.

Using η^2 (read eta squared)[1] as the measure of effect size, the significant interaction between 'context' and 'orientation' in the baseline state accounted for approximately 14% of the total variability in the spike rate index values.

[1] Note that the effect value η^2 is dependent upon the magnitude of the other effects, as it is calculated SS_{effect}/SS_{total}. Thus, some researchers report instead η^2_p (partial eta squared) that is calculated $SS_{effect}/SS_{effect}+SS_{error}$, which is essentially the equivalent to the η^2 value one would have obtained in a single factor design with the other factor(s) in the design held constant (Maxwell & Delaney, 2005). As η^2 is described to already overestimate the true value in the population (Howell, 2008), and η^2_p is always equivalent to or even larger than the η^2 value, it seems more appropriate to report η^2. For a more detailed description see also Levine & Hullett (2002) who discuss limitations and strengths of different estimates for effect sizes.

Table 3.2 | *Analysis of Variance for Spike Rate Indices in Dependence of the Factors 'Context' and 'Orientation'.*

Source	MS	df	F	η^2	p
		Between units			
orientation	.008	1	.119	.001	.730
error	.063	87			
		Within units			
context	.007	1	.355	.004	.553
context x orientation	.272	1	14.073	.139	.000
error	.019	87			

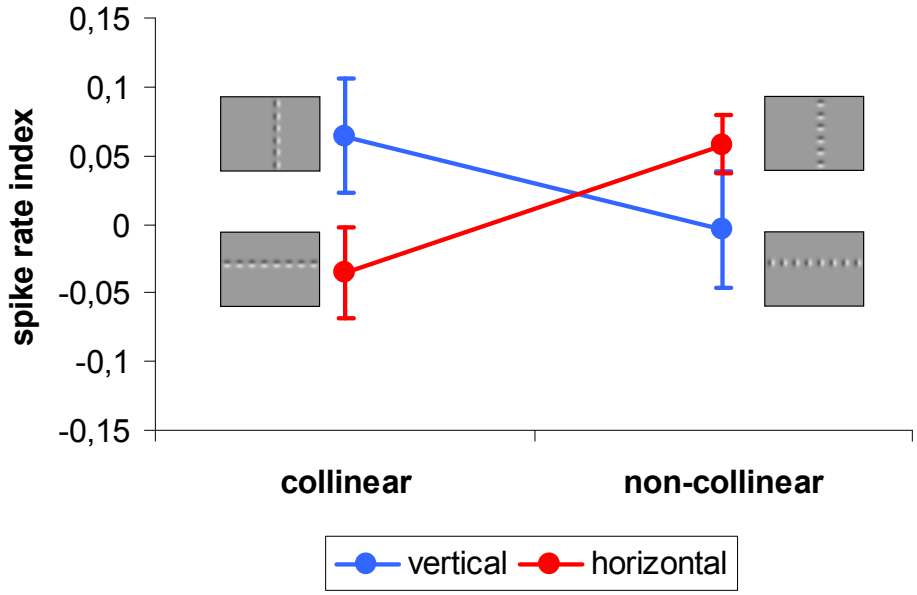

Figure 3.1 | Significant interaction between the factors 'context' and 'orientation' during baseline recording
Units of horizontal orientation preference showed an on average lower response to collinear compared to non-collinear stimulus context. In contrast, units of vertical orientation preference showed an on average higher response to collinear compared to non-collinear stimulus context. This interaction of the two experimental factors 'context' and 'orientation' during baseline recording was statistically significant. See text for more details. Error bars are SEM. N = 89 units (horizontal n = 33; vertical n = 56).

3.1.2 Cooling Effect on Recorded Spiking Activity

The second research question of this study was what role the intact primary visual cortex plays across both hemispheres in reflecting the advantage of a collinear over a non-collinear line of elements. An ANOVA was conducted to reveal the effect of 'state' on the spiking activity when stimulated with collinear vs. non-collinear 'context'. The factor of 'orientation' was again included in the design to improve the chance of possibly explaining more error variance in the data. Thus, a 2 x 2 x 2 mixed-design ANOVA was used for analysis. Here, the first repeated measures variable was 'context' with two levels, 'collinear' vs. 'non-collinear'; the second repeated measures variable was 'state' with two levels, 'baseline' vs. 'cooling'. The third variable was a group variable for the two sets of units with different 'orientation' preference, i.e. vertical vs. horizontal. The reader please note that the previous ANOVA conducted for baseline recording only, can be considered as a conditioned analysis of the present ANOVA including the factor of 'state'.

As can be seen in Table 3.3, the ANOVA results revealed no significant main effect for any of the three factors on the spike rate index values. The two experimental levels for the factor 'context' were not significantly different ($F(1, 87) = .495$, $p = .484$, $\eta^2 = .002$). The factor 'state' did not reveal any significant main effect either ($F(1,87) = .150$, $p = .699$, $\eta^2 = .001$). And the main effect for the factor 'orientation' was not significant either, ($F(1,87) = .547$, $p = .462$, $\eta^2 = .006$).

Further, the first order interaction revealed a significance between the factors 'context' x 'orientation', ($F(1,87) = 32.977$, $p < .05$, $\eta^2 = .015$) but neither interaction between 'context' x 'state', ($F(1,87) = .007$, $p = .935$, $\eta^2 = .000$) nor 'state' x 'orientation', ($F(1,87) = 1.226$, $p = .271$, $\eta^2 = .005$) was significant. The significant interaction between the factors 'context' x 'orientation' was already revealed in the previous ANOVA calculated for baseline (i.e. prior to cooling) data only, as the first research hypothesis had addressed only that state. The interaction effect remains significant despite the joint consideration of baseline and cooling data. However, the effect measure dropped from $\eta^2 = .139$ for the 'context' x 'orientation' interaction in the baseline state to only $\eta^2 = .015$ taken baseline and cooling state together. Thus, the later accounts for approximately 2% of the total variability in the data.

Table 3.3 | *Analysis of Variance for Spike Rate Indices in Dependence of the Factors 'Context', 'State' and 'Orientation'*

Source	MS	df	F	η^2	p
		Between units			
orientation	.133	1	.547	.006	.462
error	.243	87			
		Within units			
context	.015	1	.495	.002	.484
context x orientation	1.003	1	32.977	.015	.000
error	.030	87			
state	.004	1	.150	.001	.699
state x orientation	.036	1	1.226	.005	.271
error	.030	87			
context x state	.000	1	.007	.000	.935
context x state x orientation	.070	1	15.029	.059	.000
error	.005	87			

Finally, the second order interaction between all three variables 'context' x 'state' x 'orientation' was significant, $F(1,87) = 15.029$, $p < .05$, $\eta^2 = .059$. This second-order interaction indicates that a first order interaction differs significantly between the levels of a third factor, here the previously mentioned interaction between 'context' and 'orientation' differing between baseline and cooling 'state' (Figure 3.2). At first glance the mean spike rate indices for collinear context differ even more during cooling state between the two neuronal groups of orientation preference. However, to address the second research question the following display of results emphasizes the change of mean spike rate indices from baseline to cooling 'state' for all four combinations of levels for 'context' and 'orientation' (Figure 3.3). The mean

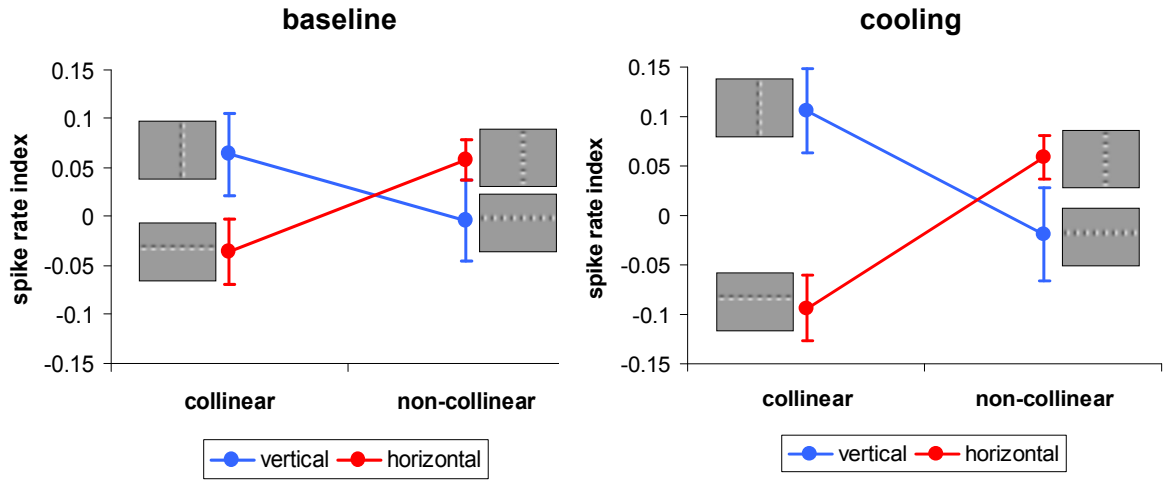

Figure 3.2 | Interaction between 'context' and 'orientation' differs on the two levels of 'state'.
The pattern of results for units of vertical vs. horizontal orientation preference in response to different stimulus contexts is compared for baseline (left) and cooling (right) state. The most notable difference between the two states is for collinear stimulus context where the mean values during cooling differ even more between units of vertical vs. horizontal orientation preference. Error bars are SEM.

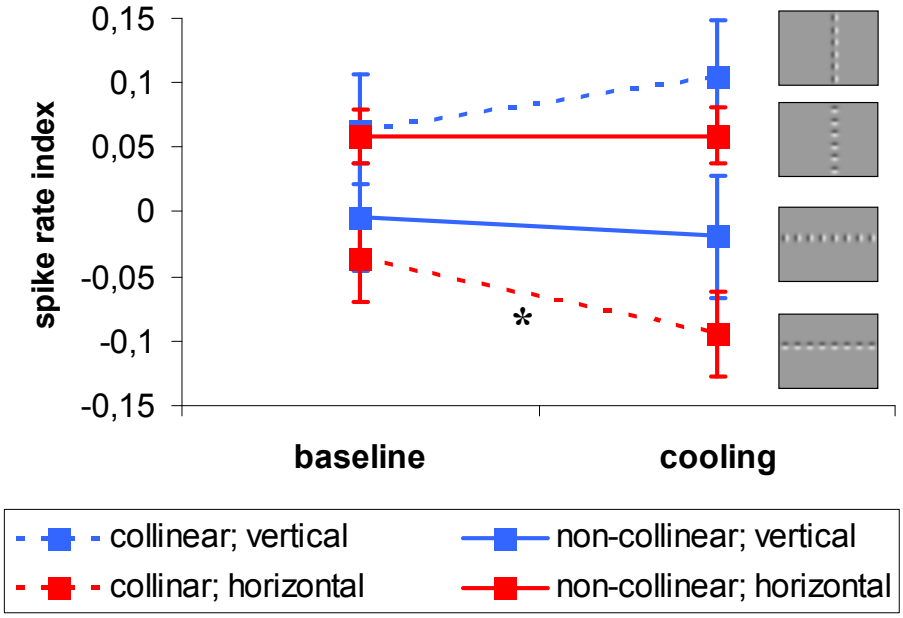

Figure 3.3 | Significant second order interaction between the factors 'context', 'orientation' and 'state'.
Units of horizontal orientation preference showed on average a decrease in mean spike rate index from baseline to cooling for collinear stimulus context, but on average an increase for collinear stimulus context. In contrast, units of vertical orientation preference showed on average an increase in mean spike rate index from baseline to cooling for non-collinear stimulus context and vice versa for collinear stimulus context. This three way interaction was statistically significant. See text for more details. Error bars are SEM. N = 89 units (horizontal n = 33; vertical n = 56). * $p < .05$

collinear index for v-units increased from baseline (M = .064, SEM = .042) to cooling (M =.106, SEM = .043) state, while for the same group of units the mean non-collinear index decreased from baseline (M = -.004, SEM = .042) to cooling (M = -.019, SEM =.047) state. For h-units the effect of cooling on the different context levels was the opposite. Here, the mean non-collinear index increased (slightly) from baseline (M = .058, SEM = .021) to cooling (M = .059, SEM = .022), while their mean collinear index decreased from baseline (M = -.036, SEM = .033) to cooling (M = -.094, SEM = .033) state. Note that the mean indices that were positive during baseline state remained so and even increased during cooling, while mean indices that were negative during baseline state dropped even lower during cooling.

Using η^2 as the measure of effect size, the significant interaction between 'context', 'orientation', and 'state' accounted for approximately 6% of the total variability in the spike rate index values.

In the frame of the second research question it had been hypothesized that especially the representation of contextual lines crossing the vertical midline would be affected by temporal deactivation of V1 in one hemisphere. In particular, it was proposed that neuronal activity in response to a collinear stimulus crossing the vertical midline would be more affected than in response to a non-collinear stimulus represented in both hemispheres. Thus, the mean spike rate indices for the two stimulus conditions crossing the vertical midline, i.e. collinear line of horizontally oriented elements vs. non-collinear line of vertically oriented elements, were compared pair wise between baseline and cooling state. Results revealed a significant decrease in mean spike rate index from baseline (M = -.036, SEM = .033) to cooling (M = -.0936, SEM = .033) state for h-units in response to a collinear stimulus context, $t(32) = 2.476$, $p < .05$. On the other hand, for v-units the decrease in mean spike rate index in response to the non-collinear stimulus context revealed no significant difference between baseline and cooling state, $t(55) = .569$, $p = .57$.

It should further be noted that the mean spike rate index for the collinear line consisting of vertical elements, thus running parallel to the vertical midline, showed even an increase from baseline (M = .064, SEM = .042) to cooling (M = .106, SEM = .043). This trend was analyzed with a t-test that revealed no significance, $t(55) = -1.358$, $p = .18$.

3.2 Results from Optical Imaging Experiments

Optical Imaging was performed in five animals. In four animals one data set was recorded each, and in one animal two data sets were recorded (independently, on different days) Thus, all together the results presented in the following are based on a sample of N = 6 data sets. Each of the six data sets consists of different images taken under specific stimulus conditions. First, it was determined where on the imaged cortical region the center Gabor stimulus (which all conditions had in common) was represented. As visualized exemplarily for one data set in Figure 3.4, this 'region of interest' (ROI) was marked on each image and the data analysis was focused on the pixels therein. Thus, for all stimulus conditions, a collinear line of vertical elements, a non-collinear line of vertical elements, and a collinear and non-collinear line of horizontal elements respectively, a map of cortical activity was imaged. Each image contained pixel grey values at a spatial resolution of 1 pixel = 12 x 12 μm^2, the data information was binned by 2. Dark spots in the image indicated high cortical activity and bright spots indicated low cortical activity (see Figure 3.4 right side). For normalization, pixel values for each of the four images captured under a certain stimulus condition were put in relation to the image value taken for the respective single Gabor condition. Refer again to section '2.5 Experimental Design' for a more detailed explanation of how the normalization was calculated. By definition, the resulting activity index for each pixel in a given image was in the range from -1 to 1 (but note that data values did not actually occupy the whole range), where a positive value indicates higher cortical activity for the respective line stimulus, and a negative value indicates an activity advantage for the single Gabor stimulus. In addition, cortical activity maps taken beforehand for whole field gratings of 0°, 45°, 90°, or 135° orientation (refer again to Figure 2.21) were processed to reveal an angle map (Figure 3.4, bottom right) of the imaged cortical region. Note that angles in between are interpolated during data processing. All pixels within the given ROI can then be assigned to the stimulus orientation that it responded most to, i.e. similar to a neuron's orientation preference in electrophysiology recording.

Next, all values of pixels assigned to vertical orientation preference (± 22,5°), i.e. pixels assigned to angles from 0° to 22,5° and 158,5° to 179°. Along the line all values of pixels assigned to horizontal orientation preference (± 22,5°), were also averaged, i.e. angles from 90°± 22,5°. Thus, for each of the six data files there are 8

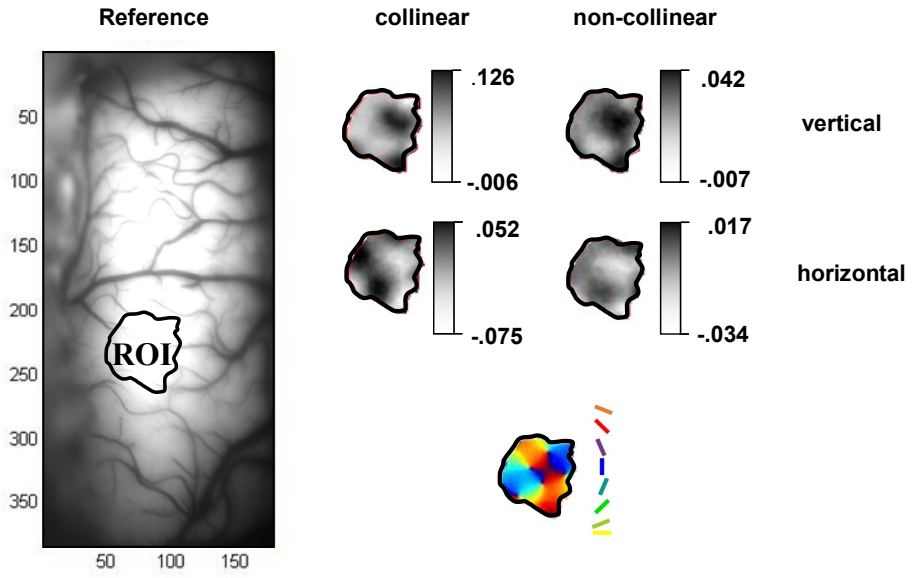

Figure 3.4 | Example for optical imaging data.
Optical images were taken of the V1 cortical surface in Experiment 091608b which is 180 x 384 pixels in size (due to 2 x 2 binning of data this corresponds to 4,42 x 9,2 mm). Refer again to Figure 2.10 for a better understanding of where the camera was positioned over the cat cortex. The cortical area representing the location of the center Gabor stimulus was determined, i.e. region of interest (ROI). The reference image (left side) shows the ROI in relation to the blood vessels visible on the cortex surface.

The four ROIs of the activation maps under different stimulus conditions are shown on the right. Activation maps contain dark pixels for active cortical areas under the given stimulus setting, and bright pixels for areas that were not responsive. Scale Bars to the side indicate maximum and minimum pixel index values for each of the four activation maps. Below in color is the distribution of optimal orientation preferences which can be assigned to each pixel of the given image.

Note the correspondence of high pixel values (dark) in each image with the corresponding color coded below, i.e. dark blue for vertical stimulus conditions, and yellow for horizontal stimulus conditions.

resulting mean activity indices when combining all experimental variables: 2 (vertical & horizontal) x 2 (collinear & non-collinear) x 2 (baseline & cooling).

It was decided to look at the results for each experiment separately because when recording the images during the experiments, on first impression the data appeared very different across the sample. Thus, in the frame of this thesis it appeared fair to describe the optical imaging data for each data set separately. However, a mean activity index for each data set ROI was calculated over approximately thousand pixel values. In consideration of this large number the mean variance resulted

so small that it became redundant to conduct a statistical modeling, instead meaningful differences are visible by the eye when plotting the means of each data set.

Referring again to Figure 3.4 (right side) for the data example taken from a baseline recording of one of the experiments (091608b). The activity appears to change across the different stimulus conditions. In particular, when stimuli of local vertical orientation were presented (Figure 3.4 right side, the two ROIs in the top row), the dark patches indicate high activity in vertical orientation columns as indicated in blue color in the angle map ROI below. Here, for the presence of both stimulus conditions, collinear or non-collinear, the ROI for the respective image represents exactly the same stimulus element, namely the center Gabor of vertical orientation. The only difference when either image was taken was the surrounding context. Note that for the collinear line of vertical elements the maximum value, i.e. the darkest pixel, was .126, while for the non-collinear line of vertical elements the maximum value was .042. Thus, the activity indices decreased from collinear to non-collinear stimulus condition. For the second orientation, when stimuli of local horizontal orientation were presented (Figure 3.4 right side, the two ROIs in the lower row), the dark patches indicate high activity in horizontal orientation columns as color coded in yellow in the angle map ROI below. Note, that the maximum activity indices for both context stimuli in the horizontal local orientation condition (max = .052 and .017) are much smaller than those in the vertical local orientation condition (max = .126 and .042). But also for the horizontal condition the maximum value for the collinear condition is larger (max = .126) than for the non-collinear condition (max = .042).

3.2.1 Contextual Effect on Imaged Cortical Signal

The first research question was whether neuronal activity in the primary visual cortex already reflects the perceptual advantage of a collinear line over a non-collinear line of oriented elements, as the Gestalt law of collinearity proposes. To address this question, the mean activity indices for the two kinds of stimulus context were compared within baseline state only. For both orientation groups of pixels separately, the activity indices were averaged in each image. Figure 3.5 visualizes for each of the six data files individually the mean pixel index (Y axis) for the two context stimulus conditions (X axis). The means are presented separately for each orientation group of pixels (red for horizontal group of pixels vs. blue for vertical group of pixels). The top right corner in each of six graphs indicates the experimental code as

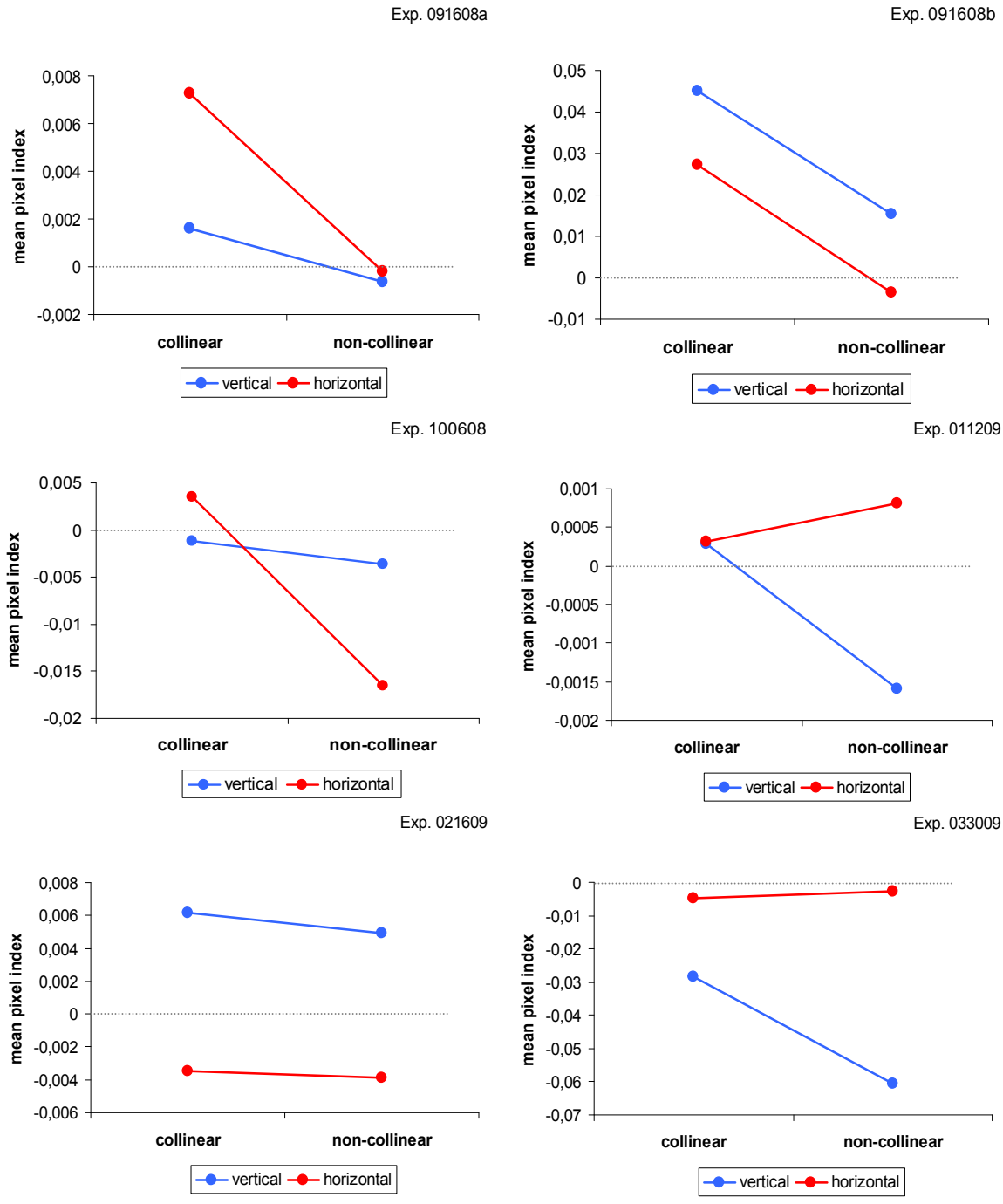

Figure 3.5 | Mean pixel index values for imaged cortical activity in dependence of stimulus context and assigned pixel orientation preference.
Each graph shows the mean pixel index values (Y axis) individually for each of the six experiments (see respective experiment code in every top right corner). Mean values for collinear and non-collinear stimulus context (X axis) are displayed separately for the group of pixels assigned to vertical (blue) vs. horizontal (red) orientation preference. Changes in mean value from one to the other stimulus condition is visualized by a line connecting the two. Results show some similar and some different 'shapes' of data for each experiment. For further description refer to section '3.2.1 Context effects on imaged cortical signal'.

listed in an overview in table 2.1 in the methods chapter. The lines in each graph connecting the data points between the two levels of the context variable help to visualize whether the mean value increased or decreased from one to the other. The scaling of the mean pixel indices (on the Y axis) was chosen individually for each experiment to frame the respective minimum and maximum mean value in each graph. Thus, one can compare the data 'shape' more easily. However, note that the actual mean values differ quite extensively across the six data files, with the axes showing min = -.06 in Exp. 033009 and max = .001 in Exp. 011209 as two extreme examples considering their absolute value.

Overall, the following similarities and differences were found in comparing the mean values in baseline recording for all experiments (see Figure 3.5). In all six cases the mean value for collinear vertical elements was higher than for non-collinear vertical elements in the group of vertically assigned pixels. For the group of horizontally assigned pixels this change from collinear to non-collinear was only found in four out of six experiments. More specifically, the mean collinear activity index for the horizontal orientation group were positive in four out of six experiments, thus indicating a higher cortical activity when the collinear line was present compared to the single Gabor. In contrast, the mean non-collinear activity indices were negative in five out of six experiments, thus indicating a lower cortical activity when the non-collinear line was present compared to the single Gabor. A similar pattern of results is found for the vertical orientation group of pixels though in different experiments: four out of six showed positive mean collinear activity values, and four out of six showed negative non-collinear activity values.

Further, for both orientation groups of pixels in half the experiments the mean values for collinear stimuli are higher compared to those for non-collinear stimuli. In all but one experiment the advantage of either orientation group over the other is the same for collinear and non-collinear stimulus context.

3.2.2 Cooling Effect on Imaged Cortical Signal

The second research question of this study was what role the intact primary visual cortex plays across both hemispheres in reflecting the advantage of a collinear over a non-collinear line of elements. To address this question, the mean index pixel values for the two levels of stimulus surround context were compared across the two levels of state, separately for the two orientation groups of pixels (see Figure 3.6).

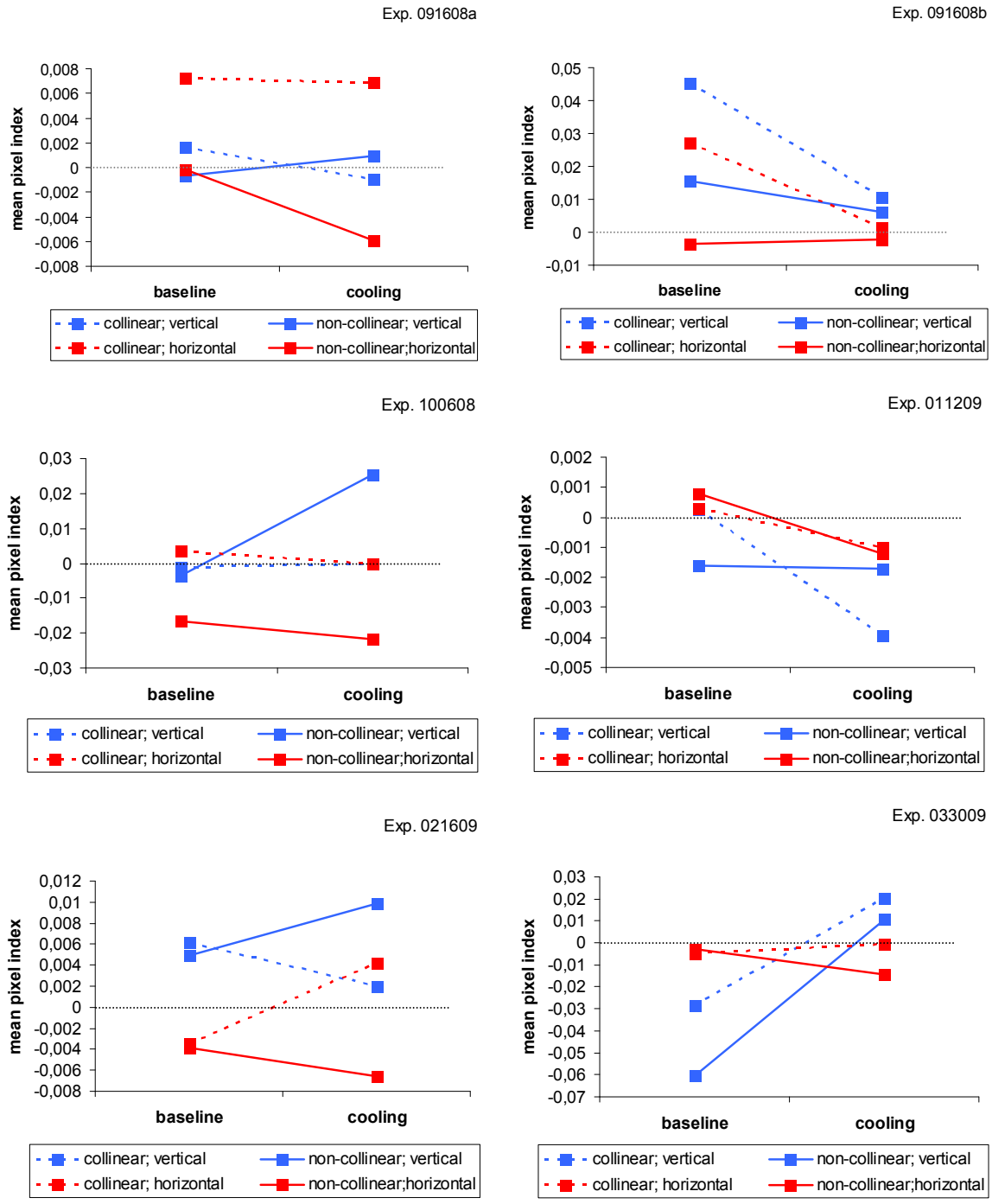

Figure 3.6 | Mean pixel index values for imaged cortical activity in dependence of stimulus context, state and assigned pixel orientation preference. Each graph shows the mean pixel index values (Y axis) individually for each of the six experiments (see respective experiment code in every top right corner). Increase or decrease of mean values from baseline to cooling state (X axis) for collinear (dashed line) and non-collinear (continuous line) stimulus context are displayed separately for the group of pixels assigned to vertical (blue) vs. horizontal (red) orientation preference. Results show some similarities but also differences in the 'shape' of the data for each experiment. Refer to text for further descriptions.

Note again that results are displayed individually for all six experiments and the scaling of the mean values was chosen respectively to the minimum and maximum for each experiment.

Overall, the following similarities and differences were found in comparing the mean values across the variable levels for all experiments (see Figure 3.6). The mean indices decreased from baseline to cooling for the horizontal orientation group in five out of six experiments for the non-collinear context, and in four out of six experiments for the collinear context. For the vertical orientation group, the results were similar, with four out of six experiments decreasing in their collinear mean value and also four out of six experiments decreasing in their non-collinear mean value from baseline to cooling state.

The findings described in the frame of both research questions are summarized in Table 3.4 listing propositions in the rows, and indicating the six experiments in the column heads. The matrix columns are filled with T = true or F = false depending on whether an experiment confirmed the given proposition or not.

The last column of the matrix indicates the proportion of how many experiments confirmed with that proposition, e.g. 4/6 indicating 4 experiments out of six. The last row indicates the number of propositions that each experiment was assigned false to. Note that out of all propositions examined, the Exp. 091608a was always consistent with the majority of propositions. Further, the majority of experiments showed highest consensus in the following propositions:

1) Mean collinear pixel index value for vertical orientation group is larger than for the non-collinear stimulus (in 6 / 6 experiments).

2) The mean non-collinear pixel index for horizontal group of pixels is a positive value, thus indicating higher cortical activity for the non-collinear line over the single Gabor condition (in 5 / 6 experiments; not in Exp. 011209).

3) The advantage of one group of pixels over the other remained under collinear and non-collinear context stimulation (in 5 / 6 experiments; not in Exp. 100608).

4) The non-collinear mean pixel index for the horizontal orientation group decreased from baseline to cooling state (in 5 / 6 experiments; not in Exp. 091808b)

Table 3.4 | *Summary of which Experiments Confirmed on Descriptive Propositions Regarding the Two Research Questions.*

	propositions	091608a	091608b	100608	011209	021609	033009	confirm
	baseline state only							
1	coll ver > nc ver	T	T	T	T	T	T	6 / 6
2	coll hor > nc hor	T	T	T	F	T	F	4 / 6
3	coll hor > coll ver	T	F	T	F	T	T	4 / 6
4	nc hor > nc ver	T	F	F	T	F	T	3 / 6
5	coll hor pos	T	T	T	F	T	F	4 / 6
6	coll ver pos	T	T	F	T	T	F	4 / 6
7	nc hor neg	T	T	T	F	T	T	5 / 6
8	nc ver neg	T	F	T	T	F	T	4 / 6
9	ori1 > ori2 for coll = nc	T	T	F	T	T	T	5 / 6
	baseline and cooling state							
10	nc hor base > nc hor cool	T	F	T	T	T	T	5 / 6
12	coll hor base > coll hor cool	T	T	T	T	F	F	4 / 6
13	coll v base < coll v cool	T	T	F	T	T	F	4 / 6
14	nc v base > nc v cool	T	F	T	F	T	T	4 / 6
	# of propositions false	0	5	4	5	3	5	

Note. T = true, F = false
coll = mean collinear pixel index value
nc = mean non-collinear pixel index value
ver = group of pixels assigned to vertical orientation preference
hor = group of pixels assigned to horizontal orientation preference
ori = orientation group of pixels
e.g. ‘4 / 6’ indicates that four out of six experiments confirmed on the proposition

4 DISCUSSION

A new scientific truth does not triumph by convincing its opponents and making them see the light, but rather because its opponents eventually die, and a new generation grows up that is familiar with it.

- Max Planck, Scientific Autobiography, 1948 -

In the present study we stimulated the receptive field of a cell in the cat primary visual cortex, or by imaging a cortical region therein, respectively, with an optimally oriented Gabor element, and varied in its surround other Gabor elements. The contextual surround was either collinear, i.e. the global axis of alignment matches the local orientation of the Gabors, or non-collinear, i.e. axis of alignment was orthogonal to local element orientation. The first research hypothesis was that the common cortical activity will be modulated by contextual surround. We also temporally deactivated half of the visual field representation and compared cortical activity to prior the deactivation. The second research hypothesis was that stimuli which are represented in both hemispheres will be most affected by this cortical disengagement.

4.1 Surround Modulations Depend on Local Orientation Preference

In favor of the first research hypothesis, our electrophysiology results confirm the findings of previous studies in the cat visual cortex. In particular, our data have shown both facilitative and suppressive influences from surround context. Our results reveal a new feature in that these different influences show a strong dependency on the orientation preference of the recorded cell. Units that preferably responded to a stimulus of vertical orientation on average increased their spike rate when that stimulus was augmented with collinear surround. In contrast, units that were categorized to horizontal orientation preference showed on average a suppressive effect by collinear surround. Interestingly, this pattern of effect reversed under non-collinear surround context. Here units of vertical orientation preference were on average sup-

pressed while units of horizontal orientation preference showed a facilitated response in comparison to receptive field stimulation only.

Previous electrophysiology studies in the cat primary visual cortex with a similar experimental setup studied the modulations by collinear surround for different stimulus contrasts (Polat et al., 1998; Mizobe et al., 2001). In their results they found stimuli outside a cell's receptive field to facilitate or suppress its response depending on the center stimulus contrast. For the majority of their recordings they found that facilitative effects diminished or reversed when the Gabor contrast placed within the cell's receptive field increased over a certain threshold. However, no matter what contrast parameter they chose their sample of recorded neurons always contained some that were facilitated, some that were suppressed, and some that were not modulated at all by collinear stimulus surround. Thus, in the present study we kept the stimulus contrast constant at 100% and found both facilitative and suppressive influences in our data sample. In contrast, recordings in the tree shrew primary visual cortex revealed only facilitative effects from the receptive field collinear surround (Chisum et al., 2003). Note that their data was gathered in 25 animals and based on altogether 35 recording sites, while our data and that from the other two cat studies (Polat et al., 1998; Mizobe et al., 2001) were carried out in 5 - 6 adult cats on the overall basis of approximately 90 recording sites. It could not be determined from the description of their study in the tree shrew cortex whether any of the experimental settings biased their overall uniform result.

Our optical imaging results confirm the findings from our electrophysiology experiments for cortical areas assigned to vertical orientation preference. For all six optical recordings the cortical activity in response to collinear surround was higher than for non-collinear surround. Imaging cortical activity and using Gabor elements for stimulation has not been performed so far in cat V1. However, the above mentioned study in tree shrew cortex by Chisum and colleagues (2003), also applied optical imaging in nine additional animals to study the influences of contextual surround. In line with our findings their individual experiments showed a mixed outcome in regards to facilitative and suppressive influences from the surround. For the same stimulus parameters as used in our study they found cortical activity strongly facilitated by collinear surround in three out of seven experiments, in the remaining four experiments results indicated modest facilitation or even suppressive influences from collinearly aligned Gabor elements. In our study we had assigned pixels in the image to a par-

ticular orientation preference, an information derived from a previous angle map calculation. Chisum and colleagues used in their study only those pixels that showed at least 50% of the maximum response. However, as they don't report what local orientation the stimulus was for each of their experimental recording our findings cannot be easily compared.

Assuming that 'the world from a cat's perspective' is more rich in horizontal contours, as Betsch and colleagues (2004) determined by attaching a camera to the head of a cat, the following explanation of our results is thinkable. Perhaps, neurons of vertical orientation preference are much more reliant on communication with others in their long-range network, because they receive less input of their preferred kind. This idea that less information demands a higher workload was also suggested by Nauhaus et al. (2009) who studied V1 activity when reducing stimulus contrast. They found that for a weak stimulus signal, lateral connections dominated in their function of integrating visual information from the surround.

4.2 Horizontal Collinear Line Depends Most on Visual Callosal Transfer

In the present study, the dominant effect when temporally deactivating half of the visual field representation was the hypothesized significant decrease in spike rate for units of horizontal orientation preference in response to a collinear stimulus context. Thus, one of the two stimulus configurations that cross the vertical midline (VM) showed a pronounced dependence on visual information communicated via callosal connections. Spiking activity in response to vertically oriented Gabor elements in non-collinear alignment was not significantly affected during cooling, however the data showed a trend in the predicted direction.

For optical recording four out of six experiments showed a decrease in cortical activity from baseline to cooling state for both stimulus configurations crossing the vertical midline. Interestingly, in all but one optical experiments cooling also diminished cortical activity when stimulated with horizontal non-collinearly aligned Gabors. The experimental variable of cooling had never before been applied to cat V1 when stimulating with contextual Gabor elements. However, previous investigators that have studied the impact of cooling in cat or ferret V1, respectively, while presenting a whole field grating stimulus reported both an increase and decrease of visually driven

activity for neurons in the intact hemisphere (e.g., Payne, Siwek, & Lomber, 1991; Carmelli et al., 2007). In particular, it was suggested that the callosal projections function on a modulatory rather than excitatory level. The most robust modulation by callosal connections was reported when both hemispheres were stimulated with the same stimulus orientation (Carmelli et al., 2007). This supported the notion that callosal axons predominantly connect neurons of the same orientation preference. However, in our study we attempted to compare callosal to intrinsic connections with regard to their role in reflecting on a neuronal basis the perceptual advantage of a collinear line. As mentioned before there is a major difference in the stimulus configuration we used compared to those studies applying whole field gratings. Given the receptive field of a V1 neuron anywhere on the pattern of the whole field grating stimulus, it receives input from the surround from along its collinear axis *and* from along the non-collinear axis. If callosal connections act as the pendant to intrinsic connections, they may represent the long range anisotropic connections for neurons of horizontal orientation preference. As supported by our data, this network is most strongly modulated by deactivating interhemispheric interaction in response to a collinear line of locally horizontal elements which is represented across both hemispheres.

4.3 Perception is not Represented but Supported by Neurons in V1

Our average results have shown that a neuron's orientation preference has an influence on whether contextual stimuli facilitate or suppress the neuron's spiking activity. Perhaps this criterion does not imply an unequal role to neurons of either orientation preference, but rather indicates a concept how the cortex deals with the respective global axis of the stimulus. Refer to Figure 4.1 which shows again the four different context stimuli used in this study. It is obvious that the line conditions can be grouped according to various arguments, not just collinear (Figure 4.1 A + D) vs. non-collinear (Figure 4.1 B + C). For example, considering their global axis the lines cross (Figure 4.1 A + B) vs. run parallel (Figure 4.1 C + D) to the vertical midline. Thus, the two lines crossing the VM are represented in both hemispheres and depend on the communication of visual information via callosal connections.

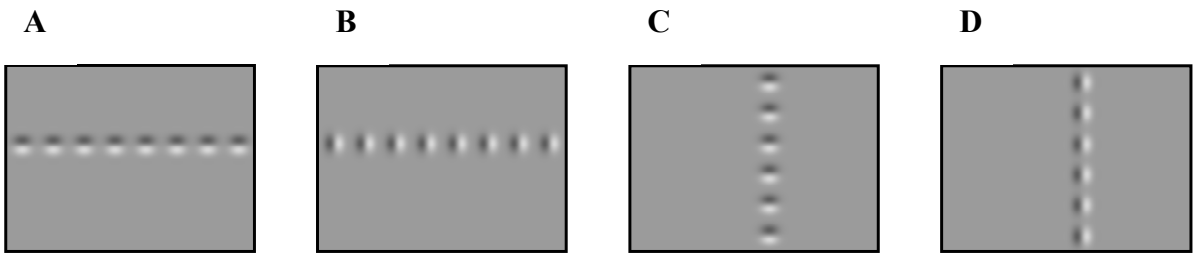

Figure 4.1 | Different groupings of line stimuli according to their properties. The line stimuli conditions were constructed to either form a collinear line **(A + D)** or non-collinear line **(B + C)**. Now consider the stimuli's position relative to the course of visual callosal connections which join the information across both hemispheres. Line stimuli in their global axis can either cross the vertical midline **(A + B)** and thus be represented in both hemispheres, or run parallel to the vertical midline **(C + D)**. Or, assuming that neurons of similar orientation preference are much further connected over their collinear axis (Schmidt et al., 1997), the connection network of horizontally preferring neurons reaches across the midline over to the opposite hemisphere **(A + C)**. In contrast the connection network of vertically preferring neurons reaches further parallel to the midline, in both cases collinear line **(D)** and non-collinear line **(B)**.

However, one could also argue that the local orientation of the context stimuli addresses two different networks of lateral connections. Given that iso-oriented neurons are connected much further along the collinear axis of their orientation preference (e.g., Schmidt et al., 1997a), the network of vertical preferring neurons stretches farthest parallel to the VM. In contrast, the network of horizontal preferring neurons is farthest across the VM, i.e. from one hemisphere to the other via callosal connections. In concordance with this argument is the anatomical finding that callosal axons connect areas of similar orientation preference also in an anisotropic way (Rochefort, in press).

These stimulus considerations suggest a new perspective on the present findings. Both recording methods of our study showed cortical responses on average to decrease when the contextual surround crossed the vertical midline. Given the proposition by Buhl and Singer (1992) that callosal sending primarily terminate from pyramidal cells, cooling temporally abolishes this excitatory input sent to the intact hemisphere. Thus, depending on whether a cell receiving callosal input is carrying an excitatory or inhibitory function itself its activity will be diminished. Consequently, the effect of cooling on cortical response to a contextual stimulus is quite complex. Two cells X and Y in V1 which are targeted from the other hemisphere via callosal axons

will receive less excitatory input during cooling. Intuitively, it appears that a neuron will decrease in its usual receptive field response no matter whether it carries an excitatory or inhibitory function itself. If the response of cell X is commonly facilitated from its surround, this effect decreases during cooling because the 'surround cells' will be diminished in their influence. In contrast, if the response of cell Y is commonly suppressed from its surround (by inhibitory neurons), it will then increase its firing under cooling, as the surround cells diminish their impact. The average results of the present study did not confirm this proposed scenario. Instead, the exact opposite was found. Units which were on average facilitated by the surround increased their advantage during cooling, while those suppressed by the surround decreased their spiking activity on average even more during cooling. Thus along the previous string of arguments, if callosal input was inhibitory, the present results could usefully augment this functional role of inhibitory connections. It has been suggested by some authors that callosal input may also be of inhibitory function (e.g., Payne, 1994) however to a minor extend (Buhl & Singer, 1992). It remains a matter of debate how excitatory and inhibitory callosal input is matched to the variable effects in the primary visual cortex.

The question arises whether the kind of surround influence, i.e. facilitation or suppression, can be predicted by some property of the cell. In other words what makes a recorded cell more or less likely to receive excitatory or inhibitory input from its collinear surround? Whereas our results are suggestive of the orientation preference of a cell to play a significant role, this variable cannot explain all of the variance in the data. Consider the situation of the variable effects in V1 from the perspective of a cell in the higher visual areas. It will receive collectively exhausted input from various V1 neurons. This input may contain information of a restricted area in the visual field but the context will be very variable, facilitative and suppressive, across all V1 neurons. Perhaps it is just that constellation of some neurons in V1 facilitated and others suppressed by collinear surround that triggers the perceptual advantage of a collinear line.

Perhaps, neuronal activity in V1 has to be variable to drive neurons further up in the visual system. A cell by itself in V1 may not represent the perceptual advantage of a collinear line, for example, but it does certainly contribute to it along the line. A single example of suppression by collinear context on V1 level must not indicate a suppression on a higher level of the visual system.

4.4 Methodological Considerations

4.4.1 Limitations of the Study

Multi-unit electrode recording was carried out in six experimental animals. For all experiments it was attempted to keep recording situations the same, besides the variations planned to address the research questions. Nevertheless, an experimental duration of at least 5 days gives room for a variety of possible differences. For example, as the recording takes place in a living organism it may make a difference what time of the day the recording took place, day or night, or the overall state of the animal in regards to its heart rate, depth of anesthesia, or recent application of medical treatment. Further, recording was performed with three different kinds of electrodes, two of them matrix electrodes but with different inter-electrode distances, and one kind a Michigan probe with not all electrodes positioned at the same height relative to cortical surface. This might have implications on the quality of data recording which in turn has an impact on the sample size for each recording. Finally, the location of electrode penetrations relative to the 17/18 border was not controlled in the data analysis as the proposed research questions had not addressed this issue. Nevertheless, the influences of context stimuli or deactivation of the contralateral hemisphere might be of different strength depending on where in the V1 area one is recording from. This last comment on interhemispheric influences had in fact been addressed in previous studies where the contribution of callosal projections to cortical domains was higher in the close vicinity of the 17/18 border (Rochefort, 2007). Thus, by sorting electrode recordings from our present study in regards to their distance from the 17/18 transition zone, a further differentiation of results might appear.

For optical imaging experiments a major limitation of this study is the dependency on good image quality through all the recording time to determine the cortical region (ROI) where the center Gabor stimulus was represented. Based on this knowledge the signal processing is reduced to this region only. For one of the experiments Exp.033009 the imaging situation was not very stable. During the recording air bubbles floated through the recording chamber and distorted the common light reflection signal. Thus, before data processing certain trials had to be excluded which improved the averaged image quality but the signal to noise ratio decreased immensely. This lead to a low certainty to determine the ROI. Nevertheless, the data file of the 0333009 experiment was included in the description of results because it showed no qualitative disagreement to the other experiments of the sample.

4.4.2 Additional Data Analysis Propositions

In an attempt to characterize neurons with regard to their contribution to the visual percept I will propose in the following an idea how else to sort units in their response properties to context stimuli. The data variable for our recorded units was an index calculated from the relative spike rate in response to a context stimulus (collinear or non-collinear) compared to a single Gabor stimulus. As discussed above, it appears that V1 neurons underlie different functions in passing on information to higher cortical areas to form a percept, some show facilitation (positive index) and some suppression (negative index) in response to their receptive field response. Remarkably, a unit can be affected by its surround always the same way independent of the kind of context, or it can respond differently depending on whether the context is collinear or non-collinear. Figure 4.2 A - D shows all units' response index to both context stimuli, to collinear context on the X axis and to non-collinear context on the Y axis. The four graphs distinguish between units of horizontal (red) and vertical (blue) orientation preference, separately for baseline (top two graphs) and cooling (lower two graphs).

For any particular unit of the sample, the index values for the collinear and non-collinear conditions could be positive for both, or negative for both or one opposite from the other. Thus by simply adding together the incidences for all possible scenarios gives an interesting additional description of our recording sample (see Figure 4.3): collinear facilitation & non-collinear facilitation (group A), collinear facilitation & non-collinear suppression (group B), collinear suppression & non-collinear facilitation (group C), collinear suppression & non-collinear suppression (group D). For units of vertical orientation preference there are more than twice as many units in group A (n = 25) and D (n = 19), where the influence of both context stimuli is in agreement - either both facilitative or both suppressive - compared to groups B (n = 9) and C (n = 3), where the influence of collinear and non-collinear stimulus is in opposition. For units of horizontal orientation preference the majority is assigned to groups A (n = 10) and C (n = 12) which both contain units facilitated by non-collinear surround. The remaining groups B (n = 4) and D (n = 7) share the characteristic of suppression by non-collinear surround. These distributions reflect again the results obtained from electrophysiological recording, however they also open a new perspective to characterize cells in the primary visual cortex. On the basis of this information the analysis of cortical response may become more distinct in future studies.

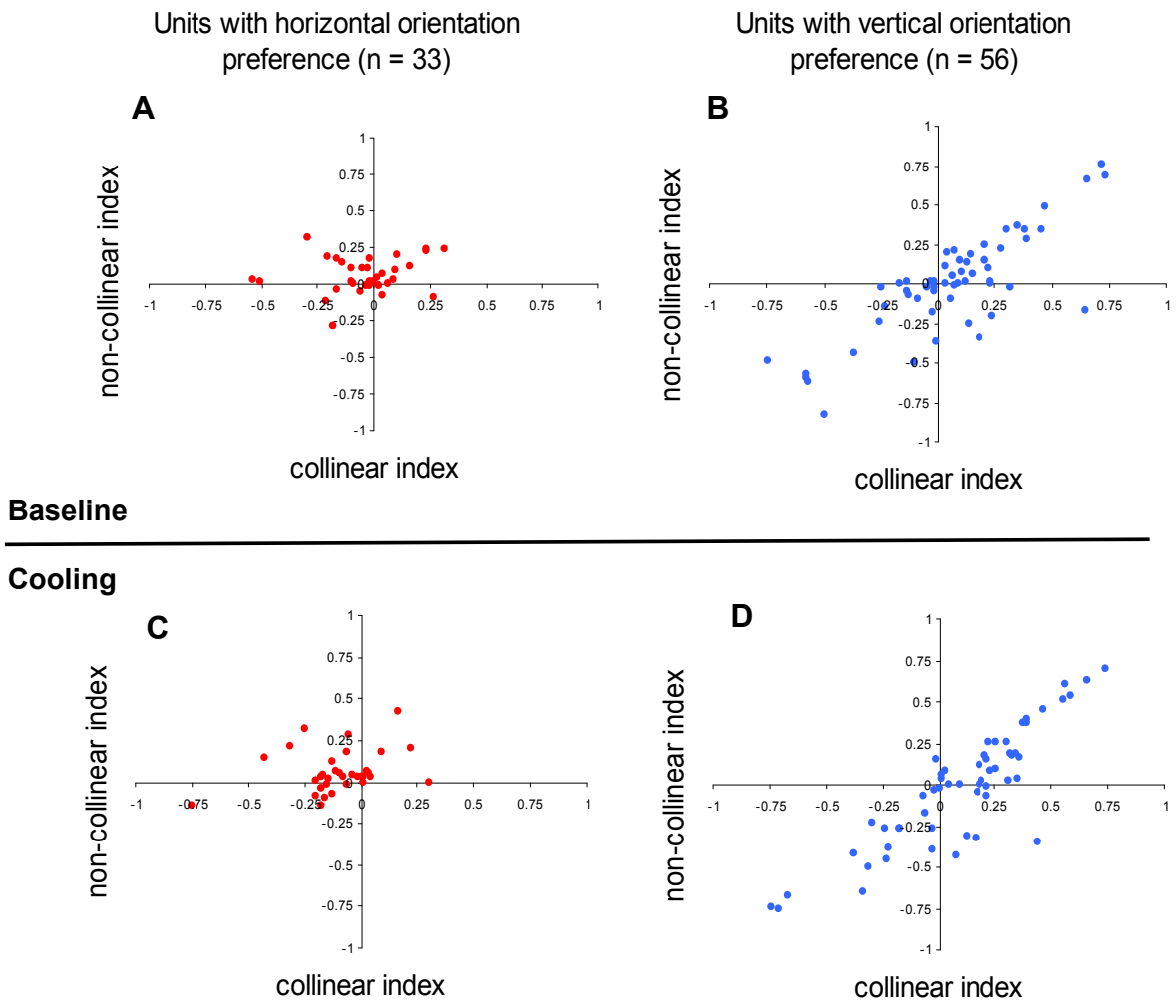

Figure 4.2 | Magnitude of spike rate index for collinear and non-collinear conditions for all units of the sample.
The grand sample of 89 units in our study contained 33 units with horizontal (red) orientation preference and 56 units with vertical (blue) orientation preference. For each unit a spike rate index value was calculated for stimulation with a collinear (X axis) or non-collinear line (Y axis), respectively. The distribution of units across the scale of index values for both context properties did not differ considerably between baseline (A + B) and cooling (C + D) state recordings. Each graph can be portioned in four quadrants, that describe a unit's response profile to both context stimuli. Recall that positive index values indicate facilitation and negative ones indicate suppression to the respective context in comparison to RF stimulation only. Starting with the quadrant in the top right corner and continuing clockwise the following four groups of neurons can be distinguished: collinear facilitation & non-collinear facilitation (group A), collinear facilitation & non-collinear suppression (group B, collinear suppression & non-collinear facilitation (group C), collinear suppression & non-collinear suppression (group D).

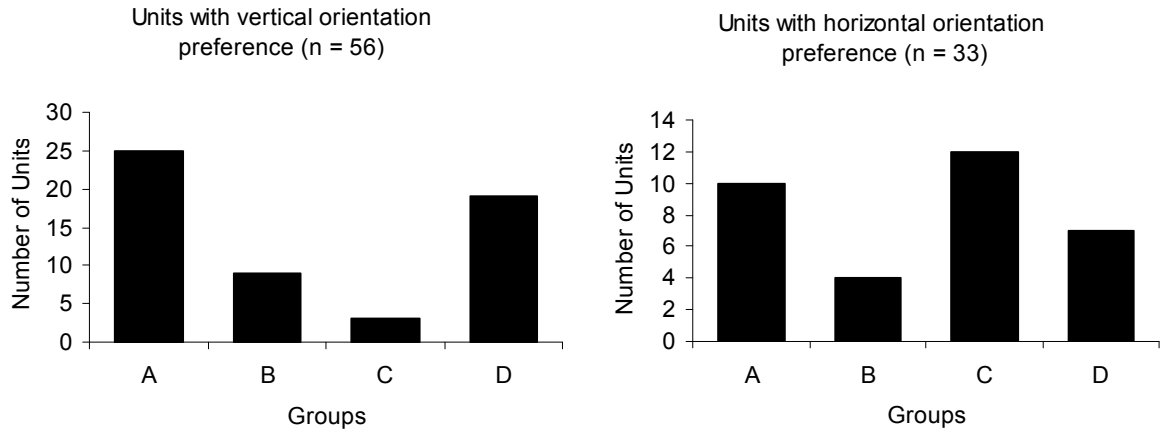

Figure 4.3 | Grouping units according to their index values on both context stimuli.
Facilitation was defined for units when they had a positive index value for the respective context stimulus, indicating that the spike rate for the context stimulus was higher (i.e. facilitated) than for the RF stimulation with the single Gabor. Suppression was defined for a negative index value for the respective context stimulus. This indicated that the spike rate for the context stimulus was lower (i.e. suppressed) than for single Gabor stimulation.
Group A: collinear facilitation & non-collinear facilitation
Group B: collinear facilitation & non-collinear suppression
Group C: collinear suppression & non-collinear facilitation
Group D: collinear suppression & non-collinear suppression
Note that for units with vertical orientation preference the majority of units (group A and D) showed agreement in their response to the collinear and non-collinear stimuli, i.e. either both facilitation or both suppression. For units of horizontal orientation preference the majority of units (group A and D) showed non-collinear facilitation.

As mentioned before, in optical imaging experiments a reliable identification of the ROI that represents the center Gabor stimulus is indispensable for meaningful results. Figure 4.4 gives an overview of the ROI placements for all experiment recordings performed in this study. Similar to the suggestion for experiments with electrode recording, the location of the ROI relative to the 17/18 border should also be planned or at least tested in future studies. This would rule out any potential influence of topographic particularities in studying contextual and/or cooling influences on the imaged cortical signal.

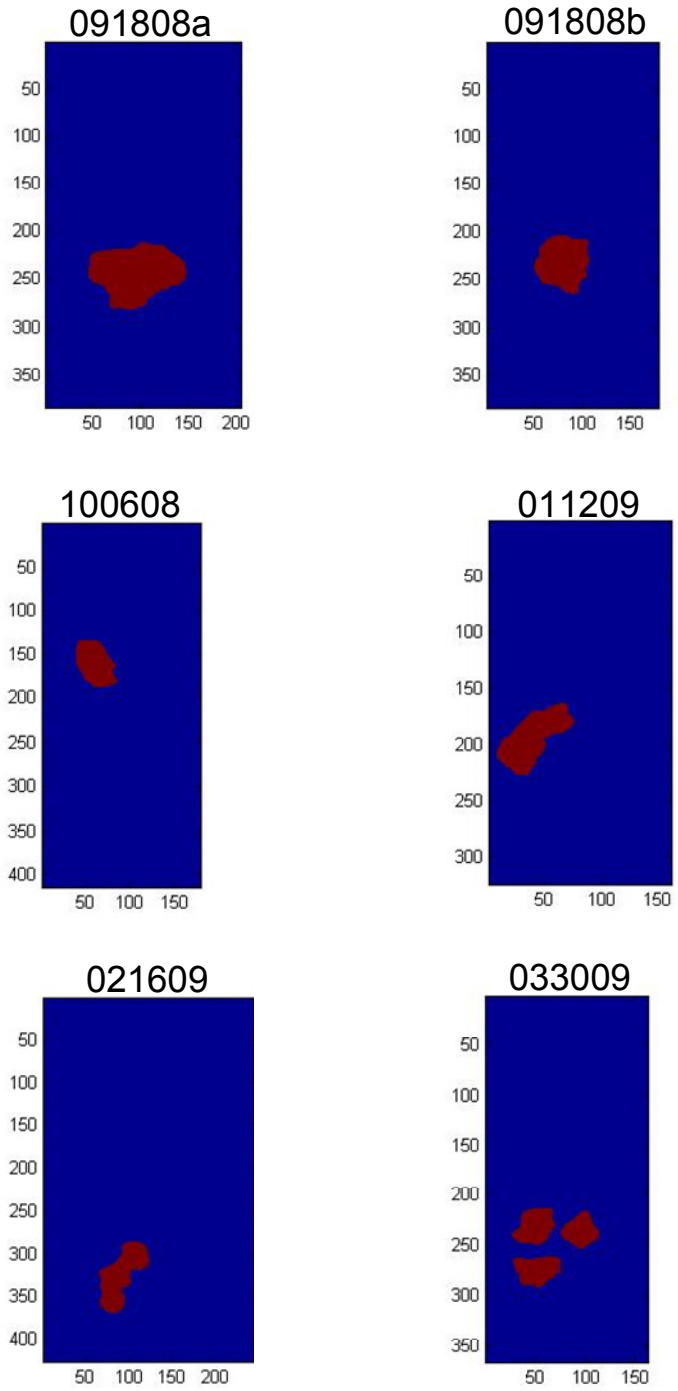

Figure 4.4 | ROI locations in the imaged cortical region for all six optical recordings of this sudy.
The numbers on top of all six graphs specify the experimental code. The values at the X- and Y- axis indicate the size of the optical image take from the cortex surface in units of pixels (1 pixel = 12 µm). The red areas on the blue background indicate the location of the ROI determined for each experimental recording. Data analysis of the pixel values was restricted to that respective ROI only. Note that the positions of the ROIs are somewhat different for all six examples, a variable that might have an impact on the recorded cortical activity. The poor image quality in experiment 033009 led to a calculation of scattered ROI particles. Data from this set was yet described for completeness.

4.5 Implications for Further Studies

With regard to our results, I will suggest some experimental ideas for future studies. First, to implement and advance the suggested grouping of neurons in V1 further types of stimuli can be applied. For example, while still stimulating the RF of a cell in its preferred orientation the non-collinear elements could be placed along the collinear axis instead of side-to-side as used before. In previous studies, this context structure has been referred to as cross-orientation (e.g. Freeman et al., 2001) which emphasizes a temporal component of inter-neuronal communication.

Second, callosal connections were suggested above as the anatomical constraint for neurons of horizontal orientation preference to connect to iso-orientation sites in an anisotropic way, i.e. across the vertical midline. Our results revealed a significant impact of cooling on the representation of a horizontal collinear line, i.e. the collinear line represented in both visual hemifields. We have so far inactivated cortical input from beyond the vertical midline and found the largest impact in the response to collinearly aligned horizontal Gabors. But this leaves the question open what happens if the opposite is done: if one could temporarily deactivate the cortical area that lies beyond the horizontal midline. Then one should see the effect in a pronounced change in cortical activity in response to a vertical collinear line.

4.6 Conclusions

Our results support the findings of previous studies in the primary visual cortex in the cat. Contextual modulation of cells' responses to an optimally oriented stimulus can be quite variable, facilitative or suppressive. Our findings suggest that a neuron's orientation preference may play a key role in how the surround influences its response property. In particular, lateral connections among horizontally preferring neurons, as also represented by callosal connections, severely influence the neuron's response. Nevertheless, the variability of contextual influences described in V1 may serve a complex coding of input information which is essential for higher visual areas to generate a percept of for example a collinear line. How the variable activity in V1 is implemented to form a particular percept remains a matter of speculations. With certainty it can be concluded that the whole percept is more complicated than the sum of its sensory inputs.

5 ZUSAMMENFASSUNG

„Das Ganze ist mehr als die Summe seiner Teile.“ Dieser Ausspruch wurde besonders durch Gestaltpsychologen wie Max Wertheimer geprägt. Es wurden Gestaltgesetze formuliert, welche unsere Wahrnehmung beschreiben. Eines dieser Gesetze betrifft die Kollinearität: Objekte, die in ihrer lokalen Orientierung mit der globalen Achse ihrer Anordnung übereinstimmen, bilden eine kollineare Linie. Diese wird im Gegensatz zu einer nicht-kollinearen Linie, bei der die lokale und globale Orientierung orthogonal zueinander sind, als „bessere“ Gestalt wahrgenommen (Wertheimer, 1923). Psychophysische Studien konnten diesen Wahrnehmungsvorteil einer kollinearen Linie bestätigen. Ein gängiger Stimulus zur experimentellen Testung ist ein Gabor Element, ein sinusoidales Streifenmuster gewichtet durch eine Gausfunktion. Versuchspersonen konnten eine Linie kollinear angeordneter Gabors umgeben von zufällig angeordneten Gabors schneller wieder erkennen, als wenn die Elemente nicht-kollinear angeordnet waren (Field & Hess, 1993). Weiterhin konnte gezeigt werden, dass ein zentraler Gabor schon bei sehr geringem Kontrast erkannt wird, wenn dieser von anderen gleich orientierten Elementen entlang der kollinearen Achse umgeben war, nicht jedoch, wenn die Elemente orthogonal zu ihrer lokalen Orientierung angeordnet waren (Polat & Sagi, 1994). Die Forscher hatten außerdem zeigen können, dass die Elemente optimaler weise 3 λ (lies: Lambda) von einander entfernt sein sollten, ein Wert der die sinusoidale Wellenlänge des Streifenmusters beschreibt (Polat & Sagi, 1993).

Den Forschern gemein war der Versuch, ihre Erkenntnisse auf Verhaltensebene neuronalen Grundlagen zuordnen zu können. Es wurde festgestellt, dass neuronale Zellen im primären visuellen Kortex (V1) bereits eine entscheidende Rolle für den beobachteten Wahrnehmungsvorteil kollinearer Linien spielen könnten.

Es ist bereits seit einiger Zeit bekannt, dass Zellen in V1 nicht ausschließlich selektiv auf Reize einer bestimmten Orientierung innerhalb ihres rezeptiven Feldes (RF) reagieren (z.B., Hubel & Wiesel, 1962), sondern auch durch die Aktivität umliegender Neurone moduliert werden (z.B., Ts’o, Gilbert, & Wiesel, 1986; Gilbert & Wiesel, 1990). Das visuelle Sichtfeld ist retinotop in V1 angebildet, mit anderen Worten, benachbarte Zellen haben auch angrenzende RF. Leitet man elektrophysiologisch die Aktivität einer Zelle in V1 ab, welche innerhalb ihres RF mit optimaler Orientierung stimuliert wird, so verändert sich die Aktivität im Beisein kollinearer oder nicht-kollinearer angeordneter Elemente im Umfeld. Interessanterweise, fanden sich in der

Fallzahl abgeleiteter Neurone stets einige, die in ihrer Aktivität verstärkt wurden und andere bei denen ein Umfeldstimulus eine Schwächung der Aktivität mit sich führte (z.B., Polat et al., 1998; Mizobe et al., 2001). Anatomische Studien konnten zeigen, dass Neurone in V1 nach einem bestimmten Prinzip miteinander verbunden sind: Zellen, die durch kollinear angeordnete Konturen stimuliert werden, sind vorzugsweise durch weit reichende Verbindungen vernetzt, auch Anisotropie der kortikalen Verbindungen genannt (z.B., Gilbert & Wiesel, 1989; Schmidt et al., 1997a). Im Gehirn der Katze existiert dieses Prinzip der neuronalen Vernetzung ebenfalls für die Verbindungen zwischen den beiden Hemisphären (Schmidt et al., 1997b; Rochefort et al., in press). Informationen der linken und rechten Hälfte des visuellen Sichtfeldes werden jeweils in der contra-lateralen Hemisphäre kortikal repräsentiert.

Das Ziel der vorliegenden Studie war es zu testen, wie sich der Wahrnehmungsvorteil einer kollinearen Linie in der Orientierungsselektivität der V1 Zellen sowie in den anatomischen Verbindungen innerhalb oder zwischen den beiden primären visuellen Kortizes widerspiegelt.

Im Rahmen der vorliegenden Dissertation in Psychologie war es von besonderer Bedeutung, zwei Methoden der Neurophysiologie detailliert zu beschreiben, die auch in der vorliegenden Studie Anwendung fanden: Elektrodenableitung und optischer Ableitung intrinsischer Signale. Beide Methoden wurden eingesetzt, um im primären visuellen Kortex einer Hemisphäre von jeweils acht anästhesierten Katzen die kortikale Aktivität zu messen. Zeitweilig wurde außerdem die topographisch entsprechende Region der anderen Hemisphäre durch Kühlen deaktiviert (siehe auch Payne & Lomber, 1999). Als visuelle Stimuli wurden neben einem optimal orientierten zentralen Gabor, Linien aus kollinear oder nicht-kollinear angeordneten Gabors verwendet.

In elektrophysiologischen Experimenten wurden in sechs Versuchstieren jeweils 32 Elektroden im marginalen Gyrus einer Hemisphäre positioniert. Die Ableitungen erfolgten extrazellulär, so dass eine Elektrode jeweils die Signale mehrerer Neurone erfasste, was im folgenden als eine Einheit bezeichnet wird. Zunächst wurden die RF aller Einheiten auf einem Stimulusmonitor vor dem Versuchstier lokalisiert, sowie die jeweils bevorzugte Stimulusorientierung bestimmt. Man kann davon ausgehen, dass die Neurone einer Einheit überlappende RF und gleiche Orientierungspräferenz aufweisen. Das aufgenommene elektrische Signal einer Einheit ist eine Potentialdifferenz, welche in ihrer Amplitude eine bestimmte Schwelle über-

schreiten kann. In diesem Fall wird ein Spike Ereignis gezählt, was über einen Zeitraum von einer Sekunde nach Stimulusbeginn und über mehrere Durchgänge zu einem Wert „Spikes pro Sekunde“ oder „Spike Rate“ gemittelt wurde. Die Einheiten, die besonders gut auf einen horizontal oder vertikal orientierten zentralen Gabor innerhalb ihres RF reagierten, wurden für weitere Analysen ausgewählt. Insgesamt wurden Daten von 89 (Neuronen) Einheiten für alle Stimulusbedingungen vor und während der Kühldeaktivierung ausgewertet.

Experimente optischer Ableitung wurden in vier Versuchstieren mit jeweils einem Aufnahmedurchgang und in einem weiteren Tier mit zwei Durchgängen durchgeführt. Zunächst wurde die Kortexregion im Kamerabild bestimmt, in der die Position des zentralen Gabors retinotop repräsentiert war. Für alle Stimulusbedingungen wurde vor und während der Kühldeaktivierung ein optisches Signal in hoher Auflösung in fünf Bildern pro Sekunde aufgenommen und über einen Zeitraum von zwei Sekunden nach Stimulusbeginn gemittelt. Die optische Aktivität wurde in einem Grauwert der Bildpixel codiert, so dass die Größe des Pixelgrauwertes entsprechend die Stärke der Aktivität beschrieb. Das optische Signal ergibt sich unter anderem durch die erhöhte Absorption von Licht durch sauerstoffarmes Blut. Es wird davon ausgegangen, dass aktive kortikale Regionen viel Sauerstoff verbrauchen und sich deswegen in ihrem Sauerstoffgehalt von nicht-aktiven Kortexregionen unterscheiden.

Die zeitweilige Deaktivierung der entsprechenden V1 Region der anderen Hemisphäre erfolgte mittels gekühltem Methanol, welches durch einen Teflonschlauch in ein dünnen Metallröhrchens gepumpt wurde. Diese Konstruktion war in Größe (ca. 0,6 x 0,4 mm) und Form (Kreislauf) der Oberfläche der zu deaktivierenden Region angepasst. Das Kühlen von Hirngewebe auf ca. 3° führt zu einer Verlangsamung der Stoffwechselrate bis schließlich der Metabolismus der Zellen zum Erliegen kommt (McCullough et al., 1999). Nach Beendigung des Kühlens erwärmt sich das Hirngewebe wieder und die neuronale Aktivität restabilisiert sich (Lomber et al., 1999).

Zusammenfassend ergaben sich für das experimentelle Design der Studie folgende Untersuchungsvariablen. Die abhängigen Variablen waren zum einen die Spike Rate für elektrophysiologische Experimente und die Stärke der Hirnaktivität ausgedrückt in Pixelgrauwerten für die Experimente der optischen Ableitung. Als unabhängige Variablen wurde zum einen der Stimuluskontext mit zwei Untersuchungsstufen, kollinear bzw. nicht-kollinear, variiert. Zur Normalisierung der Daten wurde dazu

die jeweils erhobene Hirnaktivität in Reaktion auf den zentralen Gabor alleine mit dem Aktivitätswert unter Stimulation durch eine der beiden Kontextlinien ins Verhältnis gesetzt. Die zweite unabhängige Variable war der Zeitpunkt der Aufnahme entweder vor bzw. während der zeitweiligen Kühldeaktivierung. Im Zuge der methodischen Gegebenheit, die Orientierungspräferenz der Elektrodeneinheiten zu bestimmen, wurde diese Unterscheidung als dritte unabhängige Variable in das Untersuchungsdesign mit aufgenommen. Für die Experimente optischer Ableitungen konnte dies ebenso Anwendung finden, indem zwischen Pixeln unterschieden wurden, welche Hirnregionen vertikaler bzw. horizontaler Orientierungspräferenz zuordenbar waren.

In elektrophysiologischen Experimenten konnte gezeigt werden, dass die Stärke der Spike Rate der abgeleiteten Neuroneneinheiten in unterschiedlichem Maße durch den Kontext des Stimulus moduliert wurden. Einheiten, die eine vertikale Stimulus Orientierung innerhalb ihres rezeptiven Feldes bevorzugten, zeigten im Durchschnitt eine höhere Spike Rate bei einem kollinearen im Vergleich zu einem nicht-kollinearen Stimulus im Umfeld ihres RF. Für Einheiten, die bevorzugt durch Stimuli mit horizontaler Orientierung aktiviert werden, ergab sich das gegenteilige Resultat. Hier war die Spike Rate in Antwort auf den kollinearen Stimuluskontext niedriger als auf nicht-kollinear arrangierte Umfeldelemente. Die Ergebnisse aus allen optischen Ableitungsdurchgängen konnten die kollinearen Befunde für Pixel vertikaler Orientierungspräferenz bestätigen. Nur in zwei der optischen Ableitungsdurchgänge zeigten die der horizontalen Orientierungspräferenz zugeordneten Pixel im Durchschnitt das selbe Resultat wie bei den Elektrodenableitungen.

Die Ergebnisse ergaben weiterhin, dass unter Kühlen ausschließlich die Einheiten mit horizontaler Orientierungspräferenz eine signifikante Abnahme an Aktivität für kollinearen Stimuluskontext aufwiesen. Kollinear angeordnete Stimuluselemente in lokal horizontaler Orientierung kreuzen die vertikale Mittellinie des Gesichtsfeldes und sind deshalb in beiden Hemisphären repräsentiert. Die meisten der optischen Ableitungsdurchgängen zeigten eine verringerte kortikale Aktivität während des Kühlens, unter beiden Bedingungen möglicher Stimuluskonstruktionen, welche die vertikale Mittellinie überschreiten. Das ist zum einen die bereits beschriebene kollineare Linie horizontaler Elemente, sowie die nicht-kollineare Linie vertikaler Elemente. Letzteres zeigte im Durchschnitt auch einen Abfall in der Spike Rate während der

Kühldeaktivierung im Vergleich zu vorher, dieser Unterschied wurde jedoch nicht signifikant.

Schlussfolgernd kann gesagt werden, dass unsere Ergebnisse bisherige Studien dahingehend bestätigen, dass Zellen in V1 sehr variabel durch Kontext moduliert werden (z.B., Polat et al., 1998). Es wird deutlich, dass der Wahrnehmungsvorteil einer kollinearen Linie nicht einheitlich in allen Zellen in V1 repräsentiert ist. Unsere Befunde weisen darüber hinaus darauf hin, dass die Orientierungspräferenz der Zellen eine entscheidende Rolle in den Auswirkungen des Umfeldes auf ihre Aktivität spielen könnte. Insbesondere wirkten sich kollinear angeordnete Elemente vertikaler Orientierung besonders vorteilhaft auf die Aktivitätsstärke der Zellen eben jener Orientierungspräferenz aus. Geht man recht in der Annahme, dass das Sichtfeld einer Katze vorrangig von horizontalen Konturen geprägt ist (Betsch et al., 2004), so ist es denkbar, dass Neurone vertikaler Orientierungspräferenz mehr darauf angewiesen sind, über ihr weit reichendes Netzwerk zu kommunizieren. Diese Idee, dass das Vorliegen von weniger Information einen höheren Arbeitsaufwand kortikaler Zellen bedeutet, wurde bereits von Nauhaus und Kollegen (2009) angesprochen, die neuronale Aktivität im primären visuellen Kortex in Reaktion auf verringerten Stimuluskontrast untersuchten. Sie fanden heraus, dass ein schwaches Stimulussignal, die Funktion lateraler Verbindungen hervorhob, indem diese verstärkt visuelle Information aus dem Umfeld integrierten. Die gegebene Variabilität der Aktivitätsmuster von Zellen in V1, sowohl innerhalb als auch in Kommunikation zwischen den Hemisphären, tragen vermutlich in ihrer Reichhaltigkeit erst dazu bei, dass ein Wahrnehmungsphänomen auf höherer Ebene des visuellen Systems entstehen kann. Letztendlich erscheint die Wahrnehmung des Ganzen komplexer zu sein als die Summe der eingehenden sensorischen Signale.

6 REFERENCES

Albrecht, D. G., Geisler, W. S., Frazor, R. A., & Crane, A. M. (2002). Visual cortex neurons of monkeys and cats: Temporal dynamics of the contrast response function. *Journal of Neurophysiology, 88,* 888-913.

Akasaki T., Sato H., Yoshimura Y., Ozeki H., & Shimegi S. (2002). Suppressive effects of receptive field surround on neuronal activity in the cat primary visual cortex. *Neuroscience Research, 43,* 207-220.

Beck, J. (1966). Effect of orientation and of shape similarity on perceptual grouping. *Perception & Psychophysics*, *1*, 300-302.

Betsch, B. Y., Einhäuser, W., Körding, K. P., König, P. (2004). The world from a cat's perspective – statistics of natural videos. *Biological Cybernetics, 90,* 41-50.

Birbaumer, N., & Schmidt, R. F. (1996). *Biologische Psychologie [Biological Psycology]* (3rd ed.). Berlin: Springer.

Blakemore, C., Diao, Y. C., Pu, M. L., Wang, Y. K., & Xiao, Y. M. (1983). Possible functions of the interhemispheric connections between visual cortical areas in the cat. *The Journal of Physiology Online, 337,* 331-349.

Blasdel, G., & Campbell, D. (2001). Functional retinotopy of monkey visual cortex. *Journal of Neuroscience, 21,* 8286-8301.

Bonhoeffer, T., & Grinvald, A. (1993). The layout of iso-orientation domains in area 18 of cat visual cortex: Optical imaging reveals a pinwheel-like organization. *Journal of Neuroscience, 13,* 4157-4180.

Bonhoeffer, T., & Grinvald, A. (1996). Optical imaging based on intrinsic signals: The methodology. In A. W. Toga & J. C. Mazziota (Eds.), *Brain mapping. The methods* (pp.55-97). San Diego, CA: Academic Press.

Born, R. T., & Bradley, D. C. (2005). Structure and function of visual area MT. *Annual Review of Neuroscience, 28,* 157-189.

Bosking, W. H., Zhang, Y., Schofield, B., & Fitzpatrick, D. (1997). Orientation selectivity and the arrangement of horizontal connections in tree shrew striate cortex. *Journal of Neuroscience, 17,* 2112-2127.

Braddick, O. J., O'Brien, J. M., Wattam-Bell, J., Atkinson, J., Hartley, T., & Turner, R. (2001). Brain areas sensitive to coherent visual motion. *Perception, 30,* 61-72.

Brodmann K. (1909). Vergleichende Lokalisationslehre der Großhirnrinde in ihren Prinzipien dargestellt auf Grund des Zellenbaues. Leipzig: Verlag von Johann Ambrosius Barth.

Buhl, E. H., & Singer, W. (1989). The callosal projection in cat visual cortex as revealed by a combination of retrograde tracing and intracellular injection. *Experimental Brain Research, 75,* 470-476.

Carmeli, C., Lopez-Aguado, L., Schmidt, K. E., De Feo, O., & Innocenti, G. M. (2007). A novel interhemispheric interaction: modulation of neuronal cooperativity in the visual areas. *PLoS One, 12,* 1-14.

Cass, J., & Alais, D. (2006). The mechanisms of collinear integration. *Journal of Vision, 6,* 915-922.

Chisum, H. J., Mooser, F., & Fitzpatrick, D. (2003). Emergent properties of layer 2/3 neurons reflect the collinear arrangement of horizontal connections in tree shrew visual cortex. *Journal of Neuroscience, 23,* 2947-2960.

Choudhury, B. P., Whitteridge, D., & Wilson, M. E. (1965). The function of the callosal connections of the visual cortex. *Experimental Physiology, 50,* 214-219.

Crook, J. M., & Eysel, U. T. (1992). GABA-induced inactivation of functionally characterized sites in cat visual cortex (area 18): Effects on orientation tuning. *Journal of Neuroscience, 12,* 1816-1825.

Field, D. J., Hayes, A., & Hess, R. F. (1993). Contour integration by the human visual system: Evidence for a local "association field". *Vision Research, 33,* 173-193.

Freeman, E., Sagi, D., & Driver, J. (2001). Lateral interactions between targets and flankers in low-level vision depend on attention to the flankers. *Nature Neuroscience, 4,* 1032-1036.

Freeman, T. C., Durand, S., Kiper, D. C., & Carandini, M. (2002). Suppression without inhibition in visual cortex. *Neuron, 61,* 35-41.

Freeman, E., & Driver, J. (2005). Task-dependent modulation of target-flanker lateral interactions in vision. *Perception & Psychophysics, 67,* 624-637.

Frostig, R. D., Lieke, E. E., Ts'o, D. Y., und Grinvald, A. (1990). Cortical functional architecture und local coupling between neuronal activity und the microcirculation revealed by in vivo high-resolution optical imaging of intrinsic signals. *PNAS, 87,* 6082-6086.

Gilbert, C. D., & Wiesel, T. N. (1979). Morphology and intracortical projections of functionally characterised neurones in the cat visual cortex. *Nature, 280,* 120-125.

Gilbert, C. D., & Wiesel, T. N. (1983). Clustered intrinsic connections in cat visual cortex. *Journal of Neuroscience, 3,* 1116-1133.

Gilbert, C. D., & Wiesel, T. N. (1989). Columnar specificity of intrinsic horizontal and corticocortical connections in cat visual cortex. *Journal of Neuroscience, 9,* 2432-2442.

Gilbert, C. D., & Wiesel, T. N. (1990). The influence of contextual stimuli on the orientation selectivity of cells in primary visual cortex of the cat. *Vision Research, 30,* 1689-1701.

Girardin, C. C., & Martin, K. A. (2009). Inactivation of lateral connections in cat area 17. *The European Journal of Neuroscience, 29,* 2092-2102.

Goldstein, B. (2001). *Sensation and perception* (6th ed). London: Wadsworth.

Gray, C. M., Maldonado, P. E., Wilson, M., & McNaughton, B. (1995). Tetrodes markedly improve the reliability and yield of multiple single-unit isolation from multi-unit recordings in cat striate cortex. *Journal of Neuroscience Methods, 63,* 43-54.

Gray, C. M., & Singer, W. (1989). Stimulus-specific neuronal oscillations in orientation columns of cat visual cortex. *Proceedings of the National Academy of Sciences, 86,* 1698-1702.

Grinvald, A., Lieke, E., Frostig, R. D., Gilbert, C. D., & Wiesel, T. N. (1986). Functional architecture of cortex revealed by optical imaging of intrinsic signals. *Nature, 324,* 361-364.

Hata, Y., Tsumoto, T., Sato, H., & Tamura, H. (1991). Horizontal interactions between visual cortical neurones studied by cross-correlation analysis in the cat. *The Journal of Physiology Online, 441,* 593-614.

Henle, M. (1990). Some neo-gestalt psychologies and their relation to gestalt psychology. In I. Rock (Ed.), *The legacy of Solomon Asch: Essays in cognition and social psychology* (pp. 279-318). Hillsdale: Lawrence Erlbaum.

Horsley, V., & Clarke, R. H. (1908). The structure and functions of the cerebellum examined by a new method. *Brain, 31,* 45-124.

Houzel, J. C., Milleret, C., & Innocenti, G. (1994). Morphology of callosal axons interconnecting areas 17 and 18 of the cat. *European Journal of Neuroscience, 6,* 898-917.

Howell, D. C. (2008). Fundamental statistics for the behavioral sciences (6th ed.). Belmont, CA: Duxbury Press.

Huang, P. C., & Hess, R. F. (2008). The dynamics of collinear facilitation: Fast but sustained. *Vision Research, 48,* 2715-2722.

Hubel, D. H., & Wiesel, T. N. (1962). Receptive fields, binocular interaction, and functional architecture in the cat's visual cortex. *The Journal of Physiology Online, 160,* 106-154.

Hubel, D. H., & Wiesel, T. N. (1967). Cortical and callosal connections concerned with the vertical meridian of visual fields in the cat. *Journal of Neurophysiology, 30,* 1561-1573.

Hubel, D. H., & Wiesel, T. N. (1974). Sequence regularity and geometry of orientation columns in the monkey striate cortex. *Journal of Comparative Neurolology, 158,* 267-293.

Hupé, J. M., James, A. C., Girard, P., Lomber, S. G., Payne, B. R., & Bullier, J. (2001). Feedback connections act on the early part of the responses in monkey visual cortex. *Journal of Neurophysiology, 85,* 134-145.

Innocenti, G. M., Clarke, S., & Kraftsik, R. (1986). Interchange of callosal and association projections in the developing visual cortex. *Journal of Neuroscience, 6,* 1384-1409.

Kalatsky, V. A., & Stryker, M. P. (2003). New paradigm for optical imaging: Temporally encoded maps of intrinsic signal. *Neuron, 38,* 529-545.

Kandel E. R., Schwartz J. H., & Jessell T. M. (2000). *Principles of neural science (*4th ed*).* New York, NY: McGraw-Hill.

Katzner, S., Nauhaus, I., Benucci, A., Bonin, V., Ringach, D. L., & Carandini, M. (2009). Local origin of field potentials in visual cortex. *Neuron, 61*, 35-41.

Kennedy, H., Meissirel, C., Dehay, C. (1991). Callosal pathways in primates and their compliancy to general rules governing the organization of corticocortical connectivity. In J. Cronly-Dillon, B. Dreher, & S. Robinson (Eds.), *Vision and visual dysfunction* (Vol 3, pp 324-359). London: Macmillan. Killackey HP.

Kisvárday Z. F., Tóth E., Rausch M., & Eysel U. T. (1997). Orientation-specific relationship between populations of excitatory and inhibitory lateral connections in the visual cortex of the cat. *Cerebral Cortex, 7,* 605-618.

Koffka, K. (1935). *Principles of Gestalt Psychology.* London: Lund Humphries.

Köhler, W. (1929). *Gestalt Psychology.* New York, NY: Liveright.

Kriegeskorte, N., Mur, M., & Bandettini, P. (2008). Representational similarity analysis - connecting the branches of systems neuroscience. *Frontiers in Systems Neuroscience, 2,* 1-28.

Lomber, S. G. (1999). The advantages and limitations of permanent or reversible deactivation techniques in the assessment of neural function. *Journal of Neuroscience Methods, 86,* 109-117.

Makarov, V. A., Schmidt, K. E., Castellanos, N. P., Lopez-Aguado, L., & Innocenti, G. M. (2007). Stimulus-dependent interaction between the visual areas 17 and 18 of the 2 hemispheres of the ferret (mustela putorius). *Cerebral Cortex, 28,* 1951-1960.

Mansfield, R. J. (1974). Neural basis of orientation perception in primate vision. *Science, 186*, 1133-1135.

Mark, V. H., Chato, J. C., Eastman, F. G., Aronow, S., & Ervin, F. R. (1961). Localized cooling in the brain. *Science, 134*, 1520-1521.

Maxwell, S. E., & Delaney, H. D. (2005). *Designing experiments and analyzing data: A model comparison perspective* (2nd ed.). Mahwah: Erlbaum.

McCullough, J. N., Zhang, N., Reich, D. L., Juvonen, T. S., Klein, J. J., Spielvogel, D., Ergin, M. A., & Griepp, R. B. (1999). Cerebral metabolic suppression during hypothermic circulatory arrest in humans. *The Annals of Thoracic Surgery, 67,* 1895-1899.

Metzger, W. (1966). Figurale Wahrnehmung [Figural Perception]. In W. Metzger (Ed.), *Wahrnehmung und Bewusstsein [Perception and Consciousness]* (pp. 699-714). Göttingen: Hogrefe.

Mizobe, K., Polat, U., Pettet, M. W., & Kasamatsu, T. (2001). Facilitation and suppression of single striate-cell activity by spatially discrete pattern stimuli presented beyond the receptive field. *Visual Neuroscience, 18,* 377-391.

Movshon J. A., Thompson I. D., & Tolhurst D. J. (1978). Spatial and temporal contrast sensitivity of neurones in areas 17 and 18 in the cat's visual cortex. *The Journal of Physiology, 283,* 101-120.

Müller, J. R., Metha, A. B., Krauskopf, J., & Lennie, P. (2001). Information Conveyed by onset transients in responses of striate cortical *neurons. Journal of Neuroscience, 21,* 6978-90.

Nauhaus, I., Busse, L., Carandini, M., & Ringach, D. L. (2009). Stimulus contrast modulated functional connectivity in visual cortex. *Nature Neuroscience, 12,* 70-76.

Olavarria, J. F. (2001). Callosal connections correlate preferentially with ipsilateral cortical domains in cat areas 17 and 18, and with contralateral domains in the 17/18 transition zone. *The Journal of Comparative Neurology, 433,* 441-457.

Orban, G. A., & Kennedy, H. (1981). The influence of eccentricity on receptive field types and orientation selectivity in areas 17 and 18 of the cat. *Brain Research, 208,* 203-308.

Orban, G. A., Kennedy, H., & Maes, H. (1981). Response to movement of neurons in areas 17 and 18 of the cat: Direction selectivity. *Journal of Neurophysiology, 45,* 1059-1073.

Palmer, S. E. (1999). *Vision science: Photons to Phenomenology*. Cambridge, MA: MIT Press.

Payne, B. R. (1994). Neuronal interactions in cat visual cortex mediated by the corpus callosum. *Behavioural Brain Research, 64,* 55-64.

Payne, B. R., & Berman, N. E. (1983). Functional organization of neurons in cat striate cortex: Variations in preferred orientation and orientation selectivity with receptive-field type, ocular dominance, and location in visual-field map. *Journal of Neurophysiology, 49,* 1051–1072.

Payne, B. R., & Lomber, S. G. (1999). A method to assess the functional impact of cerebral connections on target populations of neurons. *Journal of Neuroscience Methods, 86,* 195-208.

Payne, B. R., & Siwek, D. F. (1991). Visual-field map in the callosal recipient zone at the border between areas 17 and 18 in the cat. *Visual Neuroscience, 7,* 221-236.

Payne, B. R., Siwek, D. F., & Lomber, S. G. (1991). Complex transcallosal interactions in visual cortex. *Visual Neuroscience, 6,* 283-289.

Peters, A., Payne, B. R., & Josephson, K. (1990). Transcallosal non-pyramidal cell projections from visual cortex in the cat. *Journal of Comparative Neuroscience, 302,* 124-142.

Pettigrew, J. D., Nikara, T., & Bishop, P. O. (1968). Responses to moving slits by single units in cat striate cortex. *Experimental Brain Research, 6,* 373-390.

Planck, M. (1932). *Where is science going?* New York, NY: Norton.

Planck, M. (1948). *Wissenschaftliche Selbstbiographie [Scientific Autobiography].* Leipzig: Barth.

Polat, U., & Sagi, D. (1993). Lateral interactions between spatial channels: Suppression and facilitation revealed by lateral masking experiments. *Vision Research, 33,* 993-999.

Polat, U., & Sagi, D. (1994). The architecture of perceptual spatial interactions. *Vision Research, 34,* 73-78.

Polat, U., Mizobe, K., Pettet, M. W., Kasamatsu, T., & Norcia, A. M. (1998). Collinear stimuli regulate visual responses depending on cell's contrast threshold. *Nature, 391,* 580-584.

Polat, U., & Sagi, D. (2006). Temporal asymmetry of collinear lateral interactions. *Vision Research, 46,* 953-960.

Reynolds, J. H., & Desimone, R. (2003). Interacting roles of attention and visual salience in V4. *Neuron, 37,* 853-863.

Rochefort, N. L., Buzbs, P., Kisvarday, Z. F., Eysel, U. T., & Milleret, C. (2007). Layout of transcallosal activity in cat visual cortex revealed by optical imaging. *Neuroimage, 36,* 804-821.

Rochefort, N. L., Buzás, P., Quenech'du, N., Koza, A., Eysel, U. T., Milleret, C., Kisvarday, Z. F. (in press). Functional selectivity of interhemispheric connections in cat visual cortex. Cerebral Cortex.

Rockland, K., & Lund, J. S. (1983). Intrinsic laminar lattice connections in primate visual cortex. *The Journal of Comparative Neurology, 216,* 303-318.

Schmidt, K. E., Goebel, R., Lowel, S., & Singer, W. (1997a). The perceptual grouping criterion of collinearity is reflected by anisotropies of connections in the primary visual cortex. *European Journal of Neuroscience, 9,* 1083-1089.

Schmidt, K. E., Kim, D. S., Singer, W., Bonhoeffer, T., & Lowel, S. (1997b). Functional specificity of long-range intrinsic and interhemispheric connections in the visual cortex of strabismic cats. *Journal of Neuroscience, 17,* 5480-5492.

Sengpiel, F., Sen, A., & Blakemore, C. (1997). Characteristics of surround inhibition in cat area 17. *Experimental Brain Research, 116,* 216-228.

Sillito, A. M., Grieve, K. L., Jones, H. E., Cudeiro, J., & Davis, J. (1995). Visual cortical mechanisms detecting focal orientation discontinuities. *Nature, 378,* 492-496.

Sincich, L. C., & Blasdel, G. G. (2001). Oriented axon projections in primary visual cortex of the monkey. *Journal of Neuroscience, 21,* 4416-4426.

Super, H., & Roelfsema, P. R. (2005). Chronic multiunit recordings in behaving animals: advantages and limitations. In J. v. Pelt (Ed.), *Progress in brain research development, dynamics, and pathology of neuronal networks: From molecules to functional circuits* (Vol. 147, pp. 263-282). Amsterdam: Elsevier.

Toth, L. J., Rao, S. C., Kim, D. S., Somers, D., & Sur, M. (1996). Subthreshold facilitation and suppression in primary visual cortex revealed by intrinsic signal imaging. *PNAS, 93,* 9869-9874.

Ts'o, D. Y., Gilbert, C. D., & Wiesel, T. N. (1986). Relationships between horizontal interactions and functional architecture in cat striate cortex as revealed by cross-correlation analysis. *Journal of Neuroscience, 6,* 1160-1170.

Tusa, R. J., Palmer, L. A., & Rosenquist, A. C. (1978). The retinotopic organization of area 17 (striate cortex) in the cat. *The Journal of Comparative Neurology, 177,* 213-235.

Ungerleider, L. G., & Mishkin, M. (1982). Two cortical visual systems. In D. J. Ingle, M. A. Goodale, & R. J. W. Mansfield (Eds.) *Analysis of visual behavior.* Cambridge, MA: MIT Press.

Vanduffel W., Payne B. R., Lomber S. G., & Orban G. A. (1997). Functional impact of cerebral connections. *PNAS, 94,* 7617-7620.

Vicario, G. B. (1989). On Wertheimer's principles of organization. In G. Stemberger, (Ed.), *Gestalt Theory* (Vol. 20, pp 256-269). Vienna: Verlag Kramer.

Wertheimer, M. (1923). Untersuchungen zur Lehre von der Gestalt [Studies in the theory of Gestalt psychology]. *Psychologische Forschung, 4,* 301–350.

Westheimer, G. (1998). Lines and Gabor functions compared as spatial visual stimuli. *Vision Research, 38,* 487-491.